ELECTROSPUN POLY(ETHYLENE-CO-VINYL ALCOHOL) MEMBRANES FOR LEUKODEPLETION FILTERS: EFFECT OF CHEMICAL MODIFICATIONS

MAYURI P. V.

Ph.D. THESIS

2017

SREE CHITRA TIRUNAL INSTITUTE FOR

MEDICAL SCIENCES AND TECHNOLOGY, THIRUVANANTHAPURAM

INDIA

ELECTROSPUN POLY(ETHYLENE-CO-VINYL ALCOHOL) MEMBRANES FOR LEUKODEPLETION FILTERS: EFFECT OF CHEMICAL MODIFICATIONS

A THESIS PRESENTED BY

MAYURI P. V.

TO

SREE CHITRA TIRUNAL INSTITUTE
FOR MEDICAL SCIENCES AND TECHNOLOGY,
THIRUVANANTHAPURAM
INDIA

IN PARTIAL FULFILMENT OF THE REQUIREMENTS
FOR THE AWARD OF
DOCTOR OF PHILOSOPHY

2017

CERTIFICATE

I, **Mayuri P. V.**, hereby certify that I had personally carried out the work depicted in the thesis entitled, **"Electrospun Poly(Ethylene-co-vinyl alcohol) Membranes for Leukodepletion Filters: Effect of Chemical Modifications",** except where due acknowledgment has been made in the text. No part of the thesis has been submitted for the award of any other degree or diploma prior to this date.

Thiruvananthapuram

Mayuri P. V.

Reg.No: 2011/PhD/06

SREE CHITRA TIRUNAL INSTITUTE FOR MEDICAL SCIENCES & TECHNOLOGY
BIOMEDICAL TECHNOLOGY WING, POOJAPPURA
THIRUVANANTHAPURAM – 695011, INDIA
(An Institute of National Importance under Govt. of India)
Phone-(91)0471-2520221 Fax-(91)0471-2341814 www.sctimst.ac.in

Dr. P. Ramesh

Scientist G & In-charge (joint)

Division of Polymeric Medical Devices

Department of Medical Devices Engineering

BMT Wing, SCTIMST

email: rameshp@sctimst.ac.in

This is to certify that **Ms. Mayuri P. V.**, Division of Polymeric Medical Devices, Department of Medical Devices Engineering, of this Institute has fulfilled the requirements prescribed for the Ph. D. degree of Sree Chitra Tirunal Institute for Medical Sciences and Technology, Thiruvananthapuram. The thesis entitled, **"Electrospun Poly(Ethylene-co-vinyl alcohol) Membranes for Leukodepletion Filters: Effect of Chemical Modifications"** was carried out under my direct supervision. No part of the thesis was submitted for the award of any degree or diploma prior to this date.

Thiruvananthapuram
28-10-2016

Dr. P. Ramesh
(Research Supervisor)

The thesis entitled

ELECTROSPUN POLY(ETHYLENE-CO-VINYL ALCOHOL) MEMBRANES FOR LEUKODEPLETION FILTERS: EFFECT OF CHEMICAL MODIFICATIONS

Submitted by

Mayuri P. V.

for the degree of

Doctor of Philosophy

of

SREE CHITRA TIRUNAL INSTITUTE
FOR
MEDICAL SCIENCES AND TECHNOLOGY, TRIVANDRUM

Is evaluated and approved by

…….	……..
Dr. P. Ramesh	Examiner
(Research Supervisor)	

Dedicated to

GOD ALMIGHTY & MY FAMILY

ACKNOWLEDGEMENTS

It is with a deep sense of gratitude, satisfaction and with the divine blessings of God Almighty that I submit this dissertation. I take this opportunity with much pleasure to acknowledge all those who have contributed in many ways for the success of this study.

First and foremost I express my sincere gratitude and respect to my Guide Dr. P. Ramesh, Scientist G, Polymeric Medical Devices, SCTIMST for his continuous advice and encouragement throughout the course of my study. He was always accessible and took significant effort for the successful completion of this endeavour.

I am grateful to Dr. Asha Kishore, Director of SCTIMST, former Director, former Head and present Head of BMT Wing, Dr. H. K. Varma for all support provided during the course of my work. I am thankful to the Dean Dr. V. Kalliyana Krishnan, Associate Dean Dr. T. V. Kumary, Deputy Registrar Dr. Sundar Jaysingh and all members of academic division for their assistance.

I thank members of Doctoral Advisory Committee, Dr. T. V. Kumary, Scientist G, Tissue Culture Laboratory and Dr. Roy Joseph, Scientist G, Polymeric Medical Devices, for their timely suggestions, ideas and comments which helped in the improvement of the quality of this work. I express my heartfelt thanks to Dr. Roy Joseph for his sincere help and efforts taken for drafting and revising one of my publications.

I am extremely thankful to Dr. Lissy K Krishnan, Scientist G of Thrombosis Research Unit for granting me the permission to use some of their facilities. I extend my special appreciation to Dr. Anugya Bhatt, Scientist C of Thrombosis Research Unit for being with me during my biological experiments, analyzing my data and revising my manuscripts. I also extent my special thanks to Ms. Priyanka Manoj, Mr. Anil Kumar, Mr. Renjith Kartha, Ms. Reenamol and all other members of Thrombosis Research Unit for the help for their timely help and support during my biological experiments.

I express my heartfelt gratitude to Dr. Mira Mohanty, former scientist-in-charge of Histopathology Laboratory for the histological analysis of the membranes. I am extremely thankful to Dr. Sabareeswaran, Scientist E of Histopathology Laboratory for kindly doing the histological analysis, imaging, helping me to interprtet the results and for reviewing my manuscripts. I am also thankful to Ms. Sulaikhababy, Dr. Manjula, Dr. Soumya, Mr. Joseph, Ms. Lakshmi and all other staff of Histopathology Laboratory for their constant help and support.

I am grateful to Dr. Jaisy Mathai, Head of the department of transfusion medicine for providing me the blood samples for my study. I also thank all the staff of SCTIMST blood bank for their assistance and co-operation.

I thank Dr. H. K. Varma, and Mr. Nishad and all members of Bioceramics Laboratory who helped me in EDX and SEM anlysis. I would like to acknowledge Dr. K Sreenivasan, Dr. C Radhakumary and Mr. Rowsen Moses of Laboratory for Polymer Analysis for ATR-FTIR, DSC and DTA analysis; Dr. V. Kalliyana Krishnan, Mr. Satheesh and Dr. Priya of Dental Products Laboratory for the ATR-FTIR analysis; Dr. T V Kumary, Dr. P R Anil Kumar, Ms. Usha Vasudev and staff of Tissue Culture Lab for helping in cytotoxicity evaluation of the membranes; Dr. Prabha D Nair, Ms. Geetha and staff, Division of Tissue Engineering & Regenerative Technology for contact angle measurements;

I also acknowledge Er.V Ramesh Babu, Mr. Rajalingam, Mr. Subash, Mr. Prathyush, Mr. Rejikumar and Staff of Precision Fabrication Facility for designing and developing various prototypes for the study and punches for cutting the membranes.

I express my sincere gratitude to Dr. M. C. Sunny for his guidance, support and encouragement during the initial satges of my tenure. I am extremely thankful to my dear friends in the campus for their help and whole-hearted cooperation during the study. I thank Ms. Remya, Ms. Jincy, Ms. Darsana, Dr. Priya, Dr. Arjun, Dr. Kiran, Ms. Sreelakshmi, Mr. Sudhin, Mr. Arungovil, Dr. Titash, Mr. Susanth, Ms. Soorya, Mr. Sreeraj, Mr. Athiyappan, Mr. Sarath, Ms. Anitha, Ms. Aswathy, Ms. Anuja, Ms. Deepthi, Mr. Berwin Singh, Mr. Krishnachandran, Mr. Syam, Ms. Dhanya Thyagarajan, Mr. Arunkumar, Ms. Dhanya C. S., Dr. Praveen, Mr. Riju, Dr. Parvathy, Dr. Anupama, Ms. Nayana, Mr. Kumaran, Mr. Sreevisakh, Ms. Dhanya V., Ms. Vibha, Ms. Rethikala, Dr.Soumya Columbus , Ms.Reshmi, Ms. Lakshmi, Dr.Vidhu, Ms. Shanti, Ms. Shabeena, Ms. Rakhi, Mr. Dhanesh, Dr. Finosh, Mr. Vineeth, Ms. Victoriya and Ms. Sini for their friendship which relieved my stresses and made those days memorable.

I am extremely grateful to all my teachers within the campus who were involved in my PhD course work. Co-operation from staff of various administrative departments and library of the Institute is fondly remembered.

I wish to acknowledge Kerala State Council for Science Technology and Environment, Kerala, and INSPIRE programme, Department of Science and Technology, India for providing my fellowship during the study.

I have no words to express gratitude to my family members who provided the most precious support. I am indebted to my husband, parents, brothers and sisters, for their unconditional love, support, encouragement and prayers.

God almighty, I bow before you for providing me strength, courage for completing this work and for being with me in all my good and hard times.

Mayuri P. V.

TABLE OF CONTENTS

	Page No.
DECLARATION BY THE STUDENT……	i
CERTIFICATE OF GUIDE…….	ii
APPROVAL OF THESIS…….	iii
ACKNOWLWDGEMENTS…….	v
TABLE OF CONTENTS……..	vii
LIST OF FIGURES……...	xiii
LIST OF TABLES…….	xix
ABBREVIATIONS……	xxi
SYNOPSIS…….	**xxiv**
CHAPTER 1 – INTRODUCTION……...	**1**
1.1. Need for leukoreduction……..	2
1.2. Leukoreduction and leukodepletion…….	4
1.3. Universal leukodepletion (ULD) and Selective leukodepletion (SLD)……	4
1.4. Leukodepletion filters……	5
1.4.1. Types of filtrations using leukodepletion filter……..	6
1.4.2. Components and structure of a leukodepletion filter…….....	7
1.4.3. Membranes in leukodepletion filters…….....	9
1.4.3.1. Methods of fabrication…….	10
1.4.3.1.1. Melt-blowing……..	10
1.4.3.1.2. Solvent-casting and particulate leaching……	11
1.4.3.2. Requirements for leukodepletion filter membranes.....	11
1.4.4. Commercially available leukodepletion filters…….	12

1.5. Current scenario of leukodepletion in India……. 13

1.6. Strategies for developing leukodepletion filters…… 14

1.6.1. Identification of suitable polymers…… 15

1.6.2. Exploration of feasible membrane fabrication method……. 15

1.6.3. Membrane modifications…… 16

1.7. Hypothesis……..... 17

1.8. Objectives of the study…….. 18

CHAPTER 2 – LITERATURE REVIEW…… 20

2.1. Blood transfusion reactions and their prevention…….. 20

2.2. Historical developments in leukodepletion filters ……..... 23

2.3. Commercially available leukodepletion filters…….. 24

2.3.1. Clinical benefits of leukodepletion filters…… 25

2.3.2. Complications associated with leukodepletion filters……..... 26

2.4. Effect of various filter parameters on the leukodepletion efficiency: An insight to leukodepletion mechanism…….. 27

2.5. Polymeric membranes for leukodepletion filters-from laboratory to market…… 32

2.6. Significance of membrane modifications……... 33

2.6.1. Modifications by acrylate and methacrylate systems…….. 35

2.6.2. Modifications by zwitterionic systems…… 36

2.6.3. Modifications by biomolecule immobilizations…….. 36

2.7. Poly (ethylene-co-vinyl alcohol) (EVAL)……..... 37

2.8. Polyacrylonitrile (PAN)……. 38

2.9. Electrospinning-a feasible membrane fabrication method…… 39

2.10. Limitations of the current systems…… 40

CHAPTER 3 - MATERIALS AND METHODS…… 42

3.1. Fabrication of leukodepletion filter membranes by electrospinning…. 43

3.1.1. Commercial reagents…….. 43

3.1.2. Preparation of reagents…… 45

3.1.3. Development of PAN membranes by electrospinning…… 45

3.1.4. Development of EVAL membranes by electrospinning …… 46

3.2. Modifications on electrospun EVAL membranes…….. 47

3.2.1. Preparation of 2-Hydroxyethyl acrylate grafted poly(ethylene-co-vinyl alcohol) (PHEA-g-EVAL)…… 48

3.2.2. Functionalization of EVAL by incorporation of glycine (EVAL-Gly)…… …….. 49

3.2.3. Functionalization of EVAL by photografting of SMDB (PSMDB-g-EVAL)……. 49

3.2.4. Immobilization of BSA via dopamine on EVAL membranes (EVAL-BSA)……. 50

3.3. Development of prototype and leukodepletion filter…….. 51

3.4. Characterization and evaluation of the electrospun membranes……. 53

3.4.1. Structural characterization …….. 53

3.4.2. Degree of grafting (DG)…….. 53

3.4.3. Morphological analysis…… 54

3.4.4. Pore characteristics…….. 55

3.4.5. Surface wettability studies……. 55

3.4.6. Mechanical properties……. 56

3.4.7. *In vitro* release study of glycine…… 57

3.4.8. Histological analysis of the filter membranes……..... 58

3.5. Biological Evaluation …….. 58

3.5.1. *In vitro* cytotoxicity by direct contact assay …….. 58

3.5.2. *In vitro* hemocompatibility evaluation…… 59

3.5.2.1. *In vitro* hemolysis assay…… 59

3.5.2.2. Plasma protein adsorption assay…… 60

3.5.2.3. *In vitro* RBC aggregation assay……. 61

3.5.2.4. Platelet adhesion studies…… 61

3.5.2.5. Coagulation assay…….. 62

3.5.2.5.1. PTT analysis…… 62

3.5.2.5.2. Fibrinogen estimation…….. 63

3.5.2.6. Evaluation of complement activation…… 63

3.5.2.7. Blood cell consumption studies……. 64

3.5.3. Whole blood filtration studies……. 65

3.6. Statistical analysis…….. 66

CHAPTER 4 – RESULTS……. 67

4.1. Fabrication characterization and evaluation of leukodepletion efficiency of electrospun membranes…… 67

4.1.1. Fabrication of filter membranes of EVAL and PAN by electrospinning…… 67

4.1.2. Characterization of the filter membranes…… 68

4.1.2.1. Morphological analysis……. 68

4.1.2.2. Analysis of porosity…….. 71

4.1.2.3. Water contact angle measurements…… 71

4.1.2.4. *In vitro* cytotoxicity assay……. 71

4.1.2.5. *In vitro* hemolysis assay…… 72

4.1.2.6. Evaluation of efficiency of leukodepletion…… 73

4.2. Modifications on EVAL membranes and their characterization…… 88

4.2.1. Preparation of 2-Hydroxyethyl acrylate grafted poly(ethylene-co-vinyl alcohol) (PHEA-g-EVAL)..……. 88

4.2.1.1. ATR-FTIR spectroscopy ……. 88

4.2.1.2. Degree of grafting……. 90

4.2.1.3. Effect of HEA grafting on the morphology of the EVAL fibers……. 91

4.2.1.4. Effect of HEA grafting on the pore characteristics….. 92

4.2.1.5. Effect of HEA grafting on the wetting characteristics of EVAL…….. 92

4.2.1.6. Effect of HEA grafting on the mechanical properties.. 93

4.2.1.7. Effect of HEA grafting on hemocompatibility…….. 94

4.2.1.8. Evaluation of leukodepletion efficiency of PHEA-g-EVAL membranes…… 98

4.2.2. Functionalization by incorporation of glycine……. 102

4.2.2.1. Surface characterization……. 102

4.2.2.2. *In vitro* release study……. 105

4.2.2.3. *In vitro* hemocompatibility evaluation…….. 106

4.2.3. Functionalization of EVAL by SMDB…… 107

4.2.3.1. Surface characterizations……... 107

4.2.3.2. Degree of Grafting…… 110

4.2.3.3. Pore size and porosity analysis…….. 110

4.2.3.4. *In vitro* hemocompatibility evaluation…….. 111

4.2.3.5. Evaluation of leukodepletion efficiency of zwitterions bearing EVAL membranes: EVAL-Gly and PSMDB-g-EVAL membranes…….. 113

4.2.4. Fabrication and characterization of BSA immobilized EVAL membranes…….. 120

4.2.4.1. Immobilization of BSA on EVAL membranes……. 120

4.2.4.2. Surface characterization……. 121

4.2.4.3. *In vitro* hemocompatibility evaluation…….. 124

4.2.4.4. Evaluation of leukodepletion efficiency by EVAL-

BSA membranes…… 126

4.3. Comparison of leukodepletion efficiency of the various modified and unmodified filters…… 129

CHAPTER 5 – DISCUSSION…….. 131

5.1. Fabrication and characterization and evaluation of leukodepletion efficiency of electrospun membranes…… 131

5.2. Preparation, characterization and biological evaluation PHEA-g-EVAL…….. 139

5.3. Preparation, characterization and biological evaluation of EVAL membranes functionalized with zwitterionic systems…….. 149

5.3.1. Preparation and characterization of EVAL-Gly…….. 149

5.3.2. Preparation and characterization of PSMDB-g-EVAL…….. 150

5.3.3. Biological evaluation of EVAL-Gly and PSMDB-g-EVAL.. 152

5.4. Preparation, characterization and biological evaluation of EVAL-BSA……... 155

5.5. Correlation between surface chemistry, wettability and leukodepletion efficiency……... 159

CHAPTER 6 - SUMMARY AND CONCLUSION…….. 161

6.1. Summary and Conclusions……..... 161

6.2. Limitations of Study……... 165

6.3. Future perspectives …… 166

BIBLIOGRAPHY…… 167

LIST OF PUBLICATIONS…… 190

CARRICULAM VITAE……..... 192

APPENDIX…….. 194

LIST OF FIGURES

Fig. No.	Caption	Page No.
1	Schematic representation of various components of a typical leukodepletion filter……...	8
2	Schematic representation of symmetric filter and asymmetric filter….	8
3	Structure of leukodepletion filter membranes; (a) non-woven (NW) and (b) sponge form (S)…….	9
4	Schematic representation of proposed leukodepletion mechanisms; (a) blocking, (b) bridging, (c) interception and (d) adhesion…….	29
5	Structures of polymers and monomers used in the study……..	44
6	Control filter device Imuguard III RC……..	44
7	Preparation of PHEA-g-EVAL……..	49
8	Immobilization of BSA on EVAL membrane via dopamine……	51
9	The developed prototype and leukodepletion filter; (a) prototype A top view, (b) prototype A lateral view and (c) schematic representation of prototype B……	53
10	SEM images of membranes electrospun at various conditions (a) EVAL-1 mL/h-500 RPM; (b) EVAL-10 mL/h-500 RPM; (c) EVAL-1 mL/min-500 RPM; (d) PAN-1 mL/h-500 RPM; (e) EVAL-1 mL/h-1500 RPM; (f) EVAL-10 mL/h-1500 RPM; (g) EVAL-1 mL/min-1500 RPM; (h) PAN-1 mL/h-1500 RPM……..	70
11	Water contact angles of (a) EVAL membrane and (b) PAN membranes…….	71
12	Microscopic images of L929 cells grown on (a) electrospun EVAL membrane, (b) electrospun PAN membrane, (c) positive control and (d) negative control by direct contact test……..	72
13	Leukodepletion filter device after whole blood filtration; (a) filter	

assembled, (b) filter device separated, (c) membrane assembly top view and (d) membrane assembly lateral view…….. 74

14 Evaluation of leukodepletion efficiency of electrospun membranes; (a) cell adhesion, (b) hemolysis and (c) speed of filtration……... 75

15 SEM analysis of adhered cells to the EVAL filter (a-c) top layer, (d-f) middle layer and (g-i) bottom layer at different magnifications…… 76

16 Histological examination of stained cross sections (from top to bottom) of EVAL filter membrane assembly. The arrow indicates the direction of blood flow…….. 77

17 SEM analysis of adhered cells to the PAN filter (a-c) top layer, (d-f) middle layer and (g-i) bottom layer at different magnifications…… 78

18 Histological examinations of stained cross sections (from top to bottom) of PAN filter membrane assembly. The arrow indicates the direction of blood flow…….. 79

19 Comparative evaluation of leukodepletion efficiency between EVAL symmetric (EVAL-S) and EVAL asymmetric filter (EVAL-AS): (a) cell adhesion, (b) hemolysis and (c) speed of filtration……. 80

20 SEM analysis of adhered cells to the EVAL-S filter (a-c) top layer, (d-f) middle layer and (g-i) bottom layer at different magnifications... 81

21 Histological examinations of stained cross sections (from top to bottom) of EVAL-S filter membrane assembly. The arrow indicates the direction of blood flow……. 82

22 Effect of fiber diameter on the leukodepletion efficiency of EVAL-AS filter: (a) cell adhesion, (b) hemolysis and (c) speed of filtration... 84

23 SEM analysis of adhered cells to the EVAL filter (fiber diameter 0.7 µm) (a-c) top layer, (d-f) middle layer and (g-i) bottom layer at different magnifications……. 85

24 Histological examination of stained cross sections (from top to bottom) of EVAL filter (fiber diameter 0.7 µm) membrane assembly. The arrow indicates the direction of blood flow…… 86

25	SEM analysis of adhered cells to the EVAL filter (fiber diameter 3 µm) (a-c) top layer, (d-f) middle layer and (g-i) bottom layer at different magnifications…….	87
26	Histological examination of stained cross sections (from top to bottom) of EVAL filter (fiber diameter 3 µm) membrane assembly. The arrow indicates the direction of blood flow……	88
27	ATR-FTIR spectra of EVAL and PHEA-g-EVAL electrospun mats as a function of UV exposure time……	89
28	SEM images of EVAL and PHEA-g-EVAL electrospun mats:(a). Neat EVAL; (b-f). UV treated EVAL, with treatment times 10, 30, 40, 50 & 60 min, respectively; (g) fiber diameter as s function of UV irradiation time……...	91
29	Effect of HEA grafting on the pore diameter……	92
30	Stress-strain behavior of neat EVAL (indicated as '0') and PHEA-g-EVAL having different UV irradiation times……	94
31	Light microscopy images of RBC aggregation studies conducted on electrospun mats: (a) Neat EVAL; (b-f) UV treated EVAL with treatment times 10, 30, 40, 50 & 60 min respectively; (g) Positive control……	95
32	SEM images of electrospun mats after platelet adhesion studies: (a). Neat EVAL; (b-f). UV treated EVAL with treatment times 10, 30, 40, 50 & 60 min, respectively……..	96
33	SEM images of PHEA-g-EVAL membranes in the asymmetric filter collected at different speeds; (a) 500 RPM and (b) 1500 RPM……	99
34	Comparison of leukodepletion efficiency of PHEA-g-EVAL-60 and neat EVAL asymmetric filter…….	100
35	SEM analysis of adhered cells to the PHEA-g-EVAL-60 filter; (a-c) top layer, (d-f) middle layer and (g-i) bottom layer at different magnifications……	101
36	Histological examinations of stained cross sections of PHEA-g-	102

EVAL-60 filter membrane assembly. The arrow indicates the direction of blood flow……..

37 ATR-FTIR spectrum of EVAL-Gly membranes at various glycine loading……... 103

38 SEM pictures of EVAL-Gly membranes at various loadings; (a) neat EVAL, (b) EVAL-Gly-1 %, (c) EVAL-Gly-5 % and (d) EVAL-Gly-10 %..... 103

39 Wettability evaluation of EVAL-Gly membranes; (a) WCA and (b) CWST…… 104

40 *In vitro* release profile of glycine from the various EVAL-Gly membranes……. 105

41 SEM images of EVAL-Gly membranes after exposure to PRP; (a) neat EVAL, (b) EVAL-Gly-1 %, (c) EVAL-Gly-5 % and (d) EVAL-Gly-10 %..... 106

42 ATR-FTIR spectra of neat and PSMDB-g-EVAL obtained by various UV irradiation periods…….. 108

43 SEM pictures of (a) neat EVAL and (b-g) SMDB functionalized EVAL through UV irradiation periods 10, 20, 30, 40, 50 and 60 min, respectively…… 108

44 Effect of SMBD functionalization on the fiber diameter of EVAL as a function of UV irradiation periods. The ‘0’ minutes stands for neat EVAL……. 109

45 Effect of SMBD functionalization on water contact angle of EVAL as a function of UV irradiation periods. The ‘0’ minutes stands for neat EVAL……. 109

46 Degree of grafting of SMDB functionalized EVAL as a function of UV irradiation time…… 110

47 SEM images of membranes after exposure to platelets. (a) Neat EVAL and (b-g) SMDB functionalized EVAL with UV irradiation time 10, 20, 30, 40, 50 and 60 min respectively…… 113

48 SEM images of (a) EVAL-Gly-1 % and (b) PSMDB-g-EVAL membranes obtained at a speed of 1500 RPM…….. 114

49 Comparison of leukodepletion efficiency of zwitterions bearing EVAL asymmetric filters- EVAL-Gly-1 % and PSMDB-g-EVAL-60 with neat EVAL asymmetric filter……. 116

50 SEM analysis of adhered cells to the EVAL-Gly-1 % filter; (a-c) top layer, (d-f) middle layer and (g-i) bottom layer at different magnifications…… 117

51 Histological examinations of stained cross sections of EVAL-Gly-1 % filter membrane assembly. The arrow indicates the direction of blood flow…….. 118

52 SEM analysis of adhered cells to the PSMDB-g-EVAL-60 filter; (a-c) top layer, (d-f) middle layer and (g-i) bottom layer at different magnifications…… 119

53 Histological examinations of stained cross sections of PSMDB-g-EVAL-60 filter membrane assembly. The arrow indicates the direction of blood flow…….. 120

54 Mechanism of BSA immobilization on membrane via dopamine……. 121

55 ATR-FTIR spectra of EVAL-BSA membranes……. 123

56 SEM images of (a) EVAL-PD, (b) EVAL-BSA-1, (c) EVAL-BSA-2, (d) EVAL-BSA-10, (e) EVAL-BSA-50 and (c) EVAL-BSA-100…… 123

57 SEM images of EVAL-BSA membranes after exposure to PRP; (a) neat EVAL, (b) EVAL-BSA-1, (c) EVAL-BSA-2, (d) EVAL-BSA-10, (e) EVAL-BSA-50 and (f) EVAL-BSA-100……... 125

58 Comparison of leukodepletion efficiency of neat EVAL and EVAL-BSA-10 asymmetric filters…… 127

59 SEM analysis of adhered cells to the EVAL-BSA-10 filter; (a-c) top layer, (d-f) middle layer and (g-i) bottom layer at different magnifications…… 128

60 Histological examinations of stained cross sections of EVAL-BSA-10 filter membrane assembly. The arrow indicates the direction of blood flow…….. 129

61 Comparison of wettability, surface chemistry and leukodepletion efficiency of the developed filters……. 130

62 Mechanism of BP mediated photografting of HEA onto EVAL matrix……. 140

LIST OF TABLES

Table No.	Title	Page No.
1	Relationship between leukocyte number and adverse effects……	3
2	List of commercially available filters…….	10
3	Status of leukodepletion in various countries. ……..	14
4	List of prepared reagents……	45
5	The parameters for electrospinning of various membranes……..	46
6	Aqueous solutions selected for critical water surface tension (CWST) studies and their surface tension values…….	56
7	Properties of the electrospun EVAL and PAN membranes……..	70
8	*In vitro* hemolysis of electrospun EVAL and PAN membranes…	72
9	Peak intensity ratio of CH_2 stretch to C=O stretch for different UV treatment times……	90
10	Physico-chemical properties of electrospun fibroporous mats as a function of UV exposure time…….	90
11	Static and dynamic mechanical properties of electrospun mats as a function of UV exposure time…….	93
12	*In vitro* hemocompatibility evaluation: Data of hemolytic evaluation, protein adsorption and platelet adhesion on electrospun mats as a function of UV exposure time…….	95
13	*In vitro* hemocompatibility evaluation: Data of coagulation assay complement activation and interaction of blood cells on electrospun mats as a function of UV exposure time…….	98
14	Membrane properties of PHEA-g-EVAL asymmetric filter……..	99
15	Fiber diameter and pore properties of EVAL-Gly membranes…..	104
16	*In vitro* hemocompatibility evaluation of EVAL-Gly membranes	106

17	Effect of SMDB functionalization on the pore size and porosity of EVAL…….	111
18	*In vitro* hemocompatibility evaluation of PSMDB-g-EVAL obtained at various UV irradiation times……...	112
19	Membrane properties of EVAL-Gly and PSMDB-g-EVAL asymmetric filters……...	114
20	Properties of the EVAL-BSA membranes…….	124
21	*In vitro* hemocompatibility evaluation of EVAL-BSA membranes……..	125
22	Membrane properties of EVAL-BSA-10 asymmetric filter……....	126

ABBREVIATIONS

AABB	:	American Association of Blood Banks
AMO	:	N-acryloylmorpholine
ATR-FTIR	:	Attenuated Total Internal Reflection – Fourier Transform Infrared Spectroscopy
BMA	:	N-butylmethacrylate
BP	:	Benzophenone
BSA	:	Bovine Serum Albumin
CA	:	Cellulose Acetate
CB	:	Carboxybetaine
CMV	:	Cytomegalovirus
CPD-A	:	Citrate Phosphate Dextrose - Adenine
CWST	:	Critical Wetting Surface Tension
DEAEMA	:	Diethylamonoethyl methacrylate
DG	:	Degree of grafting
DMA	:	Dynamic Mechanical Analysis
DMF	:	N,N-dimethyl formamide
EDTA	:	Ethylene diamine tetra acetic acid
ELISA	:	Enzyme Linked Immuno-Sorbent Assay
EVAC	:	Poly(ethylene-co-vinyl acetate)
EVAL	:	Poly(ethylene-co-vinyl alcohol)
EVAL-AS	:	Poly(ethylene-co-vinyl alcohol) asymmetric filter
EVAL-BSA	:	Poly(ethylene-co-vinyl alcohol) functionalized with bovine serum albumin
EVAL-Gly	:	Poly(ethylene-co-vinyl alcohol) incorporated with glycine
EVAL-PD	:	Poly(ethylene-co-vinyl alcohol) functionalized with polydopamine
EVAL-S	:	Poly(ethylene-co-vinyl alcohol) symmetric filter
FDA	:	Food and Drug Administration
Gly	:	Glycine

GVHD	:	Graft Versus Host Disease
Hb	:	Hemoglobin
H&E	:	Haematoxylene and Eosin
HDPE	:	High Density Polyethylene
HEA	:	2-hydroxyethyl acrylate
HFIP	:	1,1,1,3,3,3-hexaflouro-2-propanol
HIV	:	Human Immunodeficiency Virus
HLA	:	Human Leukocyte Antigen
HTLV-I	:	Human T-Cell Leukaemia Virus I
IEC	:	Institutional Ethics Committee
LD	:	Leukodepletion
LDL	:	Low Density Lipoprotein
LMA	:	Lauryl mathacrylate
MPC	:	Methacryloyloxyethylphosphorylcholine
NHFTR	:	Nonhaemolytic Febrile Transfusion Reactions
NW	:	Non-woven
OHEMA	:	Hydroxyethyl metachrylate
PA	:	Polyamide
PAN	:	Polyacrylonitrile
PBS	:	Phosphate Buffered Saline
PBT	:	Poly(butylenes terephthalate)
PBTNF	:	Poly(butylene terephthalate) nonwoven fabric
PBTNFM	:	Poly(butylene terephthalate) nonwoven fibrous matrices
PC	:	Phosphorylcholine
PCL	:	Polycaprolactone
PD	:	Polydopamine
PEI	:	Poly(ethyleneimine)
PES	:	Poly(ethersulfone)
PET	:	Poly(ethylene terephtalate)
PHEA	:	Poly(2-hydroxyethyl acrylate)

PHEA-g-HEA	:	Poly(2-hydroxyethyl acrylate) grafted poly(ethylene-co-vinyl alcohol)
PMMA	:	Poly(methyl methacrylate)
PPP	:	Platelet Poor Plasma
PRP	:	Platelet Rich Plasma
PSMDB-g-EVAL	:	Poly(N-(3-sulfopropyl)-N-methacroyloxyethyl-N,N-dimethylammonium betaine) grafted poly(ethylene-co-vinyl alcohol)
PTFE	:	Poly(tetrafluoroethylene)
PTT	:	Partial Thromboplastin Time
PU	:	Polyurethane
PVA	:	Poly(vinyl alcohol)
PVC	:	Poly(vinyl chloride)
RBC	:	Red Blood Cell
S	:	Sponge form
SB	:	Sulfobetaine
SEM	:	Scanning Electron Microscopy
SLD	:	Selective Leukodepletion
SMDB	:	N-(3-sulfopropyl)-N-methacroyloxyethyl-N,N-dimethylammonium betaine
TC	:	Total Cholesterol
TRALI	:	Transfusion Related Acute Lung Injury
TRIS	:	Transfusion Related Immune Suppression
ULD	:	Universal Leukodepletion
UV	:	Ultraviolet radiation
VP	:	N-vinylpyrrolidone
WB	:	Whole Blood
WBC	:	White Blood Cell
WCA	:	Water Contact Angle

SYNOPSIS

Abound reports exist for the fact that leukocytes in the donor blood may be harmful to the multitransfused patients in some special circumstances of blood transfusion. These harmful circumstances appear in the form of blood transfusion reactions and these conditions have proposed the step of leukoreduction in the custom of blood transfusions. Despite the various techniques for leukocyte removal, membrane based filtration is the best choice and is one among the most widely used ones, due to its simplicity and effectiveness. Thus leukodepletion is defined as leukocyte removal by with the help of specific filters or device which can reduce the leukocytes to a level of $< 5 \times 10^6$ of residual level per transfusate.

Various polymeric membranes including polyethylene terephtalate (PET), polypropylene (PP), polybutylene terephthalate (PBT), polyurethanes (PU) and cellulose-based polymers in their pure form and in modified versions have already been recommended to fabricate leukodepletion filters. Most of these filters uses fiber based non-woven membranes.

Due to the high cost and significantly high platelet adhesion for the commercialized filters, the use of leukodepletion filters is presently not much implemented in India. So developing a cost-effective and efficient leukodepletion filter indigenously will be worth to the patient community in India in near future. In this background, the main goal of the study was (1) to explore the technique of electrospinning to fabricate membranes efficient for leukodepletion filters, out of suitable polymers (2) to optimize the various membrane parameters that affect their leukodepletion performance and (3) to modify the electrospun membranes to alter

their surface chemistry and thereby enhance the leukodepletion efficiency. The study is presented in six chapters. The background and introduction of the work are elaborated in Chapter 1. It explains in detail about the leukocyte mediated adverse reactions, need for leukoreduction, universal leukodepletion and selective leukodepletion programs, methods of filtration, structure and components of leukodepletion filter, membranes used for leukodepletion filters, their fabrication methods, ideal properties required for such membranes, commercially available filters and their limitations, and the current scenario of leukodepletion filters in India. The chapter also discussed the various strategies for developing efficient leukodepletion filters.

Hypotheses put forward on the basis of current knowledge are: *(1) Fibrous or fibroporous polymeric matrices can give better leukodepletion and thus efficient leukodepletion filter membranes can be developed from appropriate choice of blood compatible polymeric material by the application of suitable fiber fabrication method.*

(2) Leukodepletion and the mechanism of the same by fibroporous membranes are influenced by its properties including filter structure fiber diameter, pore diameter and porosity. Hence optimization of these parameters will generate excellent leukodepletion filter membranes

(3) Altering the chemical functionality of such membranes may affect its physico-chemical properties and also its leukodepletion efficiency. Thus the leukodepletion performance of the fibroporous membranes can be enhanced by proper choice of modification.

Major objectives of the current study are identified as follows.

- To fabricate leukodepletion filter membranes out of polyacrylonitrile (PAN) and poly(ethylene-co-vinyl alcohol) (EVAL) by electrospinning.
- To study the physico-chemical properties, blood material interactions and leukodepletion efficiency of PAN and EVAL membranes.
- To assess the effect of filter structure, fiber diameter, pore diameter and porosity upon the leukodepletion efficiency of EVAL membranes.
- To modify the EVAL membrane to alter its surface chemistry by photografting with 2-hydroxyethyl acrylate (HEA), functionalization by incorporation of glycine (Gly), photografting with N-(3-sulfopropyl)-N-methacroyloxyethyl-N,N-dimethylammonium betaine (SMDB) and immobilization of bovine serum albumin (BSA) via dopamine spacer.
- To study the effect of these modifications on the physico-chemical properties, mechanical properties, blood-material interactions and leukodepletion efficiency of the EVAL membranes and thus derive a correlation between the surface chemistry, wettability, and leukodepletion efficiency of membranes.

In Chapter 2, exhaustive literature review has been carried out to understand the current status of polymeric membranes for leukodepletion. The topics reviewed include blood transfusion reactions and remedies, membranes for leukodepletion filters, membrane modifications to enhance the leukodepletion efficiency. It also reviews the importance of electrospinning in membrane fabrication process. Review

also summarises the significance of various systems which are used for the membrane modification in our study.

In Chapter 3, experimental design in order to achieve the objectives of the proposed study is elaborated. It includes detailed description of materials employed, experimental protocols and instruments employed for the present study. Fabrication of leukodepletion filter membranes by electrospinning of EVAL and PAN is discussed in Section 1. The various approaches for modification of electrospun EVAL membranes are described in Section 2. The development of prototype and leukodepletion filter devices out various electrospun modified and unmodified membranes are explained in Section 3. Section 4 includes the physico-chemical characterization and evaluation of the various modified and unmodified electrospun membrane systems. The biological evaluation including the *in vitro* cytocompatibility evaluation and *in vitro* hemocompatibility evaluation, and also the evaluation of leukodepletion efficiency of the various membranes systems are detailed in Section 5. ATR-FTIR technique was adopted for structural characterization of various membrane systems. The degree of grafting (DG) was also reported by gravimetric analysis method. Measurements and analysis of surface morphology using Scanning Electron Microscopy (SEM) and surface wettability using goniometer as well as critical wetting surface tension (CWST) are also detailed. Estimation of the fiber diameter and pore properties was done by the ImageJ analysis. Mechanical testing using Universal Testing Machine was adopted to study mechanical properties of the membranes. Experimental details are also given for *in vitro* release profile of glycine (UV spectrophotometer). Cytotoxicity

evaluation of electrospun membranes using direct contact and live/dead assay, *in vitro* hemocompatibility evaluation of the various membrane systems as per ISO 10993-part 4 are provided. Details of whole blood filtration experiments for assessing the efficiencies of the various membrane systems are also explained. Post-filtration analysis of the filter membrane by SEM and histology is also described in this section.

Chapter 4 includes results presented substantiated by figures, tables and graphs. EVAL and PAN membranes were successfully fabricated by electrospinning, and their fiber diameter and pore properties were reported. Both the membranes were found hydrophobic from their water contact angle values. Both membranes were non-cytotoxic to fibroblast cells and non-hemolytic. The filtration studies showed that EVAL filter possessed leukodepletion efficiency which was comparable to that of the commercial filter while PAN filter gave a very poor efficiency and hence PAN filter was excluded from further study. Further, it was found that EVAL asymmetric filter can grant better leukodepletion efficiency than that by EVAL symmetric filter. The better leukodepletion was obtained when the fiber diameter in the EVAL membranes were ≥ 1.8 μm. The various modified EVAL membranes including HEA grafted EVAL (PHEA-g-EVAL), glycine incorporated EVAL (EVAL-Gly), SMDB grafted EVAL (PSMDB-g-EVAL) and BSA immobilized EVAL (EVAL-BSA) were characterised for their physico-chemical properties and biological evaluation. All the modifications enhanced the overall hemocompatibility of the EVAL membranes while altered its leukodepletion performances to different extends. Thus a correlation between the surface chemistry, wettability and leukodepletion was established.

Hence it was found that the PSMDB-g-EVAL had the appropriate degree of wettability and surface chemistry for enhanced leukodepletion.

In Chapter 5, results are discussed and analyzed with the aid of current literature. It is shown that electrospun EVAL has the potential to be used as leukodepletion filter membranes and appropriate modification on the membranes can enhance its hemocompatibility and leukodepletion performance. The importance of present study has also been highlighted.

Chapter 6 summarises the results and conclusions which are drawn from the present study. Leukodepletion filter membranes were successfully developed out of electrospun polymers. The electrospun EVAL membranes can be recommended to be used for leukodepletion filters. However, its performance can be improved by various chemical modifications. Out of the various modifications adopted in the study, the modification by incorporation of zwitterions, the PSMDB-g-EVAL membranes have the appropriate surface chemistry, wettability, hemocompatibility and leukodepletion efficiency. Thus it is concluded that the method of electrospinning can be recommended in future for fabrication of highly efficient leukodepletion filters out of suitable blood compatible polymers which have the desirable combination of appropriate surface chemistry/composition, wettability, surface energy and degradability. The limitations of the current study have been identified. Citations are listed in the bibliographic section.

CHAPTER 1

INTRODUCTION

Blood constitutes a major part of human circulatory system and is composed of plasma and formed elements. The term blood transfusion is defined as the process of receiving whole blood or blood products into one's circulation intravenously. During blood transfusions, the blood or blood products acts as drug for curing blood related decease conditions like thalassemia, anemia etc. or to replace a heavy blood loss due to accidents and surgeries (von Ahsen *et al.*, 2001). In each of such cases the donor's blood serve as very important entity in saving one's life, however, there are chances of adverse reactions to occur as a result of such transfusions. These adverse reactions are collectively termed as blood transfusion reactions.

It has been established that the major culprit behind these reactions are the leukocytes or white blood cells (WBC) present in the donor blood (Sahu and Verma, 2014). Sometimes, these leukocytes may mediate the transmission of certain viral infections to the recipient (Chu, 1999). Hence the only remedy to prevent the occurrence of these reactions is to reduce the leukocyte count to a safe level before transfusion. Thus the removal of leukocytes from the donor's blood is termed as leukoreduction (Capasso and Pisano, 2014). There are several methods for leukoreduction including differential centrifugation, sedimentation, freezing and thawing, cell washing and filtration (Meryman and Hornblower, 1986). Among these, filtration serves as the best method due to its

simplicity and effectiveness (Bruil *et al.,* 1995). Thus membrane based filtration of blood has been proven as the most practical approach for leukocyte reduction and has been paid much attention since 1990s. In this context, the evolution of polymeric non-woven fiber networks has greatly contributed to the fabrication of membrane bed filters for leukodepletion. A number of these kinds of filters is available in the market and made the filtration process much easier.

1.1. Need for leukoreduction

Leukocytes in the donor blood may be harmful to the multi-transfused patients in some special circumstances of blood transfusion. These harmful circumstances appear in the form of blood transfusion reactions. Some of these commonly recurring troubles caused by the administration of leukocyte rich blood have been identified in 1950s, and include nonhaemolytic febrile transfusion reactions (NHFTRs), decreased immune defense to infections, alloimmunization to human leukocyte antigens (HLA Alloimmunization), transfusion related acute lung injury (TRALI), transfusion related immune suppression (TRIS), graft versus host disease (GVHD) or transfer of viral infections such as those caused by cytomegalovirus (CMV) or human T-cell leukaemia virus I (HTLV-I) etc. (Kim *et al*., 2009; Mijović *et al*., 1983). The balance between these adverse effects and the leukocyte number has been published previously and is provided here in Table 1 (Lane *et al.,* 1992). Now it becomes clearer that these effects are minimizable if the leukocyte counts are below a threshold of 10^6. The American Association of Blood Banks (AABB) recommends this count more specifically to be less

than 5 × 10^6/unit after leukoreduction (3 log reduction giving 99.9 % leukocyte removal) with almost 85 % of other blood components retained (Ariga *et al*., 2003). Reports of Novotny *et al* also strongly support that leukoreduction to a level of < 5 × 10^6 of residual level per transfusate could prevent primary HLA alloantibody formation (Novotny *et al*., 1995). However the European Council guidelines propose this count better to be lesser than 5 × 10^6/unit (Guo *et al*., 2012; Yomotovian *et al*., 2001). Food and Drug Administration (FDA) guideline also was previously mandatory about the leukoreduction to lesser than 5 × 10^6/unit residual leukocytes, but presently little more stringent to counts recommended by European Council (FDA guidelines 1996; FDA guidelines 2012).

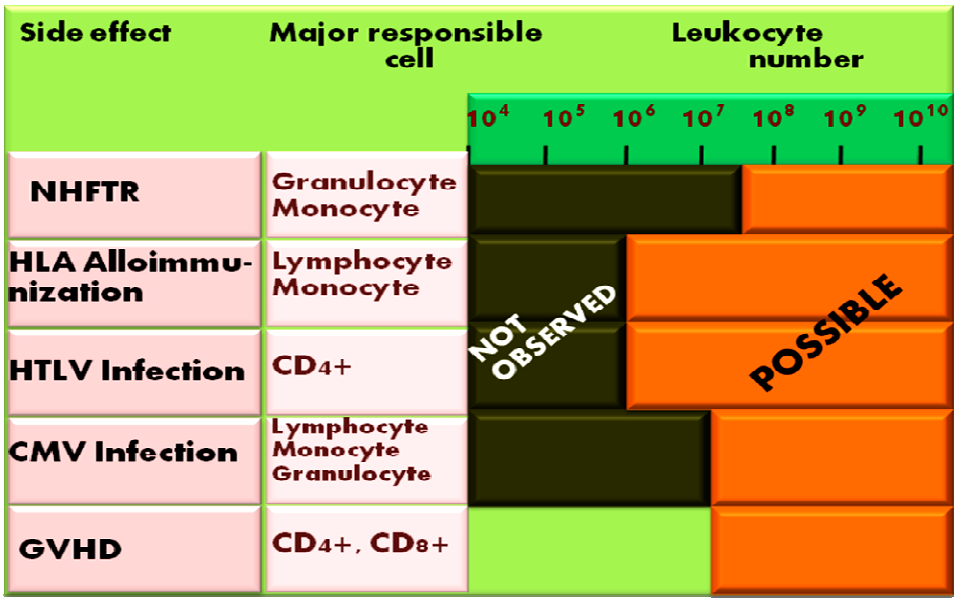

Table 1. Relationship between leukocyte number and adverse effects

With such inconsistency in monitoring the leukoreduction, contradictions also exist with respect to the minimization of above mentioned risks. Receipt of leukoreduced

blood is indeed and unavoidable for some special subjects like allogenic bone marrow transplant recipients (Sharma and Marwaha, 2010).

1.2. Leukoreduction and leukodepletion

As the two terms are used very frequently and interchangeably, “leukoreduction” and “leukodepletion”, we would like to follow the distinction between them as done by Sharma *et al* that leukoreduction and leukodepletion are respectively leukocyte removal by gross method and leukocyte removal with the help of specific filters or devices (Sharma and Marwaha, 2010). Thus a leukodepletion filter can be defined as a filter which can remove the leukocytes from blood to a count of $< 5 \times 10^6$ per unit while retaining more than 85 % of other functional and viable blood components. Defining the efficiency of the leukodepletion may vary according to the various guidelines mentioned above.

1.3. Universal leukodepletion (ULD) and Selective leukodepletion (SLD)

As it is proven that the step of leukodepletion is necessary in transfusion, this is implemented either to all patients through a universal leukodepletion (ULD) program or to selective groups of patients. Thus according to universal leukodepletion program (ULD), all the blood components have to be leukodepleted before transfusion while the selective leukodepletion (SLD) demands that only specific components have to be leukodepleted (Sharma *et al.*, 2014). Both have their own issues. While cost pulls the universal leukodepletion, the difficulty in predicting the need of leukoreduced blood at

the time of component preparation reduces the significance of selective leukodepletion (Sharma and Marwaha, 2010). European countries and some states of USA follow the ULD while the other is predominant in world's other parts. Still the debate is going on the implementation of ULD/SLD (Sharma and Marwaha, 2010; Yomtovian *et al.*, 2001).

1.4. Leukodepletion filters

Defining a leukodepletion filter is now very obvious. They are specific filter devices which are used to remove the leukocytes from the blood to the safe level, as mentioned by the various guidelines, while retaining other functional and viable components. It was Fleming who reported the use of cotton wool matrix for effective leukodepletion (Fleming, 1926). Further research and developments in the exploration of membrane based filtration of blood for leukodepletion has been paid much attention in the past years. Studies have also evinced that such membrane based leukodepletion filters are also able to remove tumor cells, bacteria, endotoxin etc. and can prevent the occurrence of virally transmissible diseases (Frühauf *et al.*, 2001; Högman *et al.*, 1997; Oldhafer *et al.*, 2013; Petsch *et al.*, 1998; Waters *et al.*, 2003). Recent studies also reported that membrane based leukodepletion are effective in separation of components in amniotic fluid (Campbell *et al.*, 2012). So knowing more about the structure, components and performance efficiencies of leukodepletion filters will be worth for understanding the current status of leukodepletion filters.

1.4.1. Types of filtrations using leukodepletion filter

Filtrations are performed in two different ways using leukodepletion filters. They are pre-storage filtration and post-storage filtration (Sharma and Marwaha, 2010). As their name indicates, the pre-storage filtration is done with the freshly collected blood from the voluntary donor immediately after the collection. After filtration, the filtered blood will be either stored or processed for further component separation. The post-storage filtration is performed with the stored blood or blood components only when required for the patient (Sharma and Marwaha, 2010). Hence the post-storage filtration is also called as bed-side filtration. The pre-storage filtration is always preferred to the other one due to its advantages mentioned below (Buchholz *et al.*, 1994; Rider *et al.*, 2000; Sharma and Marwaha, 2010)

Advantages of pre-storage filtration

- It eliminates the scope of inflammatory cytokine accumulation and prevents adverse reactions.
- It minimizes the risk of leukotropic virus transmission.
- It helps to perform leukocyte quality control in the laboratory rather than by the patient's bedside.
- During pre-storage filtration blood components can be thoroughly studied and various factors affecting the process of leukodepletion can be modified accordingly.

1.4.2. Components and structure of a leukodepletion filter

A typical leukodepletion filter consists of leukodepletion filter membranes perfectly assembled in an outer case. The filter will be supplied with two openings – inlet and outlet. The inlet functions for directing the blood to be filtered, to the filter while the outlet serves for collecting the filtered blood. A schematic representation of the interior of a leukodepletion filter is provided in Figure 1.

Depending on the structure and properties of the membranes, the filters are again classified into two different types- (1) symmetric filter and (2) asymmetric filter. Symmetric filter is one in which the pore size of all the membranes will be uniform where as in asymmetric filter, there will be a gradual decrease in the pore sizes of different layers from top to bottom (or in the direction of flow of blood) (Figure 2) (Bruil *et al.*, 1991). Several previous studies on the comparative evaluation of these two types of filters emphasize that asymmetric type of filter is preferred to symmetric filter, because in symmetric filter, there will be more chance for cell clogging on the membranes which ultimately results in pore plugging and prevents the retention of other components. However, in asymmetric filter, the chances for pore plugging will be minimum thus ensuring maximum retention of other functional and viable blood components (Bruil *et al.,* 1991) (Figure 2).

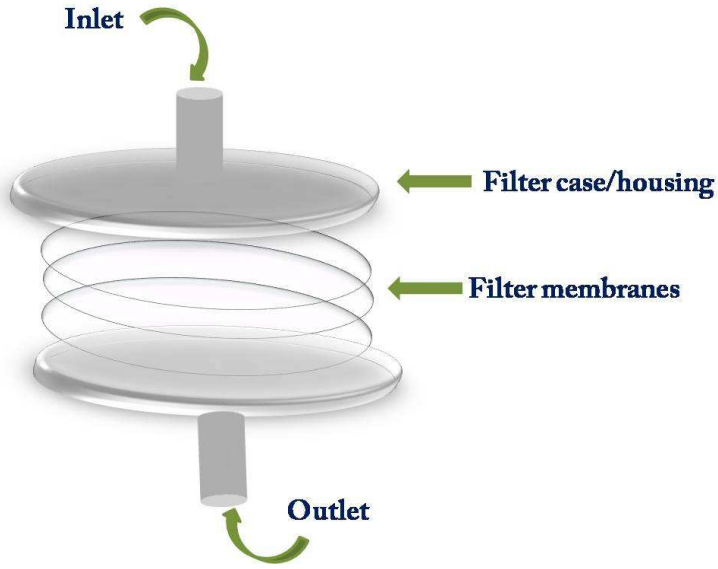

Figure 1. Schematic representation of various components of a typical leukodepletion filter

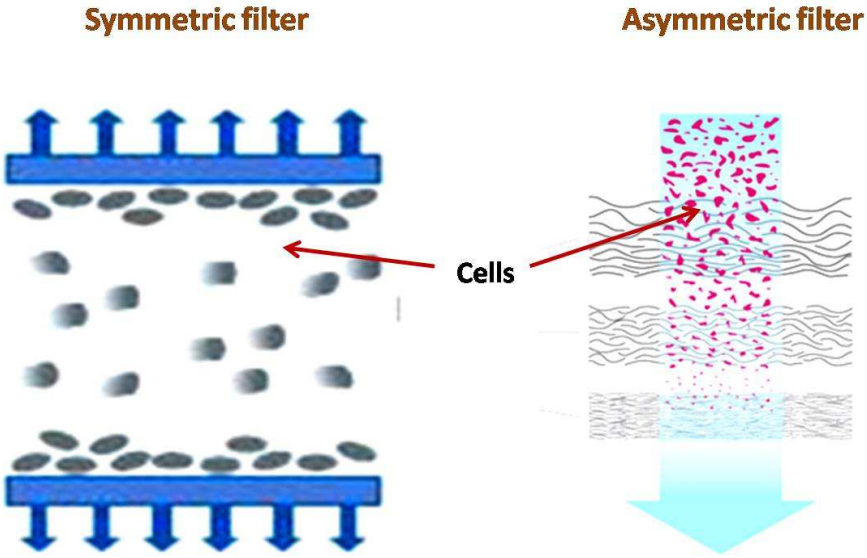

Figure 2. Schematic representation of symmetric filter and asymmetric filter

1.4.3. Membranes in leukodepletion filters

It was seen that commercialized leukodepletion filters are composed of polymeric membranes in either sponge like structure (open cellular form) or non-woven form. But most of them uses polymeric fiber based non-woven membranes. The membrane dimensions including the pore size, porosity, thickness, area etc. vary from filter to filter. Poly(ethylene terephthalate) (PET), poly(butylenes terephthalate) (PBT), polyurethanes (PU), poly(vinyl alcohol) (PVA) etc. and their modified forms have been widely used as membranes in leukodepletion filters either in sponge form (S) or non-woven (NW) form (Bruil *et al.,* 1993; Bruil *et al.,* 1991; Guo *et al.,* 2013; Henschler *et al.,* 2005; Kim *et al.,* 2009). Figure 3 shows the morphological dissimilarity of both types of membranes. Table 2 summarizes the properties and structure of some of the commercialized leukodepletion filter membranes.

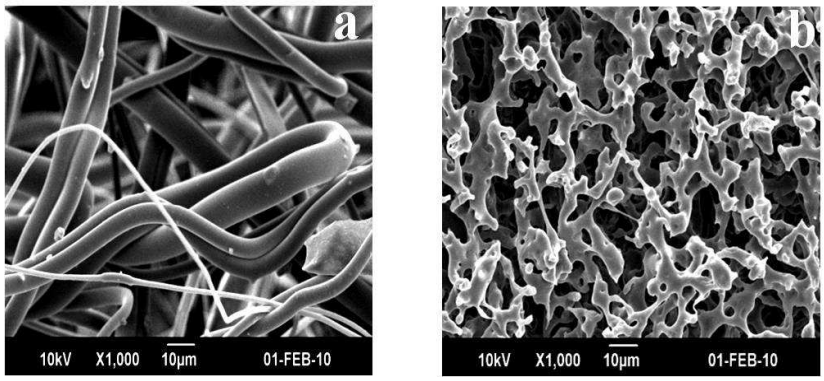

Figure 3. Structure of leukodepletion filter membranes; (a) non-woven (NW) and (b) sponge form (S)

Trade name	Manufacturer	Material	Membrane form	Pore size (µm)	Depletion WBC (%)	Recovery RBC (%)	Platelet removal (%)
Imuguard IG500	Terumo, Japan	Cottonwool	S	NA	93 - 98	85 - 97	68.4
Erypur G-0	Organon, Netherlands	Cellulose acetate fiber	NA	NA	96 - 98	90 - 99	87.9
Cellselect	NBPI, Netherlands	Cellulose acetate fiber	NA	NA	>99	75 - 88	NA
Optima		Polyester fiber	NA	NA	95 - 99	86 – 92	NA
Ultipore-SQ40S	Pall, New York	Polyester fiber	NW	40	84.8	92.7	44.8
Fenwal 4C2423	Fenwal, US	Polyester fiber	NA	20	65	73	63.5
Sepacell	Asahi, Japan	Polyester fiber	NW	20	99.7	89.8	96.4

Table 2. List of commercially available filters; NA-not available, NW-non-woven, S-sponge form

1.4.3.1. Methods of fabrication

The polymeric leukodepletion filter membranes are typically fabricated by conventional techniques, mainly (1) melt blowing and (2) solvent-casting and particulate leaching.

1.4.3.1.1. Melt-blowing

Melt blowing generates non-woven (NW) networks of polymers. It is a type of melt-spinning in which molten polymer streams are injected into a high velocity gas/air jets. This high velocity jets impinge upon the polymer and the drag forces caused by the air helps to form self-bonded web which is collected on a moving surface (Hassan *et al.*,

2013). Mel-blown membranes possess high surface area and good barrier properties which make them excellent candidates for various filtration applications (Hassan *et al*., 2013). From Table 2, it can be seen that Sepacell and Pall filters are composed out of melt-blown non-wovens.

1.4.3.1.2. Solvent-casting and particulate leaching

In this method a composite of the polymer solution is initially prepared by mixing the polymer solution with salt particles of specific size. Then the solvent is allowed to evaporate which leaves the solidified polymer membrane with the salt particles in it. Finally the porous membranes are generated by immersing the membrane in water so that all the salt particles leach out leaving the pores in the membranes (Wosek, 2015). Highly porous membranes can be generated by this method [Figure 3(b)]. A major limitation of this method is that only thin membranes can be fabricated by this method.

1.4.3.2. Requirements for leukodepletion filter membranes

The efficiency of leukodepletion by filters is determined by physico-chemical properties of the membranes, blood parameters and filtration parameters. But the membrane properties remain more significant than the others. Generally, the membrane parameters including, material chemistry/composition or surface chemistry, surface charge, pore diameter, fiber diameter, porosity, wettability etc. significantly influences the performance by leukodepletion filter membranes. However, the effect of some of these parameters on the membrane performances were established, but the effect of other parameters are still not manifested. It is reported that negatively charged leukocytes

adhere by van der Waals and electrostatic interactions and is dependent on pore size and flow rate (Curtis, 1973; Skalak *et al.*, 1982; Van Oss, 1975). Certain functionalities including –OH, zwitterions, -NH_2 are suggested to favor leukocyte binding (Curtis *et al.*, 1983; Ertel *et al*., 1992; Lee *et al*., 1991; Owens *et al*., 1988). The effect of fiber diameter on leukodepletion efficiency has also been disclosed (Shirokaze, 2002; Umegae *et al.*, 1988). The effect of pore size and porosity is dependent on the mechanism by which the leukocytes are removed. Still some researchers suggest that the ideal pore size and porosity for leukodepletion filter membranes are respectively 5 μm – 40 μm and 30 % - 90 % (Bruil *et al.*, 1995; Morudu, 2011). Contradictory reports still exist on the effect of wettability on leukocyte adhesion. Certain studies reported that hydrophobic polymeric membrane surfaces have a strong leukocyte binding, however, some other researchers suggest enhanced hydrophilicity favor leukocyte adhesion (Bruil *et al.*, 1994; Lim and Cooper, 1990). Hence it has to be understood that a desirable level of the various parameters and their appropriate combination will ensure the maximum leukodepletion by the membranes. Still a clear knowledge on the effect of these parameters on the retention of other blood components is not completely figured out.

1.4.4. Commercially available leukodepletion filters

Some of the commercially available leukodepletion filters with their efficiencies, membrane material and pore sizes are listed in Table 2. From the table it can be inferred that most of the filters are fabricated out of polyesters and cellulose acetate fibers with their pore sizes ranging from 20 μm – 40 μm. The filters were highly efficient in WBC

depletion and RBC retention. But significant amount of platelet adhesion was also reported for some of the filters. The approximate cost for such a filter is estimated to be Rs. 2000.

Limitations of commercially available filters

The major limitations associated with currently available commercial leukodepletion filters are said to be (1) the high cost and (2) poor platelet retention (Rider *et al*., 2000; Steneker and Biewenga, 1990). The high platelet loss when using such filters are often encountered when whole blood is filtered through them. Hence in order to prevent the high platelet loss by filtration, in most cases the platelet fraction is removed from whole blood by differential centrifugation and later the remaining leukocyte rich centrifugate is allowed to filter through the leukodepletion filter (Natori and Kurita, 2007b). However, this practice is much more time consuming than the simple filtration. So developing highly efficient leukodepletion filters which can effectively filter whole blood with a high retention of platelets and RBCs is worth in the current era.

1.5. Current scenario of leukodepletion in India

The current status of leukodepletion in India can be figured out from Table 3. It is now clear that in developed countries like Europe and USA, more than 80 % of the total transfusions are leukodepleted since they follow the ULD programme. But in Asia, especially in India, the blood banks still depend on other leukoreduction methods.

Country	Donations (Million)	Without LD (Million)	LD (Million)
Europe	21.9	4.8	16.3 (80 %)
USA	13.5	2.6	10.9 (82 %)
Asia	23.3	19.1	4.2 (25 %)

Table 3. Status of leukodepletion in various countries. LD-leukodepletion

Since countries including India follow SLD, leukodepletion filters are used only in critical conditions (Sharma and Marwaha, 2010). Hence according to the current scenario, India doesn't have any indigenous efficient leukodepletion filters. So we are forced to import highly efficient leukodepletion filters from the developed countries whenever needed. This result in high cost for such filters that normal patients in India may not be able to afford. However, the possibility for recommending ULD as a mandatory requirement in India, in the near future, cannot be neglected. In such a case, developing highly efficient and cost effective leukodepletion filters indigenously may reduce the filter cost and will be of significant importance to the patient community.

1.6. Strategies for developing leukodepletion filters

While developing an efficient leukodepletion filter, strategies for overcoming the limitations of the commercialized filters have to be undertaken. Taking into account, the high cost of such filters can be assigned to the manufacturing method employed. Generally, the membrane fabrication by melt-blowing technology is costly when

compared to other conventional methods (Ward, 2005). Hence there are three important approaches which one should consider while developing an efficient and cost effective leukodepletion filter. They are detailed below.

1.6.1. Identification of suitable polymers

A number of polymers have already been established to be used as leukodepletion filter membranes. However, a lot more polymers which are highly blood compatible and non-degradable suitable for membranes in leukodepletion filter still exist uninvestigated. Suggesting a few include poly(ethylene-co-vinyl alcohol) (EVAL), poly(ethylene-co-vinyl acetate) (EVAC), poly(tetrafluoroethylene) (PTFE), polyacrylonitrile (PAN), polycarbonate (PC), poly(ethersulfone) (PES) etc. Most of these polymers have been recommended for some other blood contacting application owing to their excellent blood compatibility, however, their leukodepletion efficiencies have not been reported till date (DeWitt *et al*., 2005; Jin *et al.*, 2008; Nie *et al.*, 2015; Wan Kim and Jacobs, 1996). Some other blood compatible biodegradable polymers including polycaprolactone (PCL) can also be experimented if their degradability can be tuned accordingly. Thus exploring novel cheaply available polymers with required properties might resolve the proposed limitations of the commercialized filters and thus replace the currently available polymers

1.6.2. Exploration of feasible membrane fabrication method

Another approach for developing efficient and cost effective leukodepletion filters is to explore a feasible membrane fabrication method. Since most of the commercial filter membranes are composed of non-woven matrices produced by melt-blowing, alternative

fiber fabrication method will serve best for the purpose. In this context the method of electrospinning seems very relevant. Electrospinning generates non-woven membranes whose morphological features resemble that of melt-blown non-wovens (Ramakrishna *et al.,* 2005). The technique has gained much attention in the past two decades in the area of biomedical engineering. Filtration membranes are one among the noteworthy uses of electrospun membranes. The membranes can be easily designed and modified according to the filtration requirements by the alteration in the spinning parameters (Ramakrishna *et al.,* 2005). A number of electrospun polymers have been reported to be best membranes for the purification of air and water (Guibo *et al.,* 2013; Gule *et al.,* 2012; Zhang *et al.,* 2010). Yet it seems like electrospinning has been concealed by the various other conventional techniques when concerned with the fabrication of leukodepletion membranes. The method can be considered while developing leukodepletion filter membranes with ideal properties and can serve as the best alternative to melt-blowing method for generating non-woven fabrics.

1.6.3. Membrane modifications

As already mentioned earlier that the membrane properties can influence their leukodepletion efficiency, modifications of membranes by various approaches serve as yet another strategy for developing efficient leukodepletion filters. Membrane modification also offers to achieve the required properties to the desired level. The surface composition, surface charge, wettability etc. can be modified by the appropriate modifications. Membranes can be modified by various approaches like coating of the

membrane surface with suitable materials, grafting of other monomers, incorporation of suitable additives, attaching different functionalities by coupling reactions, attaching biomolecules like proteins, anticoagulants including heparin etc. (Chang *et al.,* 2011; You *et al.,* 2011). Several investigations have been reported so far on the various modification strategies to the leukodepletion filter membranes. In one study, it was reported that coating the filter fabrics with various amphiphilic copolymers enhanced the overall performance of the fabric (Natori and Kurita, 2007a). Several other studies also reported better results after modification by different monomers including sulfbetaines, carboxybetaines etc. (Wang *et al*., 2013; Yuan *et al.,* 2008). Incorporation of hydroxyapatite was also proven to encourage the leukodepletion efficiency of PET filter fabrics (Kim *et al.,* 2009). The limitations associated with commercialized filters can also be resolved by the proper modification to those filter membranes. Thus the various strategies for modification of existing membranes open new pathways for replacing the search for exploring new materials.

1.7. Hypothesis

It is now obvious that exploring novel membrane materials by alternative fabrication methods is highly relevant in developing efficient leukodepletion filters capable for whole blood filtration. Moreover, the feasibility of membrane modification for tuning the desirable properties to the desirable extend also facilitates to develop an ideal leukodepletion filter. Hence it is conceptualized that generating non-woven membranes out of excellent hemocompatible polymers and their appropriate modification can give

outstanding filter fabrics which can replace the currently available leukodepletion filters. In order to accomplish this, we put forward the hypothesis as follows.

(1) Fibrous or fibroporous polymeric matrices can give better leukodepletion and thus efficient leukodepletion filter membranes can be developed from appropriate choice of blood compatible polymeric material by the application of suitable fiber fabrication method.

(2) Leukodepletion and the mechanism of the same by fibroporous membranes are influenced by its properties including filter structure fiber diameter, pore diameter and porosity. Hence optimization of these parameters will generate excellent leukodepletion filter membranes.

(3) Altering the chemical functionality of such membranes may affect its physico-chemical properties and also its leukodepletion efficiency. Thus the leukodepletion performance of the fibroporous membranes can be enhanced by proper choice of modification.

1.8. Objectives of the study

1. To fabricate leukodepletion filter membranes out of polyacrylonitrile (PAN) and poly(ethylene-co-vinyl alcohol) (EVAL) by electrospinning.
2. To study the physico-chemical properties, blood material interactions and leukodepletion efficiency of PAN and EVAL membranes.

3. To assess the effect of filter structure, fiber diameter, pore diameter and porosity upon the leukodepletion efficiency of EVAL membranes.
4. To modify the EVAL membrane to alter its surface chemistry by photografting with 2-hydroxyethyl acrylate (HEA), functionalization by incorporation of glycine (Gly), photografting with N-(3-sulfopropyl)-N-methacroyloxyethyl-N,N- dimethylammonium betaine (SMDB) and immobilization of bovine serum albumin (BSA) via dopamine spacer.
5. To study the effect of these modifications on the physico-chemical properties, mechanical properties, blood-material interactions and leukodepletion efficiency of the EVAL membranes and thus derive a correlation between the surface chemistry, wettability, and leukodepletion efficiency of the membranes.

CHAPTER 2

LITERATURE REVIEW

The major objectives of the present study are to explore the technique of electrospinning to fabricate efficient leukodepletion filter membranes out of suitable blood compatible polymers and to tune their physico-chemical properties to enhance their overall leukodepletion efficiency. To accomplish this goal, it is necessary to establish the current progress in this field. The following chapter on literature review elaborates in detail, the various blood transfusion reaction and their preventive measures and, history, development and significance of leukodepletion filters. The mechanism of leukocyte removal by filtration is also discussed. The historical development of various polymeric membranes in leukodepletion filters is discussed. In addition, the method of electrospinning for fabrication of membranes is also described. Thus it is possible to deduce the experimental design strategies for the current study with the help of these published literatures.

2.1. Blood transfusion reactions and their prevention

Leukocytes are the cells of immune system which are involved in fighting against the foreign invaders and thus protecting the body from infections. It has been well established that during the process of blood transfusion, the circulating donor leukocytes may identify the recipient as foreign and may produce immune responses. These responses are undesirable in the recipients, especially in multitransfused patients, and are

called blood transfusion reactions (Mijović *et al.*, 1983). The major blood transfusion reactions clinically encountered in patients are NHFTR, HLA alloimmunization, TRALI, TRIS, GVHD etc. NHFTR is caused by the antibodies directed against donor leukocytes and HLA antigens is one among the most frequently occurring transfusion reactions (Yomtovian *et al.*, 2001). According to the report from USA in 2010, the rate of NHFTR was 0.9 per 100,000 units of plasma transfusion (Serious Hazards of Transfusion (SHOT) annual report, 2002). Another retrospective study by Narick *et al* reported that the occurrence of NHFTR due to leukocyte contaminated plasma transfusion was 1:4,476 (Narick *et al*., 2012). NHFTR are also seen associated with leukocyte contaminated platelet transfusions (Serious Hazards of Transfusion (SHOT) annual report, 2002). Although these reactions carry a low risk, repeated occurrences may make the patient very apprehensive and reluctant to subsequent blood components. Alloimmunization results in the production of anti-human leukocyte antigen (anti-HLA) antibodies against the donor leukocytes and result in the rejection or transfer of viral infections such as those caused by cytomegalovirus (CMV) or human T-cell leukaemia virus I (HTLV-I) (Pandey and Vyas, 2012).

The prevention of occurrence of these reactions is accomplished by leukoreduction of blood and blood components before administration to the recipient. This is evidenced by clinical studies also. A very earlier report by Fischer *et al* has recommended that reducing the leukocyte counts to 10^6 per unit could effectively prevent the occurrence of HLA alloimmunization and other reactions (Fisher *et al.,* 1985). There are several leukoreduction methods which are in usual practice. Bruil *et al* and Wenz

have described in detail the various methods for preparing leukocyte-poor blood (Bruil *et al.*, 1995; Wenz, 1986). Differential centrifugation of blood to reduce the leukocyte count is the earliest method and still remains as the most frequently used one. However, this method consists of on open system handling and gives a poor leukocyte removal (Bruil *et al.*, 1995). Hence various modifications to this basic technique were also applied and include inverted centrifugation, double centrifugation, upright centrifugation etc. (Meryman and Hornblower, 1986). There exists another method in which molecules with high dielectric constant are deliberately added to the blood which causes the spontaneous sedimentation of RBCs and separation of the leukocyte containing buffy coat. This technique gives approximately 80 % leukocyte removal, however, is time consuming and associated with risk of bacterial contamination of the resulting products (Bruil *et al.*, 1995; Wenz, 1986). Washing of RBCs using the readily available cell washers followed by centrifugation also achieves 70 % - 95 % of the leukocyte removal (Bruil *et al.*, 1995). The disadvantages associated with this method are long processing time, high cost and open-system handling. Another technique, the freeze-thaw method, have also been considered as efficient method for preparation of leukocyte poor blood components, however, the associated difficulties like requirement of expensive equipment render this method the least considered one (Bruil *et al.*, 1995). The capability for leukocyte removal by these methods have also been reviewed by Sharma *et al* and according to their study, centrifugation could achieve removal to 10^8 (1 log reduction) leukocytes, whereas washing and freeze-thawing could make it to 10^7 (1-2 log reduction) and 10^6-10^7 (2-3 log reduction) respectively (Sharma and Marwaha, 2010).

Apparently, leukocyte removal by filtration, or leukodepletion, has achieved more attention than the above mentioned methods. During the early stages of development of such filters, the most commonly used filters were micro-aggregate filters which effectively removed the micro-aggregate debris from the stored blood thereby preventing emboli formation in the recipient (Morudu, 2011). These types of filters were also reported to possess sufficient leukodepletion. But the currently available leukodepletion filters are not specifically intended for micro-aggregate removal since they are highly efficient and commonly applied for pre-storage or bedside purposes. Various researchers investigated and compared the leukodepletion to other leukoreduction methods and established the advantages of leukodepletion over to other methods as

- Filtration is very simple, clinically effective and less time consuming.
- It doesn't require an open-system handling thus avoiding risk of contamination and preserve the shelf life of filtered products.
- It can be performed at patient's bedside (Bruil *et al.,* 1995).

2.2. Historical developments in leukodepletion filters

The first membrane based leukodepletion was reported in 1926 by Fleming who used a cotton wool matrix tightly plugged into a custom made glass tube (Fleming, 1926). Blood was forcefully driven through this and the cell counts were analyzed by hemocytometer. The filter could efficiently remove the leukocytes as well as platelets with high RBC recovery. Following this glass bead based filters were later developed

(Vaughan, 1939). Later Greenwalt *et al* investigated the leukocyte removal capacity of 3 different fibrous materials – Dacron, Teflon and Nylon – and reported that nylon has high leukodepletion efficiency than the others (Greenwalt *et al.,* 1962).

Serious researches have been carried out in 1970s exploring new natural and synthetic materials efficient for leukodepletion. Notwithstanding the search for new materials, a compromise in the design and parameters of the filter has also successfully experimented. However in last decade more progressive research have been reported and currently a number of new generation filters are readily available which gives 99.995 % leukocyte removal integrated with very fast filtrations (de Vries *et al*., 2005).

2.3. Commercially available leukodepletion filters

Several leukodepletion filters are commercially available in the market which differ in their specific purpose whether pre-storage or post-storage, material type, configuration and efficiencies. Some of such filters and their specifications are provided in Table 2. The post-storage or bedside filters are generally micro-aggregate leukodepletion filters whose pore sizes are made intentionally larger, approximately 170-240 μm, to accomplish the effective removal of micro-aggregate debris and blood clots along with the leukocytes (Morudu, 2011). These filters made the filtration process much easier and found clinically effective, however, critical reviews have also been reported.

2.3.1. Clinical benefits of leukodepletion filters

The clinical benefits of various leukodepletion filters have been unveiled by various researchers. Sirch *et al* demonstrated that when 3 different types of RBC concentrates were leukodepleted through Pall RC 100 filter and transfused to thalassemic patients, the occurrence of NHFTR was reduced (Sirchia *et al.,* 1990). Similarly the HLA alloimmunization was also significantly reduced in patients with poly-transfused oncohematology and hematologic malignancies as a result of transfusion of leukodepleted blood obtained by filtration through Imuguard IG 500 filter (Andreu *et al.,* 1988; Sniecinski *et al.,* 1988).

The beneficial aspects of use of leukodepletion filters in preventing bacterial and viral transmission have also been evidenced. Bowden *et al* presented that use of Pall filters noticeably reduced the CMV infection when CMV seronegative blood products were filtered (Bowden *et al.,* 1995). Sundry other clinical trials recommended that various commercially available leukodepletion filters could prevent the conveyance of *Yersinia Enterocolitica* contamination (Nusbacher, 1992). Pre-storage filtration using filters Sepacell R-500 reduced the likelihood of significant bacterial proliferation because of the removal of microorganism along with the WBCs during filtration (Buchholz *et al.,* 1994). In addition to the leukodepletion, the potential of these filters in other applications have also been disclosed recently. The first clinical use of leukodepletion filters for the effective tumor suppression was proved through the *in vitro* study by Oldhafer *et al* (Oldhafer *et al.,* 2013). Oncologic surgeries are always associated with high risk of tumor cell circulation into venous blood. Hence they used LG6 (Leukoguard 6 filter from Pall)

and this filter was integrated with the veno-venous bypass system of patients undergoing extended liver surgery for secondary hepatic malignancy. The filters could effectively and safely carry out the cytokeratin positive (CK+) cell depletion (Oldhafer *et al.,* 2013). Fruhuf *et al* also recommended leukodepletion filters could be used for the effective reduction of various human primary tumor cells (Frühauf *et al*., 2001). Another interesting study very recently reported by Campbell *et al* illustrated that leukodepletion filters could be successfully used for the removal of components of amniotic fluids (Campbell *et al.,* 2012).

2.3.2. Complications associated with leukodepletion filters

Despite of the beneficial aspects of leukodepletion filters, it is also worthy to note that there are some reported troubles associated with such filters. There is no such a clear-cut idea about the minimum level of leukocytes for preventing the viral infections and hence leukodepletion filters may not be trustworthy in such cases (Morudu, 2012). Supporting to this, a prospective study by Collier *et al* evidenced that leukodepletion provided no clinical benefits in patients due to leukodepleted RBC concentrate on the survival and complications of CMV and HIV infections (Collier *et al*., 2001). Another significant drawback of the leukodepletion filters is the very low platelet recovery (de Vries *et al*., 2005; Johnson *et al*., 1983; Natori and Kurita, 2007a; Rider *et al.,* 2000; Sirchia *et al*., 1990; Zwarts and de Vries, 2002). It is accounted that more than 40 % of the platelets are lost due to adhesion to the filters (de Vries *et al*., 2005). It becomes apparent that platelets have a strong affinity towards the filter membranes than the leukocytes and this indirectly helps the leukocyte binding. A favorable fact in this is that

such removal of platelets will reduce the thromboxane release and vasoconstriction (de Vries *et al*., 2005). However, loss of sufficient amount of such platelets will lead to wastage of blood products. Due to this, whole blood filtration through leukodepletion filters are not much implemented, but, filtrations are usually preformed after the removal of the platelet fraction by any other methods. This again becomes a time consuming process there by disfavoring the straightforwardness and liability of filter technology.

2.4. Effect of various filter parameters on the leukodepletion efficiency: An insight to leukodepletion mechanism

The performance by leukodepletion filters are affected by various parameters which can be generally classified into filtration parameters and filter parameters. The effects of these parameters, although not complete, have been reviewed by various investigators. However, a prior understanding on the mechanisms by which leukocytes are depleted will help to analyze the effects of the above mentioned parameters on the leukodepletion. Several researchers have suggested the possible mechanisms of leukodepletion by membranes but the exact mechanism is not yet manifested (Bruil *et al.*, 1995; Natori *et al*., 2006). According to Rider *e al*, the mechanism of leukodepletion by current filters is through directly by barrier retention and indirectly by adsorption to fibers (Rider *et al.*, 2000). Similarly, Stenekar *et al* found that the WBC and platelet removal is partially due to the formation of cell clusters on the surface of the layers and the major mechanism was trapping or mechanical sieving of the cells by the pores in the fibrous networks rather than adhesion (Steneker and Biewenga, 1990; Steneker *et al.,* 1992).

However, a more vivid idea about the leukodepletion mechanism was provided by Bruil *et al* According to Bruil *et al,* the selective removal of cells is based on the difference in degree of deformability and adhesiveness between the various cell types (Bruil *et al.*, 1995). It is understood that leukocytes as well as platelets have poor deformability and high adhesiveness while RBCs have high deformability and poor adhesiveness. Hence during blood flow through the filter, RBCs are easily deformed and escapes through the filter pores while other cells get adhered to the filter. Leukocyte removal occurs by the mechanisms like blocking or straining, bridging, interception and adhesion (Bruil *et al.*, 1991; Bruil *et al.*, 1995). A schematic representation of these is provided in Figure 4. Blocking occurs when the particle size is larger than the pore size; Bridging becomes relevant at a high particle concentration; Interception is the trapping of the leukocytes at dead ends of the filter or filter sites other than pore sizes; Adhesion is significant when the ratio of cells to pore size is in 10^{-4} to 10^{-1}. All these mechanisms acts accordingly depending on the conditions and parameters of filtration, however, adhesion is predominant while the contribution from other mechanism are negligible. Mathies *et al* also found that adhesion is significant in fibrous membrane due to the presence of several "cross-over" points in the fibrous network (Matheis *et al*., 2002). However, the studies of Steneker *et al* suggest that the removal of leukocytes by non-woven fibrous membranes is presumably due to mechanical sieving by the pores (Steneker and Biewenga, 1990; Steneker *et al.,* 1992). Investigations made by Zwarts and de Vries also support that the major leukodepletion mechanism by non-woven membranes is adhesion (Zwarts and de Vries, 2002).

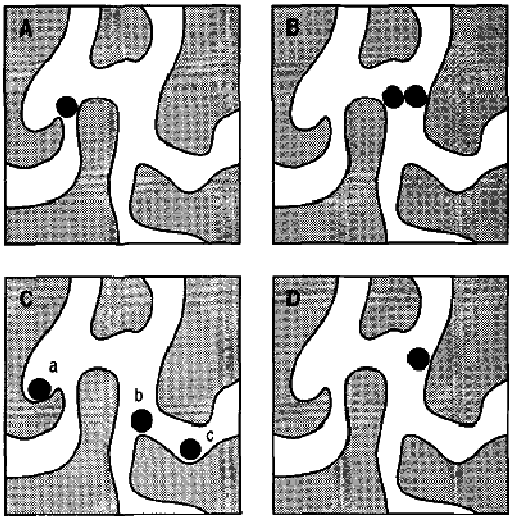

Figure 4. Schematic representation of proposed leukodepletion mechanisms; (a) blocking, (b) bridging, (c) interception and (d) adhesion. (Bruil *et al.*, 1995)

Deliberation on the effects of various parameters on the leukodepletion by filters can now be realized based on the mechanisms. Effect of temperature, one among the filtration parameters, has been examined by many and delineated that leukodepletion is maximum at low temperature preferably at 4 °C (Johnson *et al*., 1983; Ledent and Berlin, 1996; Meer *et al.,* 1999). This is accounted for the stiffness of the cells, their lower speed, and lower mobility at low temperatures that the leukocytes may either get trapped or get adhered. Another important parameter, the priming or pre-wetting with saline has considerable effect on the performance of leukodepletion filters. It is accounted that pre-wetting is necessary before the filtration of blood or blood components for removing the air trapped inside the filter and also for securing the cells to get adhered. Thus the leukodepletion efficiency has shown to be enhanced after the priming (Johnson *et al.*, 1983; Matheis *et al.*, 2002; Sniecinski *et al.*, 1988). However, contradictory reports are

also available. It was put forward that the efficiency of certain commercial leukodepletion filter was high even without priming (Sirchia *et al.,* 1990). Leukodepletion is also dependant on composition of blood. The presence of plasma significantly affects leukocyte adhesion. Grinnel and Feld and other researchers found that leukocyte adhesion is reduced in presence of plasma (Grinnell and Feld, 1981). However, there is a controversial report by Ledent and Berlin that presence of small amount of plasma enhanced the leukodepletion efficiency of the filter (Ledent and Berlin, 1996). It is also accounted that leukocyte adhesion is greatly influenced by the pre-adsorbed proteins and various proteins present in plasma has different effects on leukocyte interaction. Certain proteins including albumin inhibit leukocyte binding whereas globulins and fibronectin have more affinity for leukocytes (Barber *et al.,* 1978; Forrester and Lackie, 1984). The role of platelets in leukocyte adhesion has also needs to be considered seriously. In fact platelets have very high adhesiveness to any substrates than leukocytes do (Garvin, 1961). Hence platelet adhesion to filter membranes is always encountered during leukodepletion. Several studies have unanimously suggested that the adhesion of platelets highly support the subsequent leukocyte adhesion (Morley and Feuerstein, 1989; Rasp *et al.*, 1981). This is because, upon adhesion, the platelets gets activated and release their components like fibronectin, fibrinogen, von Willibrand factor etc. which then promote leukocyte binding (Morley and Feuerstein, 1989).

The filter parameters including the pore size, material chemistry, surface charge, surface wettability, surface microstructure and surface morphology are believed to play vital roles during leukodepletion. Leukocytes were successfully removed through the

pores of size equivalent to the size of leukocytes, 10 μm (Bruil *et al.*, 1991). However other studies have proven that there might be chances for clogging and thus diminishing the efficiency with such a small pore size and hence much higher pores are favorable (Callaerts *et al.*, 1993). In addition, the very small pore size may affect the RBC passage and could cause hemolysis (Blackshear Jr and Anderson, 1978). The different chemical functionalities present on the membrane affects the cell adhesion. It has been established that membranes having hydroxyl, carbonyl and amine moieties promote leukocyte adhesion (Ertel *et al*., 1992; Lee *et al.*, 1991; Owens *et al*., 1988). Contradictory data are available for the effect of carboxyl and sulfonate groups (Curtis *et al.*, 1983). However, it is not mandatory that incorporation of these functionalities may accordingly promote or inhibit leukocyte adhesion, because as a result of introduction of these groups, the overall physico-chemical properties of the membrane changes. Another interesting fact is that leukocyte adhesion is enhanced by presence of divalent cations especially Ca^{2+} and Mg^{2+} (Hoffstein *et al.*, 1981; Kvarstein, 1969). Hence the type of anticoagulant may also influence the cell trapping. For example, if EDTA or oxalate were used as anticoagulants, they might bind to the aforementioned divalent cations thereby decreasing their concentration and thus leukocyte adhesion has shown to be inhibited (Lang et al., 1988; MacGregor *et al.*, 1974). Surface charge of the membrane also has a crucial role since leukocyte binding to the membrane is partially due to the electrostatic interaction between the membrane surface and the leukocytes (Curtis, 1973; Skalak *et al.*, 1982; Van Oss, 1975). Notwithstanding the overall negative charge on the leukocyte surface, they are easily attached to both positively as well as negatively charged surfaces (Curtis *et al.*,

1983; Ertel *et al*., 1992; Lee *et al.*, 1991; Owens *et al*., 1988). This is because of the presence of pseudopodia on the leukocytes which can effectively penetrate through the electrical double layer of a negative charged surface and ultimately reach the bare surface thereby forming a strong contact with the surface (Polliack *et al.*, 1973; Van Oss, 1975). Effect of surface wettability on leukodepletion has also been reported contradictorily. Some researchers found that hydrophilic surface favors leukocyte adhesion while others published the conflicting argument that hydrophobic substrates show high leukocyte adhesion (Bruil *et al.*, 1994; Lim and Cooper, 1990). It has also been demonstrated that leukocyte adhesion on the substrates having microstructures, consisting of small micro-domains which differ in their composition, morphology, crystallinity and wettability is generally lower than the substrates without any microstructure (Kataoka *et al*., 1983; Maruyama *et al.*, 1987; Okano *et al.*, 1981; Yui *et al*., 1983). The effect of surface morphology on leukocyte adhesion was disclosed by various investigators. They found that surfaces having irregular and rough textures, promote the adhesion of leukocytes and platelets (Guidoin *et al*., 1977; Rich and Harris, 1981; Zingg *et al.*, 1981).

2.5. Polymeric membranes for leukodepletion filters-from laboratory to market

Various polymers have been found to have promising properties and excellent leukodepletion efficiencies. These have been experimentally validated in laboratory through *in vitro* studies and some of them ultimately reached the market. Polymers such polyethylene terephtalate (PET), polyamide (PA), polypropylene (PP), polyvinyl alcohol

(PVA), polybutylene terephthalate (PBT), polyurethanes (PU), nylon and cellulose acetate (CA) in their pure form and in modified versions have already been identified as outstanding filter materials (Henschler *et al.,* 2005). The distinct properties accredited to the leukodepletion ability by these polymers are surface chemistry, surface charge and the ideal pore size (Henschler *et al.,* 2005). The studies published by Kim *et al*, Guo *et al* and Yang *et al* have described the efficacy of PBT non-woven membranes towards leukodepletion (Guo *et al.,* 2013; Kim *et al*., 2009; Yang *et al.,* 2011). They investigated the effects of various parameters that affect the efficiency of PBT membranes. Brui *et al* experimented on open cellular PU membranes, prepared by salt suspension techniques, having pore size varying from 15 μm to 65 μm (Bruil *et al.,* 1991). These membranes showed very high leukocyte removal (> 99 %). It is also explicit from Table 2 that most of the commercial leukodepletion filters are based on PBT, CA, PU and PA.

2.6. Significance of membrane modifications

It is now well understood that an effective leukodepletion is highly influenced by the various physico-chemical properties of the filter membrane. Hence alterations in these properties by suitable approaches are necessary to design highly efficient leukodepletion filter membranes. It is interesting to note that the commercial Pall RC100 filter is made out of polyester fibrous membranes suitably modified for the selective adhesion of leukocytes (Sirchia *et al.,* 1990). Different researchers have focused on filter membrane modifications to tune the various membrane parameters. Bruil *et al* modified PU membranes by coating with poly(ethyleneimine) (PEI) in order to introduce amine groups

to the PU surface (Bruil *et al.,* 1993). However, upon filtration, it was found that the modification significantly enhanced the leukocyte adhesion from purified leukocytes in the absence of RBCs, platelets and plasma while leukocyte adhesion from whole blood remained unchanged (Bruil *et al.,* 1993). They concluded that morphological parameters like filter shape, roughness, porosity etc. plays more important role rather than the chemical composition of the filter in mediating the cell adhesion (Bruil *et al.,* 1993). Kim *et al* demonstrated the modification of PBTNF by incorporation of HA particles via the attachment of acrylic acid onto PBTNF by graft polymerization (Kim *et al*., 2009). They found that PBT-HA modified membranes had high leukocyte adhesion as well as high RBC recovery (Kim *et al*., 2009). Coating or covalent attachment of hydrophilic monomers or polymers synthesized from such monomers for modifying the membranes in order to alter the surface chemistry, surface charge, hydrophilicity, and WBC and platelet adhesions have been now widely accepted. Natori *et al* focused on the enhancement of platelet permeation by coating on PET non-woven filter membranes with amphiphilic copolymers synthesized from *n*-butylmethacrylate (BMA), *N*,*N*_-dimethylacrylamide (DMA), *N*-acryloylmorpholine (AMO), and *N*-vinylpyrrolidone (VP) (Natori and Kurita, 2007a; Natori and Kurita, 2007b; Natori *et al.,* 2006). These coated membranes exhibited enhanced platelet permeation. Membrane modification by acrylate and methacrylate based monomers and zwitterionic systems are another most commonly and successfully employed strategy (Yang *et al.,* 2011). In addition to these, modifications by immobilization of suitable biomolecules have also received attention.

Several researchers have investigated the effects of these modifications and are described below.

2.6.1. Modifications by acrylate and methacrylate systems

The monomers of acrylates and methacrylates as such or their polymers have been proven successful for the modification of leukodepletion filter membranes in order to achieve highly selective leukocyte removal with maximum retention of other components, especially platelets. It has been reported that the commercialized Sepacell-PL filter consists of PET nonwoven fibers coated with a copolymer of hydroxyethyl metachrylate (OHEMA) containing 5 % of diethylamonoethyl methacrylate (DEAEMA) (Dzik, 1993). Methacryloyloxyethylphosphorylcholine (MPC), also belonging to this class, has been used to modify filter membrane for preventing the high platelet adhesion (Iwasaki *et al.,* 2003; Lewis *et al*., 2000). 2-hydroxyethyl acrylate (HEA) is another widely used functional monomer for this purpose. Recently Yang *et al* modified the surface of PBTNF by UV graft polymerization of HEA and reported a very significant reduction in the platelet adhesion for the modified PBTNF (Yang *et al.,* 2011). HEA and its homopolymer, poly(hydroxyethyl acrylate) (PHEA), has been also shown to have other excellent biological properties including thermo-responsive and stimuli-responsive properties, low cytotoxicity and excellent hemocompatibility (Bian and Cunningham, 2005; McAllister *et al.,* 2002).

2.6.2. Modifications by zwitterionic systems

Functionalization imparting zwitterionic systems have proven most versatile and acquired much attention in past decade. The speciality of these zwitterionic systems is the presence of covalently linked cations and anions in the same unit. Belonging to this category, phosphorylcholines (PC), carboxybetaines (CB) and sulfobetaines (SB) have been successfully used to improve the hemocompatibility of various non-woven fabrics for blood contacting applications. A number of investigators have recommended that introduction of various zwitterionic moieties to various polymers effectively decreased the platelet adhesion to these surfaces (Ishihara *et al.*, 1990; Yuan *et al.*, 2003; Zhang *et al.*, 2003). Yang *et al* attempted to functionalize PBTNF by UV induced graft polymerization of a sulfobetaine, N-(3-sulfopropyl)-N-methacroyloxyethyl-N,N-dimethylammonium betaine (SMDB) (Yang *et al.,* 2011). The functionalization enhanced the overall hydrophilicity and wettability of PBTNF. The functionalization also enhanced the hemocompatibility of PBTNF and their platelet permeability (Yang *et al.,* 2011).

2.6.3. Modifications by biomolecule immobilizations

The immobilization of various biomolecules on membrane surfaces have been shown to alter the cell adhesion/retention or hemocompatibility of filter fabrics. Cao *et al* demonstrated that grafting of heparin onto PBTNF significantly enhanced the overall blood compatibility and altered the absorption capabilities of low density lipoprotein (LDL) and total cholesterol (TC) (Cao *et al.*, 2011). These modified fabrics could be used for selective depletion of LDL (Cao *et al.*, 2011). PBTNF was also functionalized by

attachment of a peptide Gly-Arg-Gly-Asp-Ser and Gly-Gly-Gly-Gly-Gly. These peptide modified non-wovens showed better leukodepletion efficiencies than the neat PBTNF (Gérard *et al.,* 2011). Immobilization of protein has also been an accepted strategy to reduce the platelet adhesion, aggregation and activation. As albumin has been identified as a protein which prevents the platelet adhesion, several attempts have been succeeded in modifying the membranes by albumin immobilization (De Queiroz *et al*., 1997; Weng *et al*., 2008; Zhang *et al*., 2013).

2.7. Poly (ethylene-co-vinyl alcohol) (EVAL)

Poly (ethylene-co-vinyl alcohol) (EVAL) is an important semi-crystalline, amphiphilic polymer widely used for various biomedical applications like periodontal ligament regeneration, scaffold for neural repair, wound dressing material etc. (Matsumura *et al*., 2004; Xu *et al*., 2011; Young *et al.,* 2001). In addition to these, EVAL is an excellent membrane material and have been commercially used as plasma separators under the name "Evacure-SC" (Sueoka, 1997). An earlier report of Sakurada *et al* recommends EVAL hollow fiber membranes for efficient hemodialysis (Sakurada *et al*., 1987). Similar studies revealed the capability of EVAL hollow fiber membranes as affinity membrane for purification and separation of proteins and bilirubin (Acconci *et al.,* 2000; Avramescu *et al*., 2004; Avramescu *et al.,* 2002; Bueno *et al*., 1996; Coffinier and Vijayalakshmi, 2004). Another interesting study by Acconci *et al* reported the use of histidine immobilized EVAL for the removal of endotoxin from snake antivenom (Acconci *et al.,* 2000). During these separations, it is in fact the hydrophobic and

hydrophilic segments present in EVAL which make them suitable for developing specific interactions with these biomolecules. Moreover, the excellent blood compatibility of EVAL membranes is also well known. Hence it is worth considering this polymer for fabrication of leukodepletion filters.

2.8. Polyacrylonitrile (PAN)

Polyacrylonitrile (PAN) is an attaractive engineering polymer which has a high thermal stability and resistivity to solvents, bacteria and radiation (Wang *et al*., 2007). Electrospun PAN matrices have also been identified as excellent membrane materials due to their high capture-efficiency for micro/nano particles (Nataraj *et al.*, 2012). A number of investigators have unveiled their potential as filtration media (Barhate *et al*., 2006; Li *et al*., 2007; Saufi and Ismail, 2002). It is also noteworthy that PAN hollow fiber membranes as well as poly(acrylonitrile-co-methallyl sulfonate) membranes have been used for hemodialysis (Jindal *et al.*, 1989; Klein, 1998). However, issues of high protein adsorption and fouling due to their hydrophobicity have been raised by various researchers. Hence several attempts have been executed to modify the PAN membranes to overcome these limitations. Che *et al* reported that the immobilization of heparin or insulin could enhance the hydrophilicity and hemocompatibility of PAN based membranes (Xu *et al.*, 2005). Covalent attachment of phospholipid moieties onto the various PAN derived membranes has been succeeded to enhance their hemocompatibility (Huang *et al.*, 2006; Huang *et al.*, 2005). Another interesting advantage for the PAN and PAN based membranes, the availability of surface functionality which supports further

derivatizations with desirable surface properties necessary for the concerned application, has made them a favorite membrane material (Chiang and Hu, 1990; Oh *et al.*, 2001).

2.9. Electrospinning-a feasible membrane fabrication method

Electrospinning, a fascinating fiber fabrication technique, has been widely used to generate polymeric fibroporous matrices for various applications (Ramakrishna *et al.*, 2005). Fibers are produced either from polymer melts or from polymer solutions, when the electric field overcomes the surface tension. The process is solely governed by a number of parameters like solution viscosity, conductivity, feed rate, collector composition etc. Spun fibers also offer several advantages such as an extremely high surface to volume ratio, tunable porosity, with the ability to control the nanofiber composition to achieve the desired results (Greiner and Wendorff, 2007; He *et al.*, 2008; Ramakrishna *et al.*, 2005). Such electrospun fibers have been widely used in the various fields of biomedical engineering like drug delivery, tissue engineering, wound dressing, biosensors, antifouling membranes etc (Agarwal *et al.*, 2008; Lee and Livingston Arinzeh, 2011; Namboodiri and Parameswaran, 2013; Nandakumar *et al*., 2010; Remya *et al.*, 2013; Sill and von Recum, 2008; Xu *et al*., 2011). Although the technique serves befit for the fabrication of polymeric porous membranes for leukodepletion filters, few report exist for a leukodepletion filter developed by electrospun polymeric fibers. Guo *et al* recently developed a newly designed leukodepletion filter out of poly(butylene terephthalate) (PBT) electrospun/melt-blown composite mats. A layer of electrospun PBT was assembled along with melt-blown PBT before the exit of the filter and their

performance evaluation resulted in reduced WBC adhesion inspite of the lower fiber and pore diameter of the electrospun fibers than the melt-blown fibers (Guo *et al.,* 2013). Hence it can be expected that the forthcoming studies will disclose the potential of this technique towards the fabrication of filter membranes effective for leukodepletion.

2.10. Limitations of the current systems

The benefits and drawbacks of the currently available leukodepletion filters have been reviewed in detail. It now becomes clear that the high platelet adhesion and moderate efficiency (for certain filters) in prevention of blood transfusion reactions are the serious limitations of the currently available membranes. In addition, the high cost of such filters renders the ULD to be a less practical routine to be implemented in developing countries including India.

To summarize, it can be estimated that significant progress has been made in the development of leukodepletion filters with adequate properties. However alternative membrane fabrication techniques like electrospinning and exploration of new blood compatible polymers has not yet been much explored by the investigators. In addition the various membrane modification approaches opens new pathways to developing excellent membrane materials which can overcome the limitations and thus replace the currently available filters. Hence the present work is an attempt to investigate the feasibility of electrospinning technology for developing leukodepletion filter fabrics out of blood compatible polymers, integrated with the appropriate membrane modification strategies to

tune the properties of the membranes ideally and efforts are being taken to achieve this goal.

CHAPTER 3

MATERIALS AND METHODS

In this study, efforts were made to (1) develop polymeric filter membranes for effective leukodepletion by electrospinning, (2) modify the electrospun filter membranes to enhance their hemocompatibility and (3) compare the leukodepletion efficiencies of the various modified filter membranes, thereby deducing the correlation between the material surface chemistry, wettability and leukodepletion efficiency.

The membranes were prepared by electrospinning of PAN and EVAL. Leukodepletion filters were developed out of these membranes and evaluated for their efficiency. Effect of fiber diameter, pore diameter and symmetricity on leukodepletion efficiency was also established. Later EVAL membranes were modified for enhancing their hemocompatibility by various approaches viz. photografting with HEA, incorporation of glycine, functionalization with SMDB and immobilization of BSA via dopamine. All the membrane systems were evaluated for their leukodepletion efficiencies. All experiments related to membrane fabrication are described in Section 3.1 while the modification approaches are described in Section 3.2. The development of prototype and leukodepletion filter is described in Section 3.3. The physico-chemical and mechanical property evaluation is detailed in Section 3.4. Biological evaluation of the developed membranes is described in Section 3.5.

3.1. Fabrication of leukodepletion filter membranes by electrospinning

3.1.1. Commercial reagents

Poly (ethylene-co-vinyl alcohol) (EVAL) with 44 mol % ethylene content (having melting point 191 °C and melt index 3.50 g/10 min), 2-hydroxyethyl acrylate (HEA), N-(3-sulfopropyl)-N-methacroyloxyethyl-N,N- dimethylammonium betaine (SMDB) and ninhydrin (2,2-dihydroxyindane-1,3-dione) were purchased from Sigma-Aldrich Chemical Company Inc., USA. Polyacrylonitrile was procured from Technorbital, India. Benzophenone (BP) extrapure crystals were supplied by Sisco Research Laboratories, India. 2-propanol (> 99.5 % priss, EL grade), N,N-dimethyl formamide (DMF) (puriss AR grade) and 1,1,1,3,3,3-hexaflouro-2-propanol (HFIP) was purchased from Spectrochem, India. Ethanol (99.9 %, AR grade) and glutaraldehyde solution (25 %, LR grade) were obtained from SD fine chemicals, India. Glycine (GR grade) was procured from Merck, Germany. Bovine serum albumin (BSA) and dopamine hydrochloride were obtained from Himedia, India. Acetone AR was procured from Rankem, India. The chemical structures of the polymers and monomers/molecules used for membrane modifications are provided in Figure 5. A commercial leukodepletion filter, Imuguard III RC was obtained from Terumo Corporation, Japan (Figure 6).

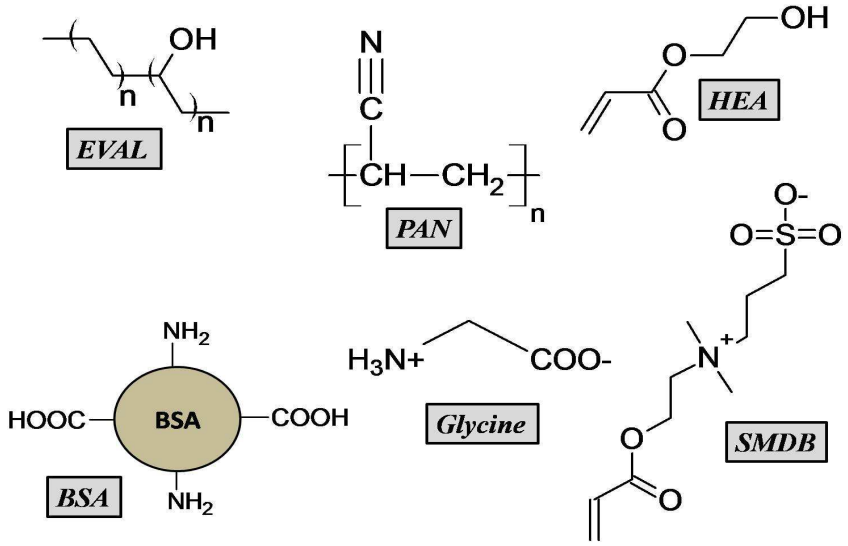

Figure 5. Structures of polymers and monomers used in the study

Figure 6. Control filter device Imuguard III RC

3.1.2. Preparation of reagents

The following reagents were freshly prepared and used according to the reported forthcoming procedures.

Name of the reagent	Concentration and diluent
Ninhydrin	0.2 % w/v in methanol
Sodium bicarbonate	0.1 M in distilled water
Glutaraldehyde	2.5 % in distilled water

Table 4. List of prepared reagents

3.1.3. Development of PAN membranes by electrospinning

10 w/v % solution of PAN was made by dissolving the required amount of PAN in DMF by overnight stirring at room temperature. The solution was then filled into a syringe supplied with blunt end needle of length 42 mm and internal diameter 1.2 mm, and mounted onto the syringe pump (Holmarc opto-mechatronics, Kochi, India). The solution was then electrospun at a rate of 1 mL/h. The spun fibers were collected onto a rotating mandrel placed at 13 cm apart from the tip of the needle. The needle gauge and the distance were constant for all the electrospinning carried out. The speed of the mandrel was set at 500 RPM and 1500 RPM in order to tune the pore properties of the membrane. A voltage of 8-9 kV (Gamma high voltage, USA) was applied to maintain the

stable jet of fibers. These parameters were also provided in Table 5. The deposited fibers were finally detached from the mandrel in the form of fibroporous membrane. The membranes were then dried at 40 °C in an air oven for the removal of residual solvent.

Polymer	Electrospinning parameters					
	Solvent	Concentration (w/v %)	Flow rate	Distance (cm)	Applied Voltage (kV)	Collection speed (RPM)
PAN	DMF	10	1 mL/h	13	8-9 kV	500
						1500
EVAL	2-propanol : water (70:30)	9	10 mL/h		11-12 kV	500
						1500
			1 mL/min		14-15 kV	500
						1500
	HFIP		1 mL/h		10-11 kV	500
						1500

Table 5. The parameters for electrospinning of various membranes

3.1.4. Development of EVAL membranes by electrospinning

EVAL was electrospun from both 2-propanol:water mixture and HFIP in order to tune the resulting membrane properties. Firstly, required weight of EVAL pellets were dissolved in 70:30 2-propanol:water mixture by vigorous stirring at 60 – 65 °C overnight to a concentration of 9 w/v %. This solution was electrospun at two different conditions. To be more specific, the flow rate was varied between 1 mL/min and 10 mL/h and, accordingly the applied voltage was also varied as provided in Table 5.

Since the flow rate cannot be reduced further below 10 mL/h using 2-propanol:water solvent mixture, EVAL was again electrospun from HFIP. The concentration of the EVAL in HFIP was 9 w/v % and the flow rate employed was 1 mL/h. Again, a voltage of 10-11 kV was required to stabilize the fiber jet. The electrospun fibers were collected onto the mandrel set at a speed of 500 RPM and 1500 RPM (Table 5).

3.2. Modifications on electrospun EVAL membranes

Electrospun EVAL membranes were subjected to various chemical modifications in order to enhance its hemocompatibility. Thus, various chemical functionalities were incorporated on the EVAL membrane in order to study the effect of these modifications on the performance of leukodepletion. Briefly, a modification by photografting of HEA was carried out to enhance the hydrophilicity of EVAL by incorporation of more –OH functionalities. Another modification was the introduction of zwitterion bearing chains. Two types of zwitterionic moieties were explored- (a) carboxylic acid derived zwitterions, glycine and (b) sulfobetaine, which is a sulfonic acid derived zwitterion, SMDB. Further approach for enhancing the hemocompatibility was carried out by immobilization of BSA via dopamine. The detailed methodology for these modifications is narrated below

3.2.1 Preparation of 2-Hydroxyethyl acrylate grafted poly(ethylene-co-vinyl alcohol) (PHEA-g-EVAL)

PHEA-g-EVAL matrices were prepared by photografting 2-hydroxyethyl acrylate monomer onto EVAL in the presence of BP as photoinitiator. A novel approach for grafting where the solution for electrospinning contained HEA monomer, BP and EVAL were adopted (Figure 7). At first polymer solution (9 w/v %) was prepared by dissolving EVAL pellets in 2-propanol:water mixture (70:30 v/v). Later HEA monomer and BP were added into the polymer solution and dissolved in it. The concentrations of monomer and BP taken were 10 % (v/v) and 4 % (w/v) respectively, of the polymer solution. Yang *et al* reported that optimum results were obtained when the initiator concentration was 4 % (w/v) (Yang *et al.,* 2011). So this concentration was fixed for the current work. The mixture was electrospun at a feed rate of 10 mL/h. A voltage of 12 kV was used for maintaining a constant and stable jet. The spun fibers were collected on a rotating mandrel set at a speed of 500 RPM located 13 cm away from the spinneret.

The fibroporous mat obtained was immediately UV treated to induce grafting. The mats were kept in a UV chamber provided with UV-A lamps (Toshiba FL15SBL, 350 nm, 15 W). Different UV exposure times ranging from 10 minutes to 60 minutes were given. The grafted fibroporous mats thus obtained were washed with acetone for 30 minutes followed by distilled water for 2 hours in order to remove any homopolymer formed, and the unreacted monomer and the initiator present in the mat. They were dried overnight at room temperature prior to oven drying at 50 °C. The grafted mats were designated as PHEA-g-EVAL and indicated with corresponding UV treatment time in

minutes for easy identification. The ‘zero’ minute UV treated EVAL stands for the neat EVAL in all the mentioned results.

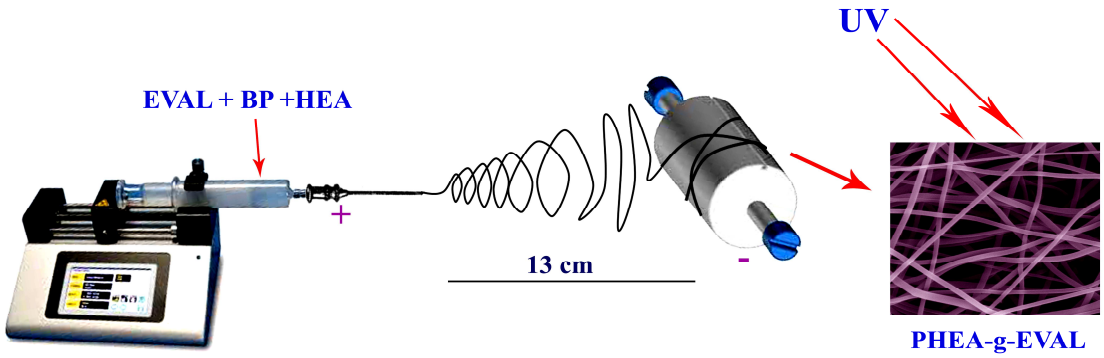

Figure 7. Preparation of PHEA-g-EVAL

3.2.2. Functionalization of EVAL by incorporation of glycine (EVAL-Gly)

Various concentrations of glycine viz. 1, 5 and 10 % (w/w to EVAL concentration) were directly dissolved in the EVAL solution. This mixture was electrospun at 10 mL/h at a voltage of 13 kV. The spun membranes were collected onto the mandrel rotating at a speed of 500 RPM. The membranes were completely dried at 50 °C in a vacuum oven. The glycine functionalized EVAL membranes were denoted as EVAL-Gly along with the corresponding concentration of glycine used for modification.

3.2.3. Functionalization of EVAL by photografting of SMDB (PSMDB-g-EVAL)

Similar to the above protocol in Section 3.2.1, the in-situ addition of the monomer SMDB and photoinitiator BP was followed to prepare PSMDB-g-EVAL electrospun mats (Yang *et al.*, 2011). A 9 % (w/v) of EVAL solution was prepared and to this solution, SMDB (10 % w/w of EVAL) and BP (4 % w/w of EVAL) were added and stirred to

dissolve. This solution was then electrospun at a flow rate of 10 mL/h using a spinneret of diameter of 1.2 mm. A voltage of 12 kV (Gamma High Voltage, USA) was needed for a smooth and continuous electrospinning. The spun fibers were collected onto a target set at 13 cm away from the spinneret rotating at a speed of 500 RPM. The obtained fibroporous membrane was directly UV treated for varying duration from 10 to 60 minutes, uniformly on both sides to induce grafting in a closed and isolated chamber fitted with UV lamps (Toshiba FL15SBL, 350 nm, 15 W). The grafted films were then washed with acetone and water to remove unreacted monomer and initiator. They were then dried under vacuum at 50 °C. The membranes were denoted as PSMDB-g-EVAL along with the UV irradiation time.

3.2.4. Immobilization of BSA via dopamine on EVAL membranes (EVAL-BSA)

Neat dried EVAL membranes, obtained by electrospinning of EVAL solution in 2-propanol:water mixture at a rate of 10 mL/h, were placed in 2 g/dL dopamine solution (10 mM in tris HCl) and incubated at 30 °C for 12 hours. During the term, the dopamine polymerizes to polydopamine (PD) particles and gets firmly attached to the EVAL resulting in black coloration to the EVAL membrane. This is also depicted in Figure 8. The PD coated EVAL membranes (EVAL- PD) thus obtained were thoroughly washed with distilled water by sonication for several times, replacing the water at each 30 minutes, for removing any unbound/loosely bound PD particles. Later the washed membranes were dried under vacuum at 50 °C. BSA solution was prepared at various concentrations 1, 2, 10, 50 and 100 g/dL by dissolving the desired amount of BSA crystals in PBS of pH 7.4. The dried membranes of EVAL-PD were immersed in the BSA

solution and incubated at 30 °C for 24 hours. Then the membranes were taken out and sonicated with distilled water to extract the unattached BSA. After washing, the obtained BSA immobilized EVAL membranes (EVAL-BSA) were dried in a vacuum oven at room temperature for 3 days. The various BSA immobilized EVAL membranes were denoted EVAL-BSA along with their corresponding BSA concentration.

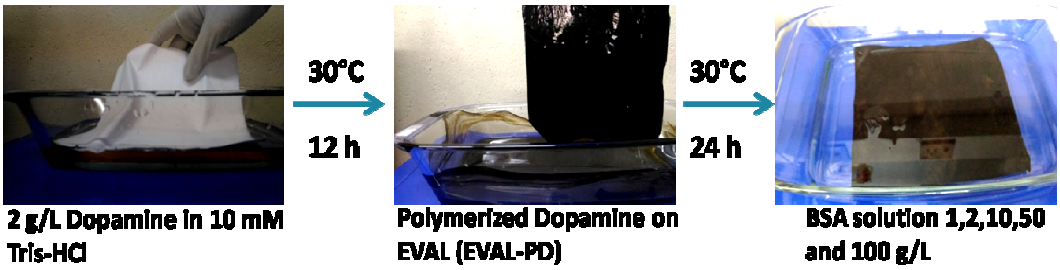

Figure 8. Immobilization of BSA on EVAL membrane via dopamine

3.3. Development of prototype and leukodepletion filter

Two different types of prototypes, namely prototype-A and prototype-B, of the leukodepletion filter was developed by machining of poly(methyl methacrylate) (PMMA) blocks into the desired specifications as detailed below.

Prototype-A was designed to employ for the typical whole blood filtration for assessing the leukodepletion efficiency of various modified and unmodified electrospun membranes. For this, the PMMA blocks were sculpted into a circular case having internal diameter 5 cm, internal cavity depth of 3 mm and provided with an inlet and outlet [Figure 9: (a) & (b)]. The inlet and outlet were retained for passing the whole blood for filtration and for collecting the filtered blood respectively.

The prototype-B was particularly engineered for screening of the various modified membranes prior to the whole blood filtration using prototype-A. For this purpose a circular chamber of diameter 4 cm was engraved in two equal PMMA blocks so that on the chamber depth is approximately 4 cm on closure of the two halves. Inlet and outlet were provided on the two halves respectively [Figure 9: (c)].

Leukodepletion filters were developed by stacking the electrospun membranes in the prototype-A in asymmetric and symmetric fashion. For designing the asymmetric filter, the membranes obtained at a collection rate of 500 RPM were placed as the top 4 layers and monolayer of membrane obtained at 1500 RPM is kept as the bottom layer just before the exit of the filter. But for the symmetric filter, all the 5 membranes were from the membranes obtained at a speed of 500 RPM.

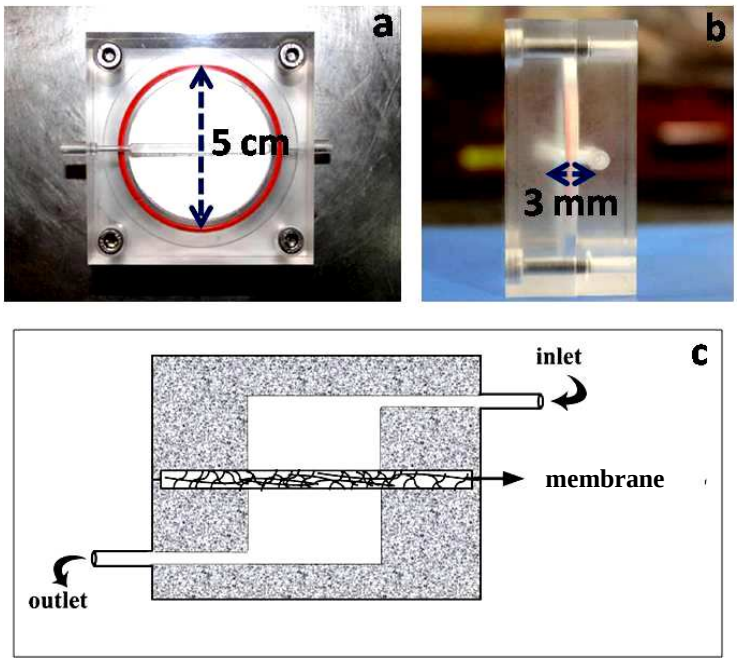

Figure 9. The developed prototype and leukodepletion filter; (a) prototype A top view, (b) prototype A lateral view and (c) schematic representation of prototype B.

3.4. Characterization and evaluation of the electrospun membranes

3.4.1. Structural characterization

Structural characterization of the neat and modified EVAL membranes were carried out using an ATR-FTIR spectrophotometer (Jasco, Model 6300, Japan) in the range of 4000-400 cm^{-1}.

3.4.2. Degree of grafting (DG)

The degree of grafting (DG) of HEA and SMDB grafted EVAL was estimated by gravimetric method. For the estimation of DG, a part of the electrospun mat, added with

the monomer and initiator, was cut before UV exposure and it was extracted to remove those additives. The extraction was done by immersing the mats in acetone and sonicating them for about 30 min. Later they were immersed in distilled water and sonicated for 2 h. The water was replaced with fresh distilled water at every 30 minutes intervals. The mats were then dried and weighed. The weight of this extracted mat was taken as W_1. Weight of grafted EVAL membrane was taken as W_2. DG was calculated using the equation given below:

$$DG\ (\%) = \frac{W_2 - W_1}{W_1} \times 100 \quad \ldots\ldots\ldots\ldots\ldots\ldots\ldots\ldots (1)$$

3.4.3. Morphological analysis

The morphology of the PAN, modified and neat EVAL electrospun membranes was investigated by scanning electron microscopy (SEM) (Hitachi model S-240, Japan) operated at 15 kV. Dried samples were mounted on aluminium stubs and sputter coated (Hitachi E101) prior to observation under SEM. The average fiber diameter was measured from the SEM images using ImageJ software.

The membranes after exposure to whole blood (WB) and platelet rich plasma (PRP) were fixed with 2.5 - 3 % glutaraldehyde followed by slow dehydration in ethanol-water mixture. Dehydration medium had the ethanol content varied from 30 to 100 %. The samples were then dried in a vacuum oven at 30 °C. Finally the samples were again gold coated and observed under SEM.

3.4.4. Pore characteristics

The pore characteristics of the electrospun membranes before and after modification were analyzed by studying the percentage porosity and pore diameter using ImageJ analysis. The SEM images of the respective membranes were converted to binary images using different thresholds. The porosity of the membrane was analyzed in different layers corresponding to these thresholds according to previously reported protocol (Ghasemi-Mobarakeh *et al.*, 2007). These porosity values for various layers were then averaged and reported as the overall porosity of the sample.

3.4.5. Surface wettability studies

The wetting characteristics of the neat and modified electrospun membranes were studied from their water contact angles (WCA) and critical wetting surface tension (CWST). The WCA were estimated with a goniometer equipped with a special optical system and a camera (Data Physics OCA 15 plus, Germany). A drop of water (5 μL) was placed on the electrospun fiber mat and the image was immediately taken at the very first point of contact between the water and the surface of the mat and sent via the camera to the computer and imaged using Imaging SCA20 software. CWST was determined by following previously established procedures (Lewis *et al*., 2000; Yang *et al.*, 2011). Briefly, a series of aqueous solutions of known surface tension were chosen in such a way that their surface tensions differ by 2-5 mN/m. A drop of each liquid was placed on the electrospun mat and visually observed it for 5 minutes. If the drop spreads on the mat it was considered as a wetting liquid and if it does not spread on the mat, it was taken as a

non-wetting liquid. CWST was taken as the average value of the surface tensions of liquids that sat at the boundary between wetting and non-wetting liquids. The set of aqueous solutions used are listed in the Table 6.

Aqueous solution	Surface Tension (mN/m)
43.2 wt % CH_3COOH	38.4
26.5 wt % CH_3COOH	43.7
26.5 wt % CH_3COOH	47.2
10.8 wt % CH_3COOH	52.5
7.2 wt % CH_3COOH	56.5
4 wt % CH_3COOH	60.4
2.5 wt % CH_3COOH	63.1
0.5 wt % CH_3COOH	67.3
0.1 M $CaCl_2$	70.4
1.7 M $CaCl_2$	74.2
2.7 M $CaCl_2$	78.3
24.7 M NaCl	81.5
27.3 M NaCl	83.5
33.3 M $CaCl_2$	86.4
35.7 M $CaCl_2$	88.0

Table 6. Aqueous solutions selected for critical water surface tension (CWST) studies and their surface tension values.

3.4.6. Mechanical properties

The static mechanical properties of neat and HEA grafted EVAL were evaluated on a Universal Testing Machine (Instron, model 3345) attached with 10 N load cell. Micro dumbbell samples having 2 mm width in the narrow portion and 15 mm length were punched out from neat and grafted electrospun EVAL mats using a cutting die.

Mechanical testing was carried out at 25 °C with a cross-head speed of 10 mm/min. The dynamic mechanical properties of electrospun mats were studied using a dynamic mechanical analyzer (Tritec 2000 DMA, Triton technology limited, UK) at a frequency of 1 Hz. The test was conducted in a tension mode at a heating rate of 1 °C/min. The test temperatures ranged from room temperature to 150 °C. The modulus and damping properties of the grafted and neat EVAL were recorded as a function of temperature.

3.4.7. *In vitro* release study of glycine

The release of glycine from the loaded EVAL membranes (EVAL-Gly) was analyzed by the UV-visible spectrophotometric method. EVAL-Gly discs of dimensions 8 mm x 0.4 mm were placed in Eppendorf tubes containing 2 mL PBS (pH=7.4). Release studies were carried out using a shaking incubator (50 RPM at 37^{o}C). At certain intervals, 500 µL of the released medium was aliquoted out and replaced with fresh buffer. This released medium was transferred to a 10 mL standard flask and mixed with 0.5 mL of sodium bicarbonate and 2.5 mL ninhydrin reagent. The mixture was heated in a water bath at 90 ± 5 °C for 20 min. Then the flasks were cooled to room temperature and subsequently, the volume was made up to the mark with distilled water. The absorbance of this solution at 568 nm was read by a UV-visible spectrophotometer (Shimadzu) (Colson, 2010). The released glycine was quantitatively estimated from the calibration curve constructed using glycine by the same method. The cumulative release of glycine was calculated using the standard plot. The experiments were carried out in triplicates and reported as average values.

3.4.8. Histological analysis of the filter membranes

After the whole blood filtration studies, the filter membranes were taken out and one half of the segment was subjected to histology analysis. Small pieces (10 mm × 2 mm × 3 mm) (l×b×h) of filter membrane were cut, removed and stapled in such a manner that would prevent the separation of different layers of membrane during processing. They were processed routinely in an automatic tissue processor (ASP300, Leica, GmbH) and embedded in paraffin. A 5 micron thin sections were cut using a rotary microtome (RM2255, Leica, GmbH) and stained with Haematoxylene and Eosin (H&E) using an autostainer (Leica, GmbH). Sections were visualised using a bright field microscope (Axioimager Z1, Carl Zeiss, GmbH) and digital images were captured at low and high magnification from top, middle and bottom layers of filter membrane using the camera AutoXL (MRc,Carl Zeiss, GmbH) attached to the microscope.

3.5. Biological Evaluation

3.5.1. *In vitro* cytotoxicity by direct contact assay

An *in vitro* cytotoxicity test using direct contact method was performed using the electrospun membranes as per ISO 10993-part 5 standard with L929 cell lines. 4 mm discs of electrospun EVAL membranes were thoroughly washed with distilled water and dried completely in a vacuum oven. These samples sterilized by ethylene oxide gas, negative controls (HDPE) and positive controls (tin compound stabilized PVC) in triplicate were placed on the cells. After incubation at 37 ± 1 ºC for 24-26 hours, cell monolayers were examined microscopically using optical microscope and Leica

Application Suit software (Leica, DMIRB, Germany) for the response around the samples and the controls.

3.5.2. *In vitro* hemocompatibility evaluation

The hemocompatibility evaluation of the various electrospun membranes was performed to assess the safety of the electrospun membranes towards the application and the tests were done according to ISO 10993 standard part 4. The following test were carried out on electrospun membranes - *in vitro* hemolysis assay, plasma protein adsorption assay, *in vitro* RBC aggregation assay, platelet adhesion studies, coagulation assay, complement activation and blood cell consumption studies. Since the modifications of PAN membranes were not taken into consideration, its hemocompatibility evaluation was assessed exclusively by the *in vitro* hemolysis assay. Moreover, some tests, mentioned above, viz *in vitro* RBC aggregation assay, coagulation assay and complement activation were done selectively for PHEA-g-EVAL membranes only. All the above mentioned tests were done using human samples as per the ethical guidelines and the study was approved by the Institutional Ethics Committee (IEC) of Sree Chitra Tirunal Institute for Medical Sciences and Technology (Approval no.: SCT/IEC/594/2014 dated 21/04/2014).

3.5.2.1. In vitro hemolysis assay

The *in vitro* hemolysis was studied in order to assess the safety of the membranes. The procedure involves quantifying the hemoglobin content, as a result of lysis of RBCs. Blood from human volunteer was collected into the anticoagulant, citrate-phosphate-

dextrose-adenine (CPD-A). The total hemoglobin in the whole blood was analyzed by Haematology Analyzer (Sysmex-K 4500, Japan). Samples, 4 mm discs in triplicate thoroughly washed and dried, were immersed in PBS for 5 minutes in polystyrene petri dishes before exposing to blood. A 1 mL blood was then added to the samples and incubated for 30 minutes under agitation at 70 ± 5 RPM using an Environ shaker thermostated at 35 ± 2 °C. Four empty polystyrene culture dishes were exposed with blood as reference. The free hemoglobin liberated into the plasma after exposure to samples was measured using Diode array spectrophotometer according to the protocol reported in ISO 10993: Part 4 and percentage hemolysis was calculated using the formula,

Hemolysis (%) = (Free Hb/Total Hb) X 100…….(2)

3.5.2.2. Plasma protein adsorption assay

Human blood from a voluntary donor was freshly collected into anticoagulant Citrate Phosphate Dextrose-Adenine (CPD-A). Plasma was separated from blood following established procedure (Thankam and Muthu, 2014). It was then diluted to a final concentration of 10 % by adding PBS. Neat and modified EVAL membranes cut into 8 mm discs, washed thoroughly and dried, were incubated at 37 ± 2 °C with 1 mL diluted plasma kept in a polystyrene well plate for 30 minutes. After the incubation, the samples were removed and the protein content in plasma fraction left was estimated by Lowry's method (Olson and Markwell, 2007). The percentage protein adsorption was calculated from the remaining protein fraction and the total protein content from the calibration curve with BSA standard.

3.5.2.3. In vitro RBC aggregation assay

For *in vitro* RBC aggregation studies, the collected anticoagulated blood was diluted 10 times with sterile 0.9 % saline. The grafted and neat EVAL membranes were extracted with PBS for 48 hours. A 100 µL of this extract was mixed with 100 µL of diluted RBC and the mixture was incubated at 37 ± 2 °C for 30 minutes. The cells were examined microscopically for aggregation. Following was the rationale behind mixing equal quantities of the extract and diluted RBC: if the volume of the extract is higher than that of RBC, RBC gets diluted and the RBC available for aggregation would be limited. In such cases if the extract caused aggregation, due to the poor availability of RBC, the aggregation may not be observed. On the other hand, if the volume of the extract is less than that of the RBC, population of RBC becomes high and it becomes difficult to distinguish between the 'true aggregation' and 'clustered RBC population'. For the sake of comparison, positive and negative controls were also used (Thankam and Muthu, 2014).

3.5.2.4. Platelet adhesion studies

The platelet-rich plasma (PRP) and platelet-poor plasma (PPP) were prepared according to the procedure reported elsewhere (Thankam and Muthu, 2014). The platelet count in the PRP was maintained with PPP. Samples were placed in PRP and incubated at room temperature for 30 minutes. After the exposure period, the samples were removed and the platelet count in the remaining PRP was noted. The ratio of platelets consumed

(%) by the materials were calculated from the initial counts and counts after exposure. The following formula was used for calculation:

$$\text{Consumption ratio } (\%) = \frac{\text{initial count} - \text{count after contact}}{\text{initial count}} \times 100 \text{.....(3)}$$

Samples were then washed with PBS and the adhered platelets were fixed with 2.5-3 % glutaraldehyde followed by slow dehydration in ethanol-water mixture. Dehydration medium had the ethanol content varied from 30 to 100 %. The samples were then dried in a vacuum oven at 30 °C. Finally the samples were gold coated and observed under SEM.

3.5.2.5. Coagulation assay

The blood coagulation assay was carried out to understand the effect of materials on the activation of clotting factor cascade. Tests were done in order to evaluate the extrinsic coagulation pathway by partial thromboplastin time (PTT) analysis and estimating the level of plasma fibrinogen, which is the major coagulation protein in blood. For these tests, the samples were placed in PRP and kept for agitation at 75 ± 5 °C in an incubator at 37 °C for 30 minutes. Aliquots were collected before and after the exposure period and analyzed by the following tests:

3.5.2.5.1. PTT analysis

PTT was determined by the plasma recalcification method using the CK PREST assay kit (Diaganostica Stago). 50 µL of PRP collected before and after the exposure with samples, were placed in the pre-warmed strip of cuvettes. A 50 µL of PTT reagent

(without kaolin) was then added to these cuvettes and incubated for 3 minutes at 37 °C. After the incubation time, 50 µL of 0.025 M $CaCl_2$ was dispensed into each cuvette and clotting times were determined by the Start 4 semi-automated coagulation analyzer (Diaganostica Stago) according to the manufacturer's instructions. The percentage change in the PTT after exposure was calculated from the PTT values obtained before and after exposure. For calibration purposes, unicalibration was used and internal control was used as a quality control on each day of testing.

3.5.2.5.2. Fibrinogen estimation

To identify the level of fibrinogen, clotting assay (Clark' method) was performed with PRP, collected before and after exposure to the materials, using the reagent Fibriprest on Start 4 semi-automated coagulation analyzer (Diaganostica Stago) according to the manufacturer's instructions. The percentage change in the expression of fibrinogen as a result of PRP exposure to materials was then calculated. Equipment calibration was done using unicalibrator and internal control was used as a quality control on each day of testing.

3.5.2.6. Evaluation of complement activation

In order to assess the complement activation induced by the membranes, the complement protein C3 was analyzed by quantifying the anaphylotoxin peptide C3a, formed as a result of C3 cleavage, using commercial C3a ELISA kit (Enzyme linked immuno-sorbent assay) from MicruoVue C3a Plus. Briefly, PRP was prepared according to the procedure mentioned in the previous section. The complement activation was

performed on selected samples only. The samples were exposed to PRP and incubated at 37 °C for 30 minutes at 70 ± 5 RPM. 100 µL aliquots of PRP were taken from each sample before and after exposure and diluted using the diluents provided in the kit. A 100 µL of this diluted PRP was then added to the microtitre plates which are pre-coated with specific monoclonal antibody for human C3a. The plates were then incubated for 1 h at room temperature so that the C3a present in the plasma binds to the antibody. The unbound C3a was then removed by washing the plates with the wash solution provided in the kit according to manufacturer's instructions. The plates were again incubated for 1 hour after adding 100 µL of the conjugate. After washing these plates with wash solution, 100 µL of the substrate solution was added and incubated for 15 minutes at room temperature. The reaction was then arrested by adding the stop solution in the kit and the absorbance at 450 nm was measured by ELISA reader (i Mark, Biorad). Concentration of C3a was estimated from the standard curve using MPM6 software. The obtained results were expressed in terms of percentage change calculated from the C3a measured before and after exposure.

3.5.2.7. Blood cell consumption studies

In advance to the whole blood filtration, it is necessary to study the interaction of the electrospun membranes with blood cells. For this, the neat and modified EVAL electrospun membranes were enclosed in the central position of the custom-made prototype-B in such a way that the membrane separates the interior cavity of the prototype into two chambers. Blood from human volunteer, collected into the anticoagulant CPD-A, was added to the upper chamber above the membrane. The whole

assembly was kept undisturbed for 30 minutes for the interaction of blood cells with the material. Afterwards, the blood was taken by a mild suction through the valve provided in the bottom chamber. The total count of WBCs, RBCs and platelets were analyzed before and after exposure with membrane using Haematology analyzer. The percentage adhesion of WBCs, RBCs and platelets were quantified by the formula,

$$\text{Adhesion (\%)} = \frac{\text{Initial count} - \text{Count after exposure}}{\text{Initial count}} \times 100 \quad \text{.....(4)}$$

3.5.3. Whole blood filtration studies

The filter devices were equilibrated with PBS by means of connected tubes to repel air and to wet the membrane surface prior to the blood filtration. Blood from human volunteer was collected into a bag added with the anticoagulant CPD-A. Study was approved by the IEC of SCTIMST and was carried out as per the ethical guidelines. The filter device was connected to the bag through the inlet and the bag was hanged at a height of 2 m from the floor. Blood was then allowed to pass through the EVAL filter under the effect of gravity. A 20 mL blood was used for each filtration. The filtered blood was collected through the outlet. The RBC, WBC and platelet count was analyzed before and after each filtration using Haematology analyzer. The adhesion of WBC, RBC and platelets were quantified by adhesion ratio, defined above.

The control filter was also evaluated by the same method. All the filtrations were performed with 6 replicates at room temperature. The neat EVAL membranes were evaluated through symmetric and asymmetric type and the performances of both were

compared. However, for all the other membranes, including the various modified EVAL membranes and the PAN membranes was evaluated by the asymmetric filter only. The speed of filtration was estimated from the time taken for filtration with respect to the volume of blood filtered. After filtration, the EVAL membrane assembly was separated from the device and further studied by SEM and histology.

3.6. Statistical Analysis

Data of all non-biological studies presented in this work were the mean of 6 samples. All the biological studies, except the whole blood filtration, were done in triplicate. Data is reported as mean ± SD. Statistical analysis was performed with one way ANOVA using Microsoft excel 2007 version. The values for which $p<0.05$ were considered as statistically significant. The number of tests for each parameter is indicated in the respective figure legends.

CHAPTER 4

RESULTS

Chapter 4 contains the results of the current study. It is divided into three subsections. The first section details the fabrication of EVAL and PAN membranes by optimized electrospinning parameters, their characterization and assessment of leukodepletion efficiency. The second section discusses the various modifications, characterization and evaluation of leukodepletion efficiencies of the modified EVAL membranes. The third section describes the comparative evaluation of the various modified EVAL filters and deriving the correlation between surface chemistry, wettability and leukodepletion efficiency of the filters.

4.1. Fabrication characterization and evaluation of leukodepletion efficiency of electrospun membranes

The main objective of this section is to discuss the fabrication of electrospun membranes by electrospinning of PAN and EVAL. Symmetric and asymmetric filters were designed out of these membranes and their leukodepletion efficiencies were compared.

4.1.1. Fabrication of filter membranes of EVAL and PAN by electrospinning

The straightforward technique of electrospinning reforms any polymers into continuous fibers. The feasibility of the technique and production of nano/micro scale

fibers with tunable properties have made this technique a most popular one. Here filter membranes were fabricated through the process of electrospinning. EVAL has been electrospun from its solution in 70/30 2-propanol/water mixture as well as from HFIP. The chosen concentration of 9 % gave rise to smooth fibers at each flow rate (1 mL/h, 10 mL/h and 1 mL/min) and collected onto a rotating mandrel. PAN membranes were obtained by electrospinning its solution in DMF. However, clogging at the tip of the needle was observed on all occasions during the electrospinning of EVAL. The PAN electrospun membranes seemed slight yellowish in color and tenuous. The speed of the collector was set at 500 RPM and 1500 RPM in order to generate membranes with different porosities. Consequently the spun membrane at 1500 RPM might be composed of more packed fibers with lower porosity than the same at 500 RPM.

4.1.2. Characterization of the filter membranes

4.1.2. 1. Morphological analysis

The morphological features of the electrospun membranes were inspected by SEM analysis and the respective images are presented in Figure 10. Subsequent image analysis described the membrane parameters and these data are compiled in Table 7. It can be seen that varying the spinning solvent from 2-propanol : water to HFIP did not alter the unwrinkled morphology of the EVAL fibers. However, the changes in the flow rate significantly affected the membrane properties. Very small fibers of average diameter 0.7 ± 0.1µm were obtained when EVAL was electrospun from its solution in HFIP at a rate of 1 mL/h (Table 7). The lowest pore diameter was also recorded for this system. The fiber

diameter was almost doubled when EVAL was electrospun form 2-propanol : water mixture at the flow rate of 10 mL/h (Table 7). Very high flow rate of 1 mL/min was also implemented to further expand the size of the EVAL fibers in the membrane. It was noticed that such a high flow rate resulted in the dropping of minor volume of EVAL solution, even at a voltage of 14 kV. The PAN fibers were fine and the diameter was found to be 1.4 ± 0.2 µm at 500 RPM. In addition, the pore diameter of the PAN membranes seemed more or less similar to that of the EVAL membrane electrospun at a rate of 1 mL/h and 10 mL/h (Table 7). Interestingly, altering the collector speed at specified flow parameters had little change on the fiber diameter for all the electrospun system. Fibers experience a hauling effect as a result of the increment in the collector speed from 500 RPM to 1500 RPM and consequently reduced the pore diameter. This variation in the pore size with reference to the change in the collector speed manifests the proposed asymmetry in the filer devices.

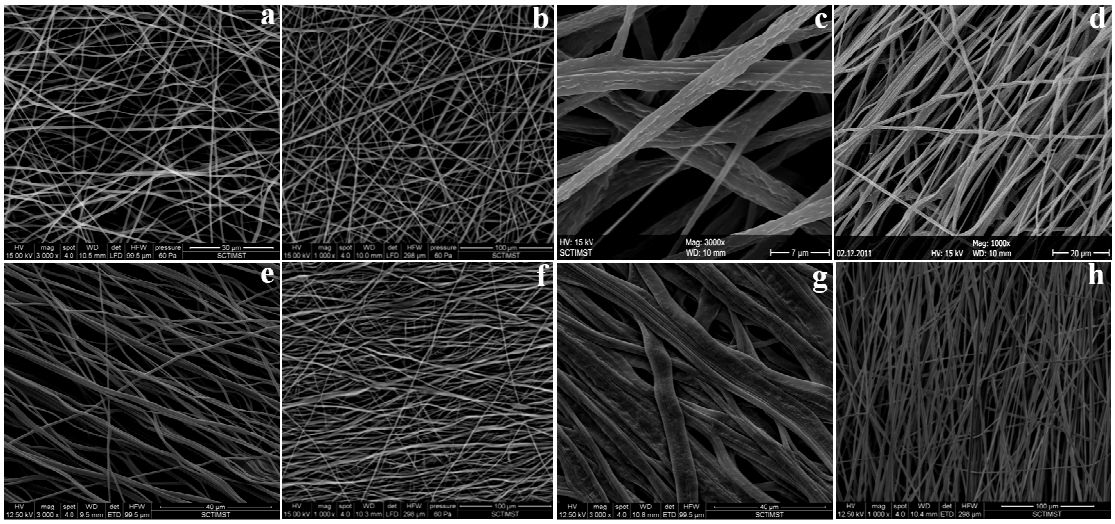

Figure 10. SEM images of membranes electrospun at various conditions (a) EVAL-1 mL/h-500 RPM; (b) EVAL-10 mL/h-500 RPM; (c) EVAL-1 mL/min-500 RPM; (d) PAN-1 mL/h-500 RPM; (e) EVAL-1 mL/h-1500 RPM; (f) EVAL-10 mL/h-1500 RPM; (g) EVAL-1 mL/min-1500 RPM; (h) PAN-1 mL/h-1500 RPM

Membrane	Fiber diameter (µm)	Pore diameter (µm)	Porosity (%)
EVAL-1 mL/h-500 RPM	0.7 ± 0.1	18.0± 3	53 ± 0.9
EVAL-10 mL/h-500 RPM	1.8 ± 0.1	23.3 ± 5	51 ± 1
EVAL-1 mL/min-500 RPM	3.0 ± 0.5	29 ± 4	51 ± 0.4
PAN-1 mL/h-500 RPM	1.4 ± 0.2	16 ± 4	50 ± 0.6
EVAL-1 mL/h-1500 RPM	0.7 ± 0.2	9 ± 3	53 ± 0.9
EVAL-10 mL/h-1500 RPM	1.7 ± 0.2	13 ± 3	51 ± 0.4
EVAL-1 mL/min-1500 RPM	4.0 ± 0.8	14 ± 3	52 ± 0.5
PAN-1 mL/h-1500 RPM	1.5 ± 0.2	9 ±2	50 ± 0.6

Table 7. Properties of the electrospun EVAL and PAN membranes

4.1.2. 2. Analysis of porosity

The porosity of the membranes were estimated by image analysis of the SEM pictures and reported as average percentage porosity in Table 7. The porosities of all the membranes were more or less equal and not significantly affected by the collection speed.

4.1.2.3. Water contact angle measurements

The wettability of membranes is of great interest when they are to be used as membrane materials for any kind of filtration. The wetting characteristics of the electrospun EVAL and PAN membranes were well established by their water contact angle measurements and the images are provided in Figure 11. Both the membranes appeared to be hydrophobic in nature, according to a contact angle of 126 ± 6 ° and 113 ± 2 ° with water for EVAL and PAN membranes respectively.

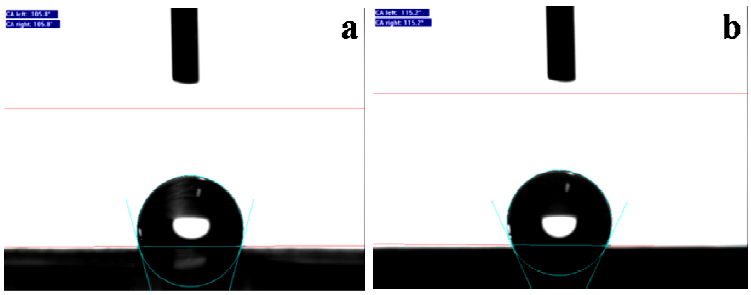

Figure 11. Water contact angles of (a) EVAL membrane and (b) PAN membranes

4.1.2.4. *In vitro* cytotoxicity assay

The toxicity of the electrospun EVAL and PAN membranes is qualitatively assessed by *in vitro* cytotoxicity assay. Representative microscopic images are shown in

Figure 12. The images reveal a good cell attachment and spreading upon the spun membranes. Cells were denser on negative control while the positive control indicated severe cytotoxic effect. No vacuolization, cell detachment or membrane disintegration was detected around the electrospun samples indicating their non-cytotoxic nature.

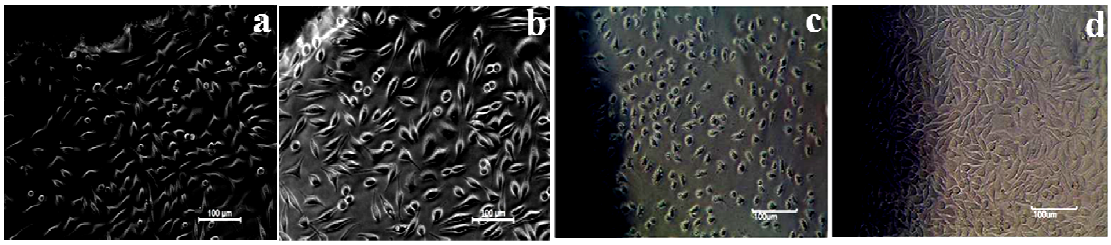

Figure 12. Microscopic images of L929 cells grown on (a) electrospun EVAL membrane, (b) electrospun PAN membrane, (c) positive control and (d) negative control by direct contact test

4.1.2.5. *In vitro* hemolysis assay

The preliminary evaluation of hemolysis is pre-requisite to assure the safety of both the electrospun membranes prior to being used as device. Data showed that EVAL and PAN membrane does not induce lysis to the exposed blood (Table 8). Percentage lysis obtained for both the membranes were well under the acceptable range of 5 %.

Membrane	Hemolysis (%)
EVAL	0.033 ± 0.005
PAN	0.090 ± 0.05

Table 8. *In vitro* hemolysis of electrospun EVAL and PAN membranes

4.1.2.6. Evaluation of efficiency of leukodepletion

Blood was filtered through the developed PAN filter and various EVAL filters under the effect of gravity. Firstly, the efficiency of EVAL asymmetric filter, composed of fibers with diameter 1.8 µm was compared with that of asymmetric PAN filter and that of the control. Further, symmetric and asymmetric filter were composed out of fibers of size 1.8 µm were compared. Finally, the performances of EVAL asymmetric filters with membranes of varying fiber size were also compared.

Continuous blood flow was observed through all the filters. Figure 13 shows the leukodepletion filter device and membrane assembly after whole blood filtration. The cell adhesion ratio calculated from the cell counts are provided in Figure 14. Electrospun EVAL asymmetric filter could remove 100 ± 0 % leukocytes, 8.19 ± 4.8 % RBCs and 91.0 ± 8.2 % of the platelets. PAN asymmetric removed 17.5 ± 13.1 % leukocytes, 3.3 ± 3.5 % RBCs and 28.9 ± 7.8 % platelets. However, the control filter Imuguard could remove 100 ± 0.01 % of leukocytes, 31.4 ± 17 % of RBCs and 98.5 ± 1.3 % of platelets [Figure 14 (a)]. The filtration speed was about 0.032 ± 0.008 mL/s for the EVAL filter, 0.029 ± 0.019 mL/s for the PAN filter and 0.042 ± 0.005 mL/s for the Imuguard [Figure 14 (b)]. The percentage hemolysis induced after the filtration by these filters was within the acceptable level [Figure 14 (c)].

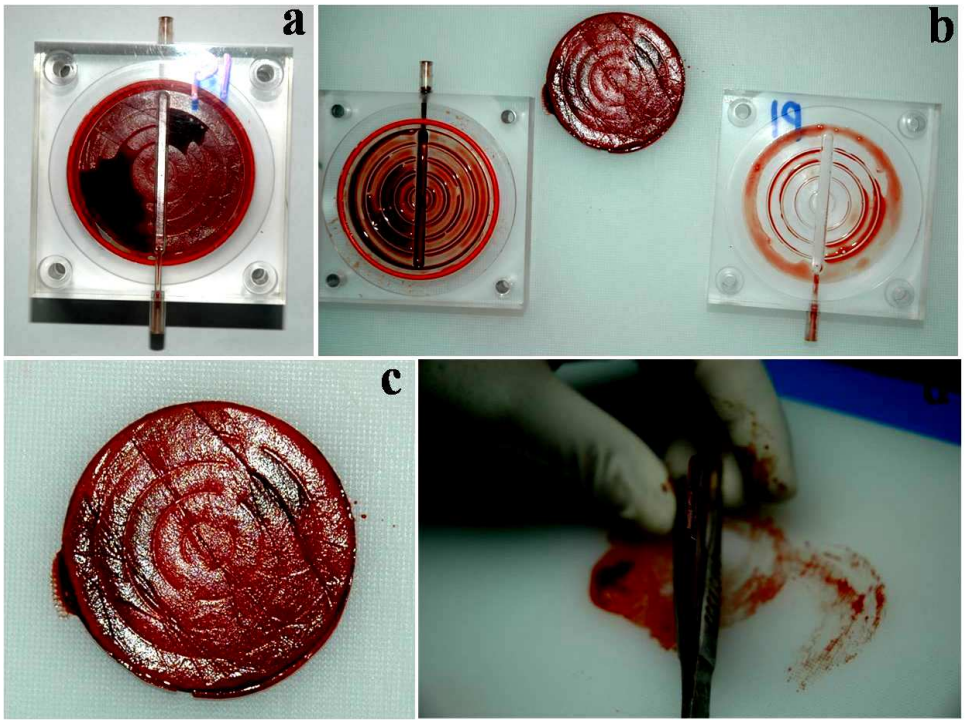

Figure 13: Leukodepletion filter device after whole blood filtration; (a) filter assembled, (b) filter device separated, (c) membrane assembly top view and (d) membrane assembly lateral view

The visualization of adhered platelet and leukocyte population on the electrospun EVAL and PAN layers were done by the SEM analysis of top, middle and bottom layers of the device (Figure 15 and Figure 17) and histological study of the stained cross sections of the filter assembly (Figure 16 and Figure 18). The leukocytes and platelets were trapped on all layers of EVAL filter according to the histology and SEM pictures. The leukocytes were even widely spread throughout reflecting a good interaction with the electrospun EVAL membrane (Figure 15). However, from Figure 17, it can be inferred that cells present on the PAN filter was comparatively lesser than that on the EVAL filter

in accordance with the quantitative data given in Figure 14. High populations of RBCs were also visible throughout the layers of PAN filter in the microscopic images provided in Figure 18.

From these observations, since the PAN filter was found to have very poor leukodepletion efficiency, it was ruled out and further studies were carried out with EVAL membranes only.

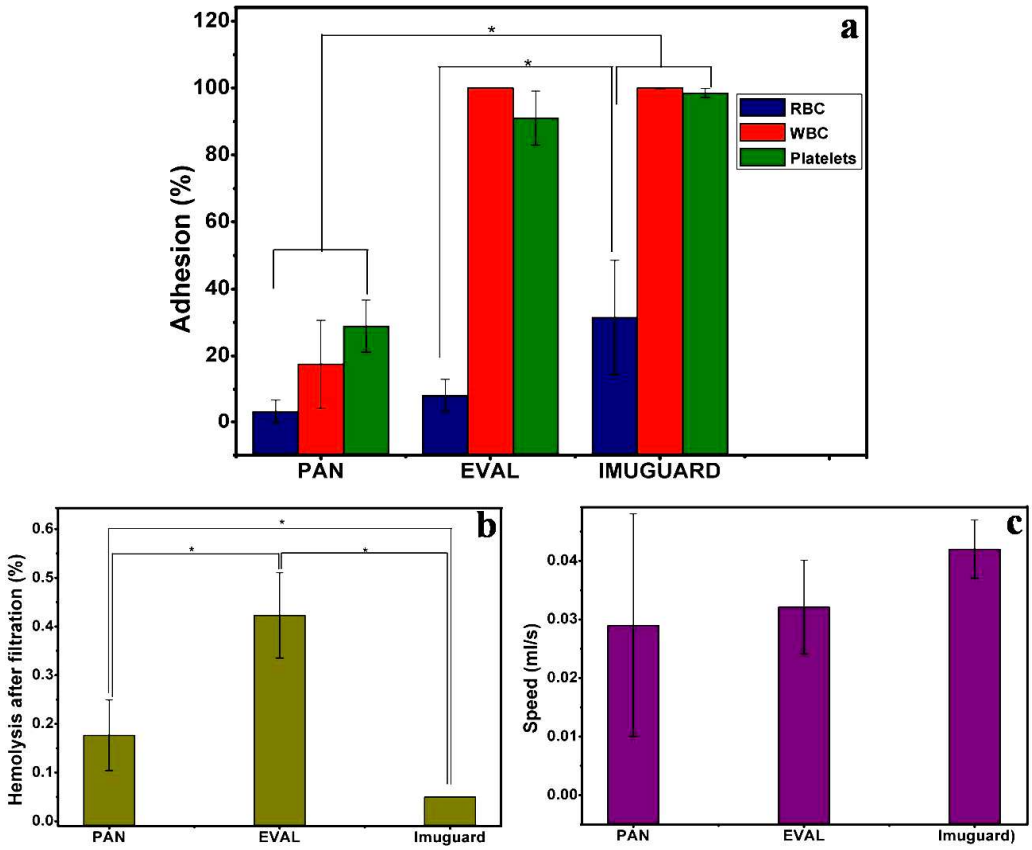

Figure 14: Evaluation of leukodepletion efficiency of electrospun membranes; (a) cell adhesion, (b) hemolysis and (c) speed of filtration

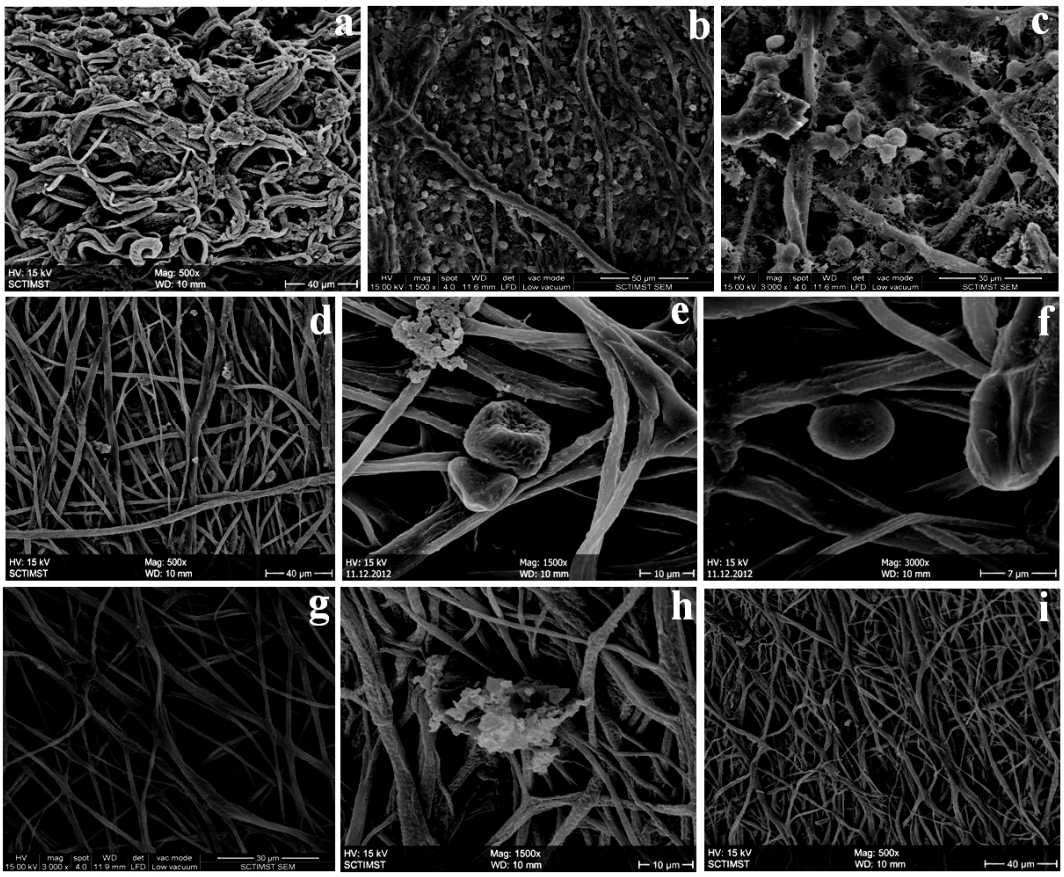

Figure 15. SEM analysis of adhered cells to the EVAL filter (a-c) top layer, (d-f) middle layer and (g-i) bottom layer at different magnifications.

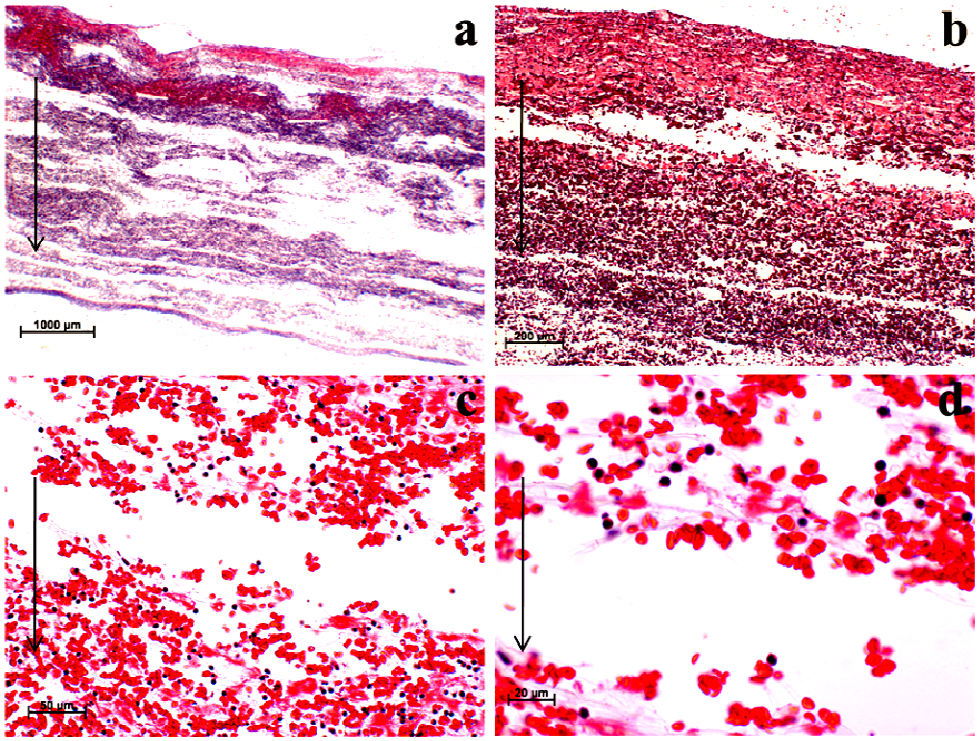

Figure 16. Histological examination of stained cross sections (from top to bottom) of EVAL filter membrane assembly. The arrow indicates the direction of blood flow

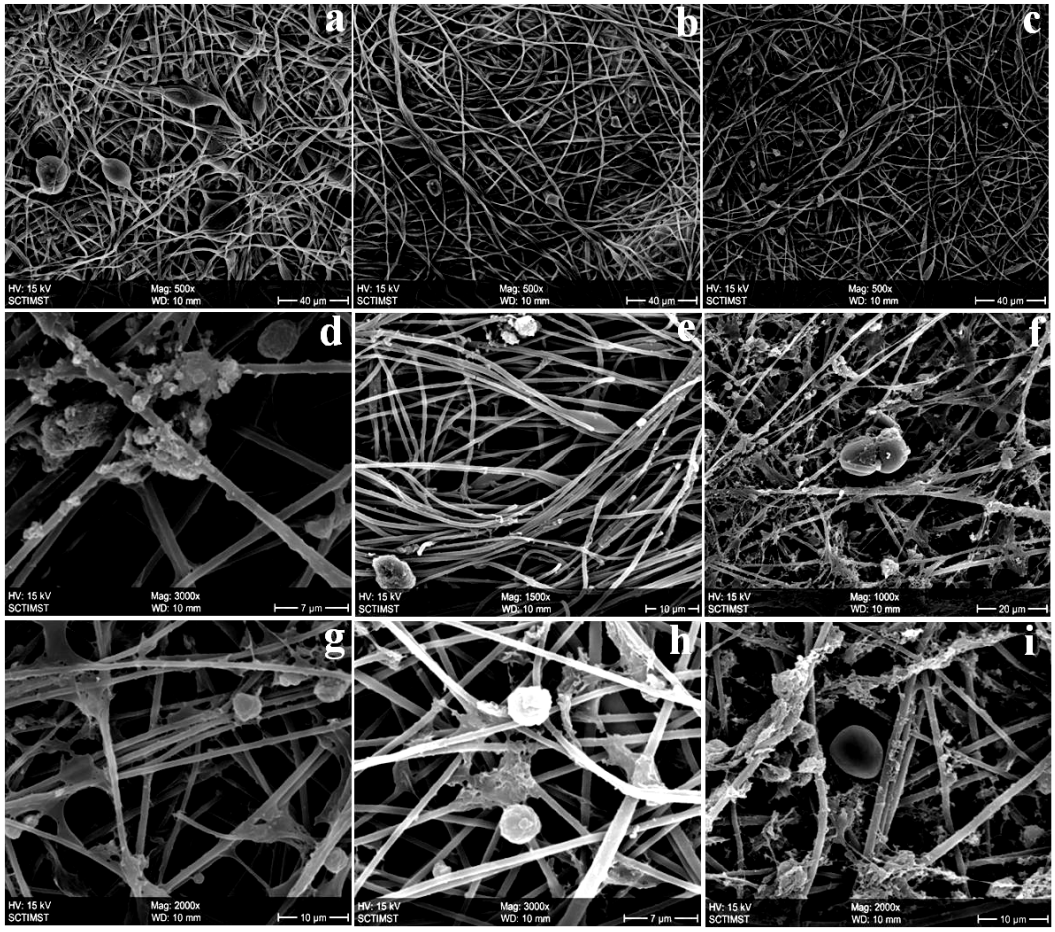

Figure 17. SEM analysis of adhered cells to the PAN filter (a-c) top layer, (d-f) middle layer and (g-i) bottom layer at different magnifications

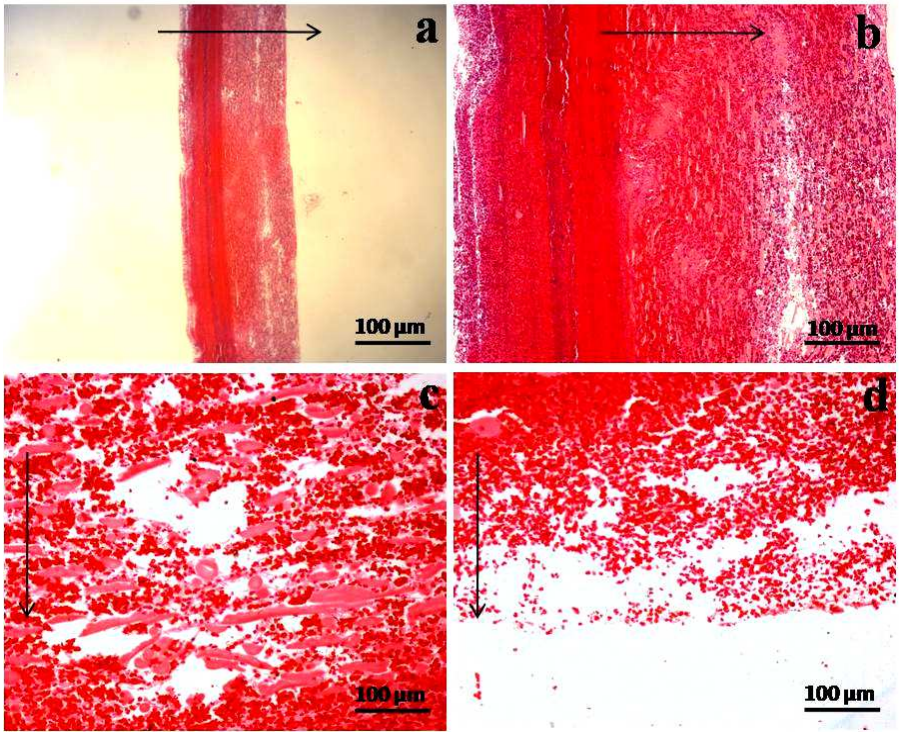

Figure 18. Histological examinations of stained cross sections (from top to bottom) of PAN filter membrane assembly. The arrow indicates the direction of blood flow

The performance of symmetric EVAL filter (EVAL-S) were also compared with the asymmetric EVAL filter (EVAL-AS) and the results were as follows. EVAL-S filter could remove 91 ± 11 % leukocytes, 22 ± 12 % of RBCs and 93 ± 8 % of platelets [Figure 19 (a)]. The percentage hemolysis induced by EVAL was negligible below the acceptable level and the speed of filtration was more or less similar to that of EVAL-AS filter [Figure 19 (b) & (c)]. The microscopic images of various portions from the stained cross-section of the EVAL-S filter, provided in Figure 21, convey that the cells were present equally on all layers. This was further supported by the SEM images provided in Figure 20.

In the light of these data, it has to be emphasized that asymmetric filters gave better performance than the symmetric one and hence further studies will be focusing on development of asymmetric filters of EVAL.

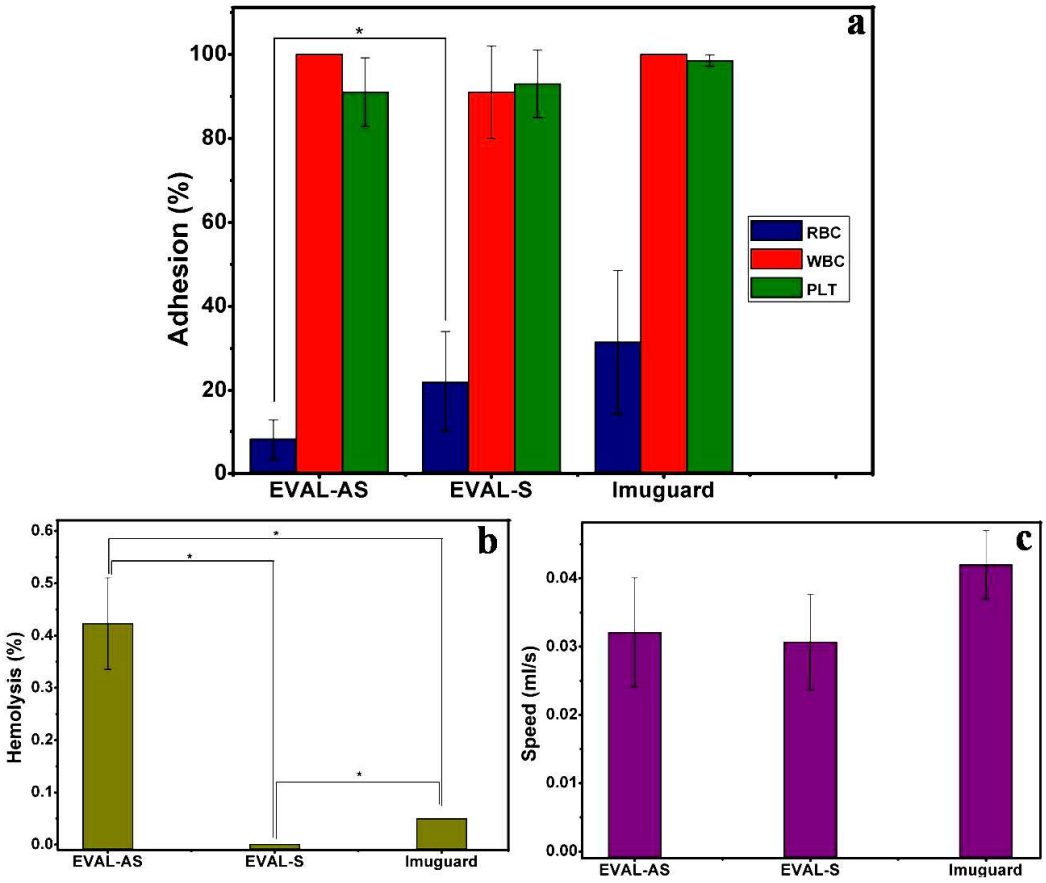

Figure 19. Comparative evaluation of leukodepletion efficiency between EVAL symmetric (EVAL-S) and EVAL asymmetric filter (EVAL-AS): (a) cell adhesion, (b) hemolysis and (c) speed of filtration

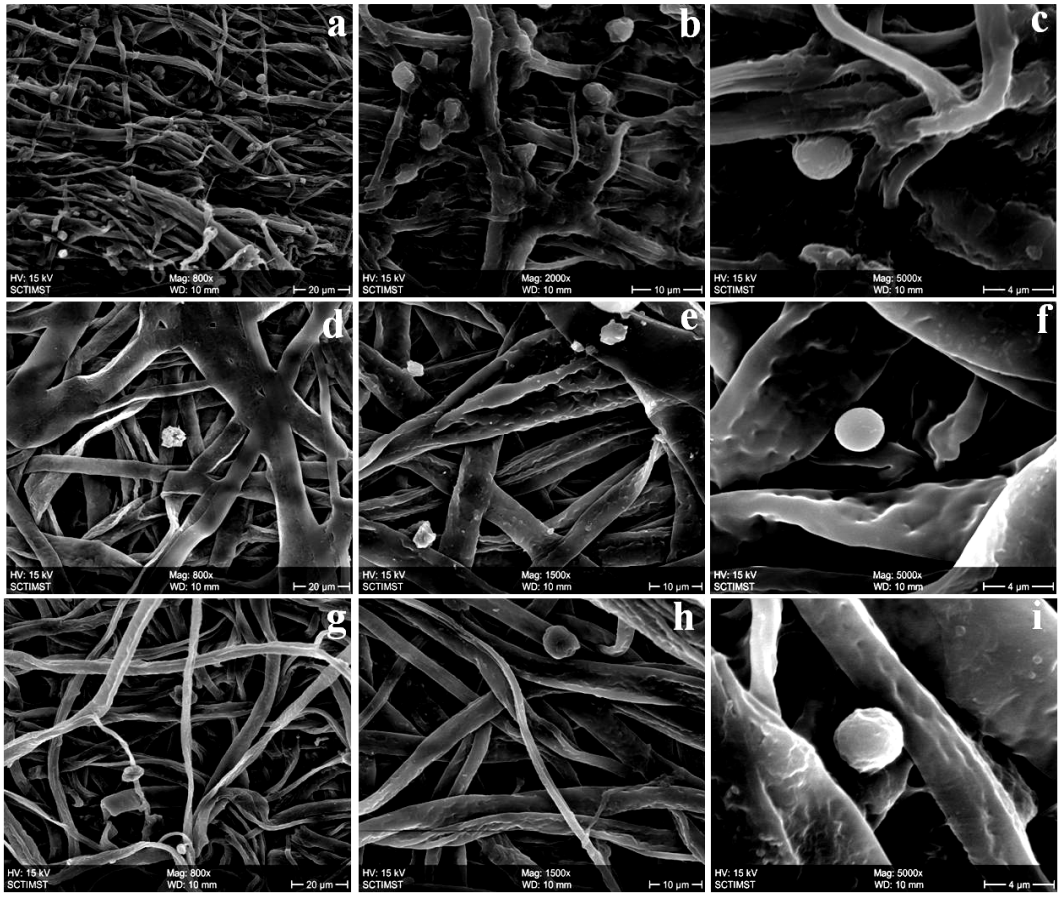

Figure 20. SEM analysis of adhered cells to the EVAL-S filter (a-c) top layer, (d-f) middle layer and (g-i) bottom layer at different magnifications

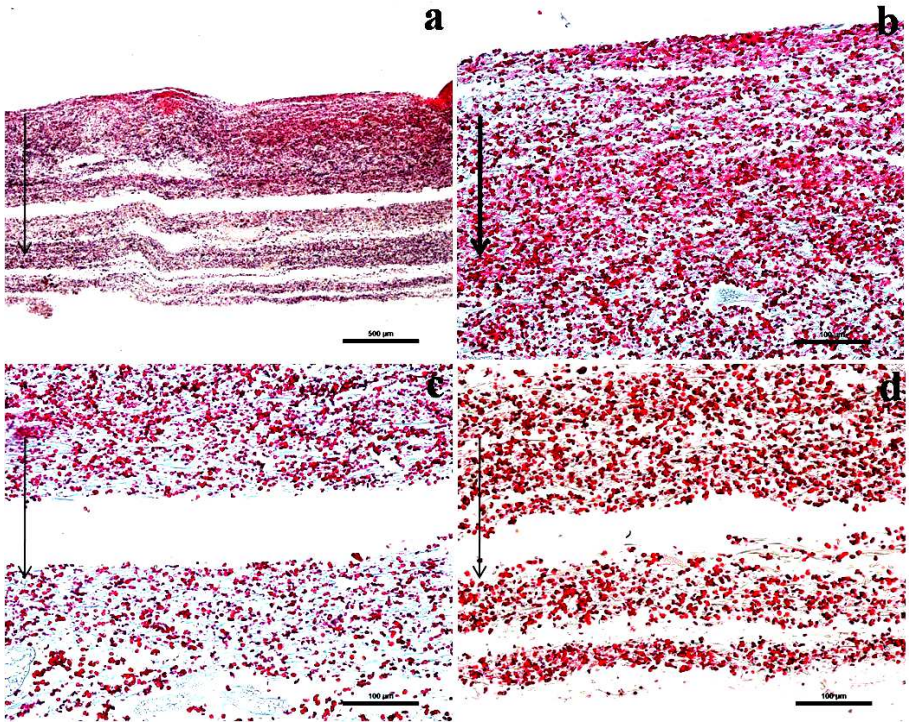

Figure 21. Histological examinations of stained cross sections (from top to bottom) of EVAL-S filter membrane assembly. The arrow indicates the direction of blood flow

Figure 22 shows the effect of fiber diameter of electrospun EVAL membranes on their overall leukodepletion efficiency. No significant difference in cell adhesion (WBCs, RBCs and platelets) was observed for the EVAL filters out of membranes with fiber diameter 1.8 µm and 3 µm [Figure 22 (a)]. However, efficiency of leukodepletion was very poor when the fiber diameter was reduced to 0.7 µm [Figure 22 (a)]. The speed of filtration for this filter was also significantly lower than the other filters having higher fiber diameters [Figure 22 (c)]. The percentage hemolysis induced by all of these filters fell under the acceptable level [Figure 22 (b)]. The cell populations on the various layers of the two filters having fiber diameter 0.7 µm and 3 µm were analyzed by SEM and

histology and are provided in Figure 23 to Figure 26. The morphology of the WBCs adhered on both the filters were spherical as evidenced by Figure 23 and 25. From Figure 23 and Figure 24, it can be inferred that the overall population of WBCs distributed throughout the different layers of the EVAL filter with fiber diameter 0.7 µm was relatively lower than that at the various layers of other two filters (Figure 25, Figure 26, Figure 15 and Figure 16), supporting to the percentage of WBC adhesion provided in Figure 22. Very few WBCs were visible in the bottom portion of the filter having fiber diameter 0.7 µm, in the microscopic images given in Figure 24, however, more WBCs were still present towards the bottom layer of other filters having high fiber diameter (Figure 16 and Figure 26).

From this data, among the various fiber diameter studied, the minimum required fiber diameter for effective leukodepletion was found to be 1.8 µm and hence the conditions for obtaining the same was followed for further studies.

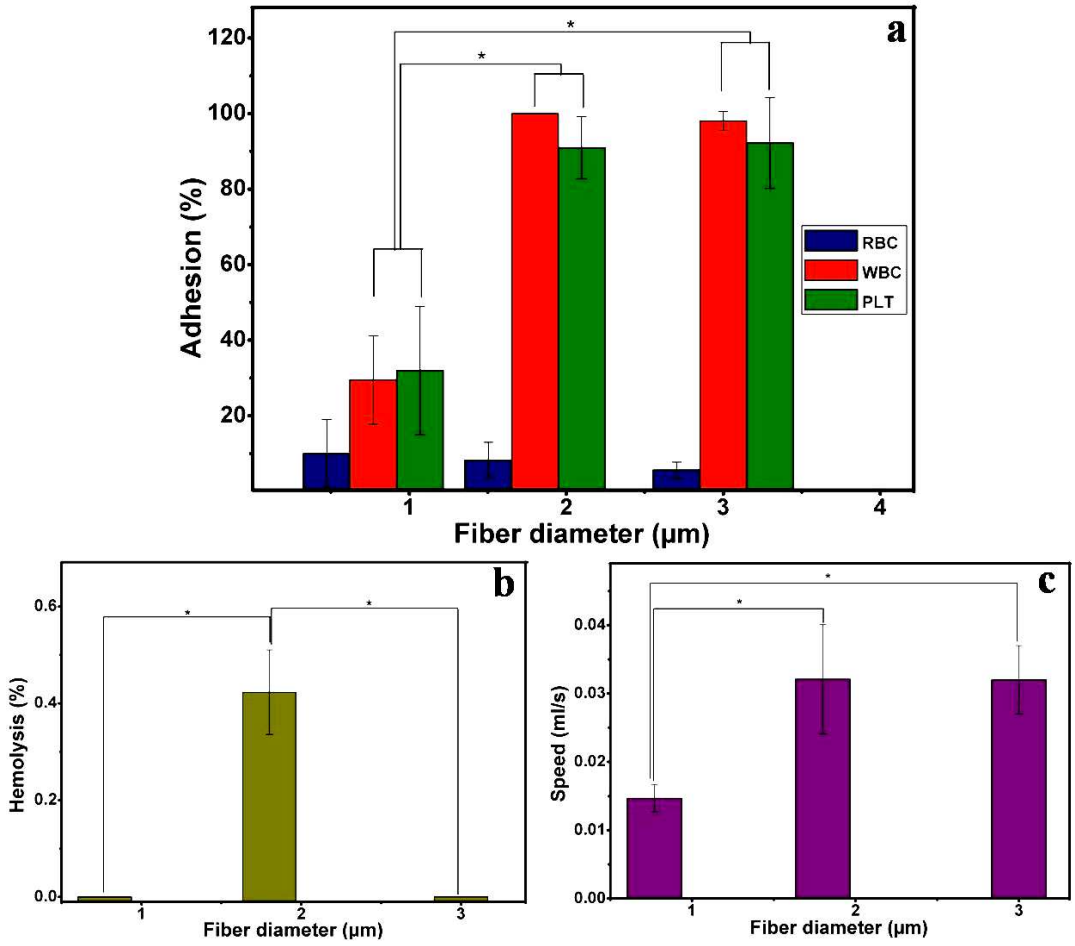

Figure 22. Effect of fiber diameter on the leukodepletion efficiency of EVAL-AS filter: (a) cell adhesion, (b) hemolysis and (c) speed of filtration

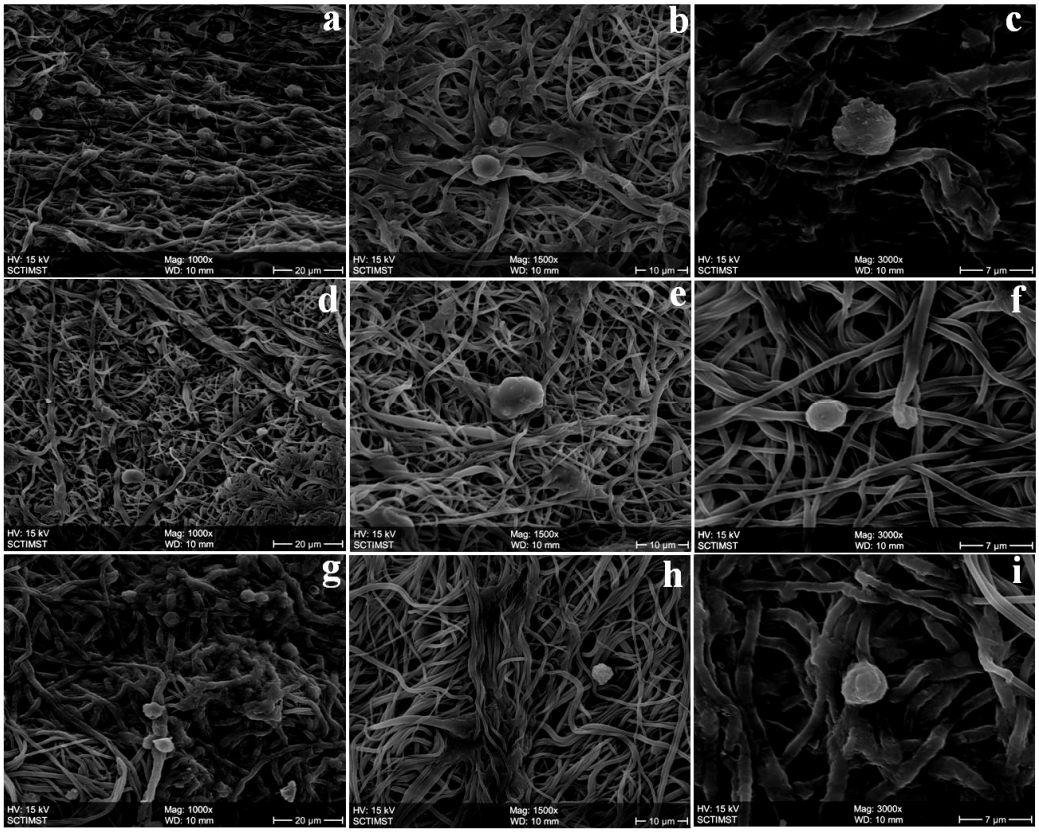

Figure 23. SEM analysis of adhered cells to the EVAL filter (fiber diameter 0.7 µm) (a-c) top layer, (d-f) middle layer and (g-i) bottom layer at different magnifications

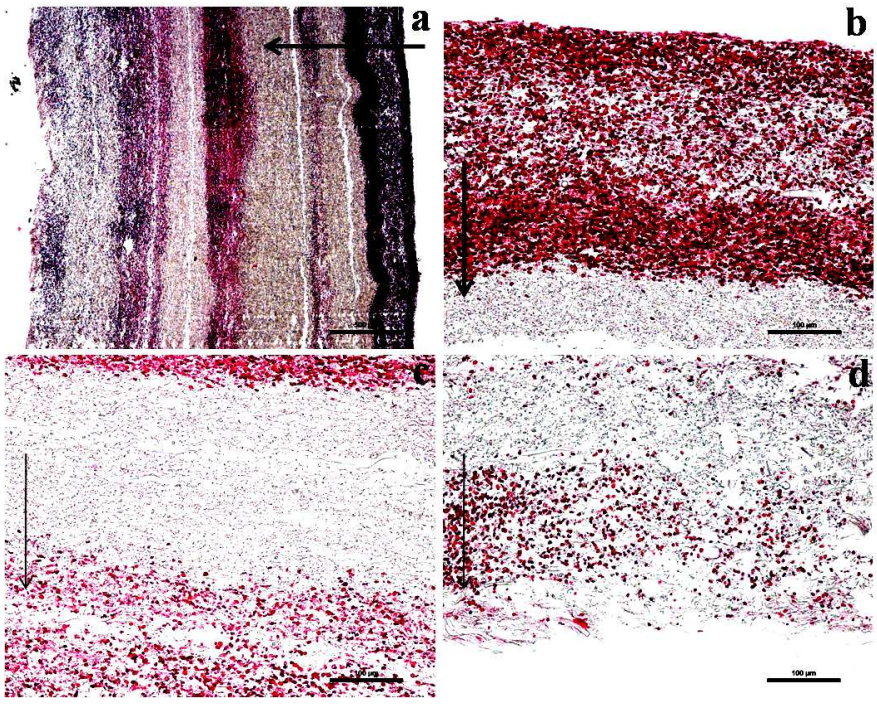

Figure 24. Histological examination of stained cross sections (from top to bottom) of EVAL filter (fiber diameter 0.7 µm) membrane assembly. The arrow indicates the direction of blood flow

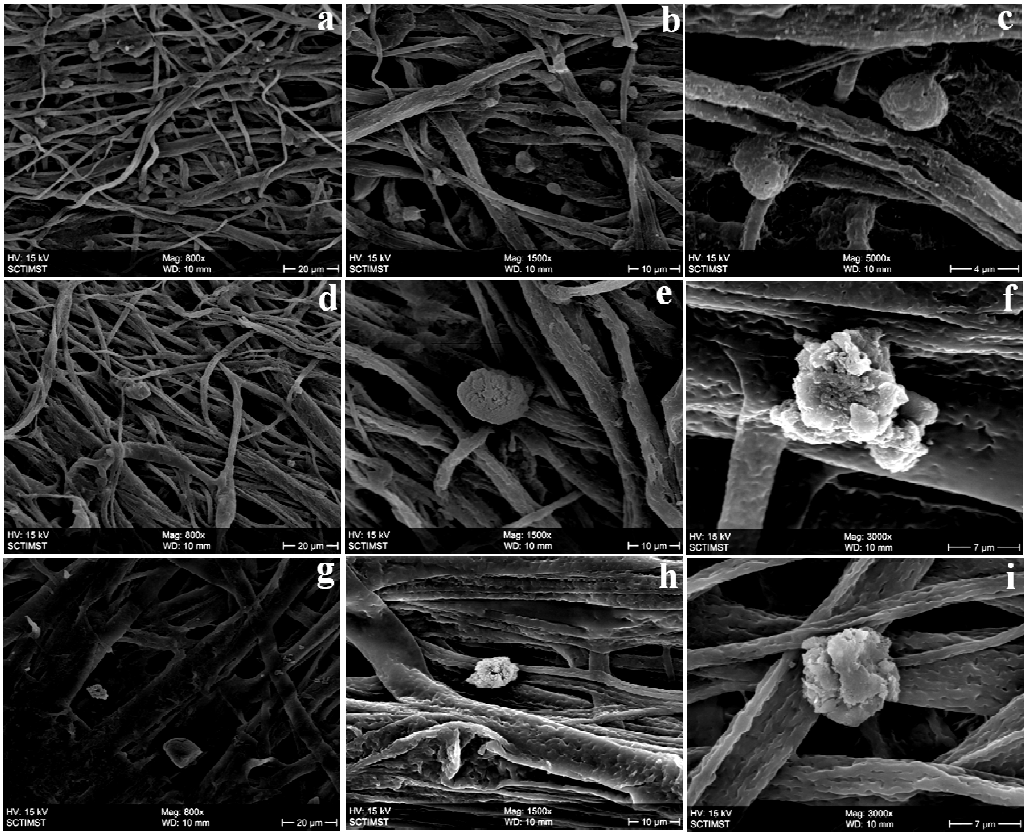

Figure 25. SEM analysis of adhered cells to the EVAL filter (fiber diameter 3 µm) (a-c) top layer, (d-f) middle layer and (g-i) bottom layer at different magnifications

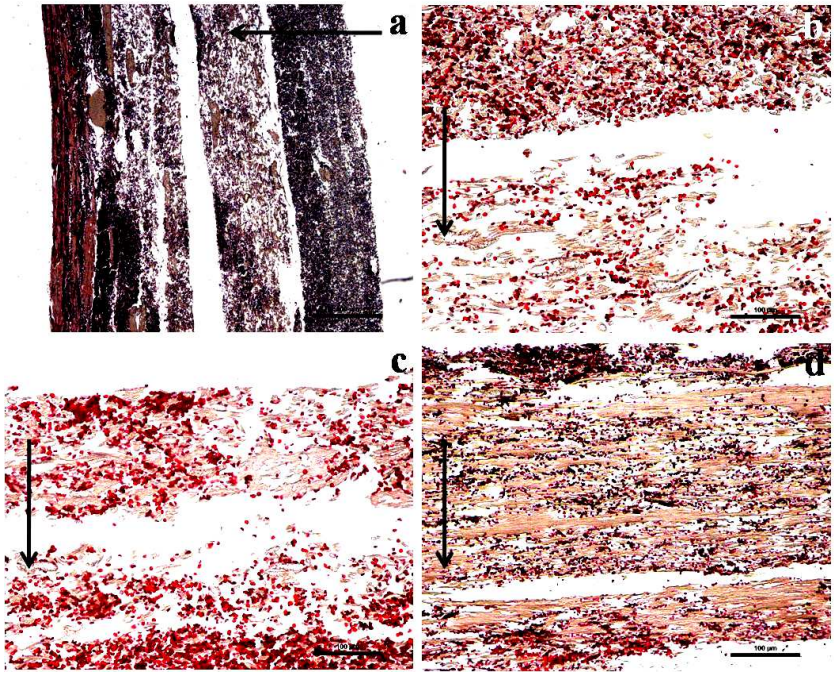

Figure 26. Histological examination of stained cross sections (from top to bottom) of EVAL filter (fiber diameter 3 µm) membrane assembly. The arrow indicates the direction of blood flow

4.2. Modifications on EVAL membranes and their characterization

4.2.1. Preparation of 2-hydroxyethyl acrylate grafted poly(ethylene-co-vinyl alcohol) (PHEA-g-EVAL)

4.2.1.1. ATR-FTIR spectroscopy

The photografting of HEA onto EVAL was confirmed by monitoring the appearance or shifting of characteristic peaks in the ATR-FTIR spectrum (Figure 27). A peak at 3288 cm^{-1} corresponding to the O-H stretch in EVAL shifted to 3360 cm^{-1} for all the grafted mats. A new peak at 1735.6 cm^{-1}, present in all the grafted mats, is due to

carbonyl stretching vibrations. Since the thickness of the samples exposed to UV varied slightly, there appear to have variations in the intensities of this peak. This is especially true for the sample exposed to UV for 50 minutes. In order to avoid ambiguity, peak at 2924.5 cm^{-1} (due to CH_2 asymmetric stretch) was taken as a reference peak and calculated the peak intensity ratios for different UV exposure times. The peak intensity ratios were calculated from the ratio of the intensity of peak at 2924.5 cm^{-1} ($I_{2924.5}$) to that of CO stretch at 1735.6 cm^{-1} ($I_{1735.6}$). Data given in Table 9 shows that peak intensity ratios are close to each other. Peaks at 1432.8 cm^{-1} and 1326.8 cm^{-1} arising from $(CH_2)_n$ bending and CH deformation, respectively, shifted to higher wave numbers. All these data are evidences that confirm grafting of HEA onto EVAL matrix.

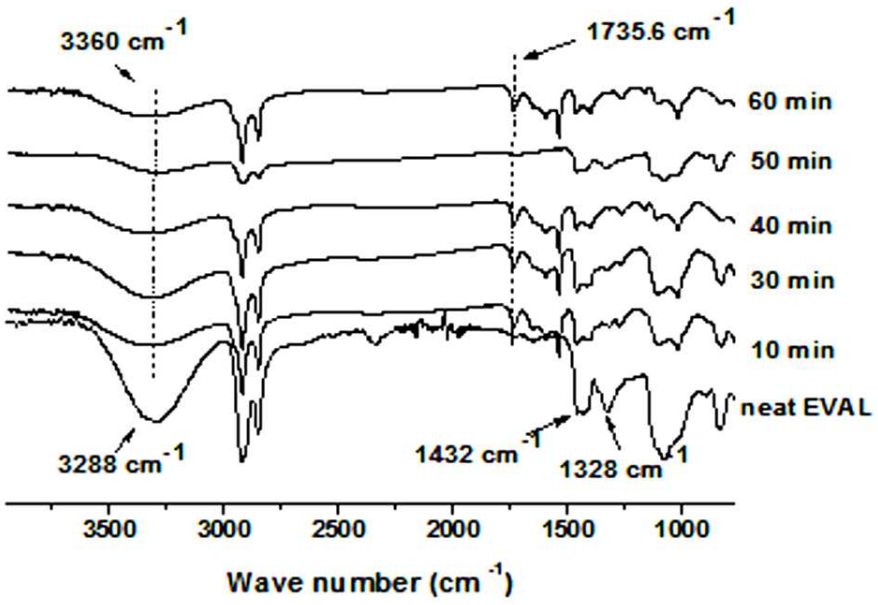

Figure 27. ATR-FTIR spectra of EVAL and PHEA-g-EVAL electrospun mats as a function of UV exposure time

UV treatment time (min)	Peak intensity ratio $= \frac{I_{2924.5}}{I_{1735.6}}$
10	0.8
30	0.7
40	0.8
50	0.8
60	0.7

Table 9. Peak intensity ratio of CH_2 stretch to C=O stretch for different UV treatment times

4.2.1.2. Degree of grafting

The degree of grafting was estimated to assess the extent of HEA grafting and the data is presented in Table 10. A gradual increase in the DG with the increase in UV exposure time was observed. DG reached its maximum when the UV exposure time was 60 min.

UV exposure time (min)	Properties (n=6)			
	DG (%)	Porosity (%)	WCA (°)* $p<0.001$	CWST (mN/m)
0	-	53 ± 1	126 ± 6	61.8
10	2.22 ± 1.10	51 ± 2	109 ± 4	68.8
30	11.11 ± 5.05	52 ± 1	85 ± 0.2	76.3
40	14.64 ± 5.11	52 ± 1	109 ± 2	79.9
50	18.99 ± 2.41	53 ± 0.2	108 ± 1	82.5
60	29.80 ± 6.20	52 ± 1	79 ± 9	---

Table 10. Physico-chemical properties of electrospun fibroporous mats as a function of UV exposure time: (DG = Degree of grafting, WCA = Water contact angle, CWST = Critical water surface tension)

4.2.1.3. Effect of HEA grafting on the morphology of the EVAL fibers

Morphological features of the fibroporous mats observed under SEM are shown in Figure 28. Images reveal the formation of smooth fibers. [Figure 28 (a-f)]. There is a significant increase in fiber diameter as a result of grafting [Figure 28 (g)]. Fusion and wrinkling of the fibers were also oberved in these SEM images and it is more predominant in the samples that were UV treated for 60 minutes. These changes in the fiber morphology and fiber diameter with UV treatment time further confirms grafting.

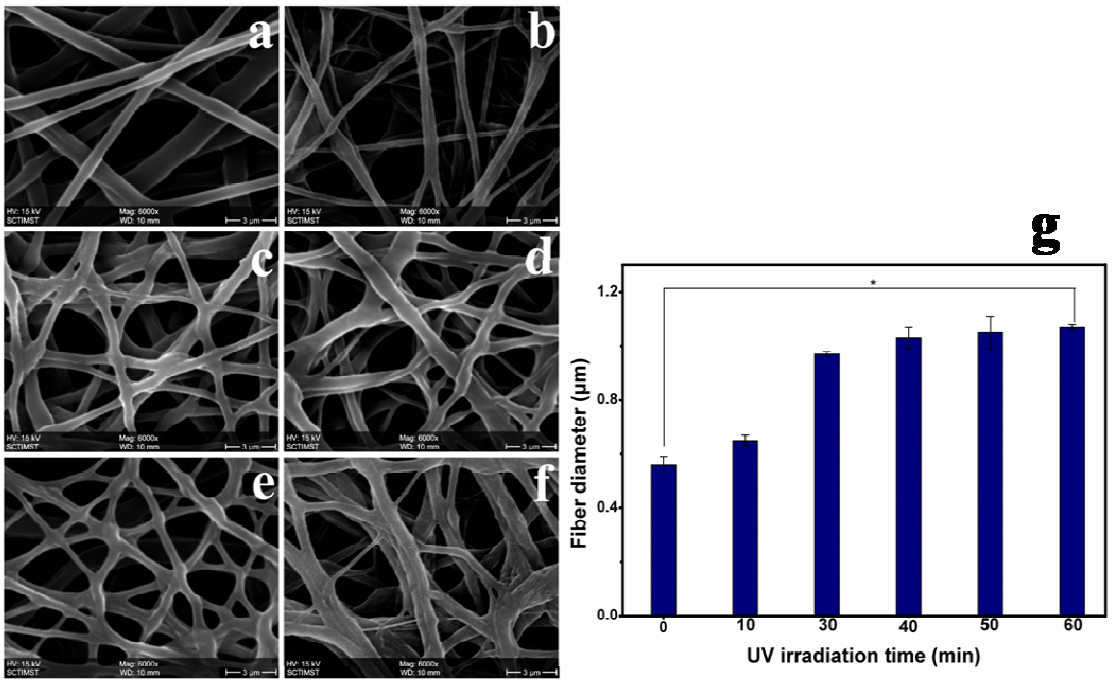

Figure 28. SEM images of EVAL and PHEA-g-EVAL electrospun mats:(a). Neat EVAL; (b-f). UV treated EVAL, with treatment times 10, 30, 40, 50 & 60 min, respectively; (g) fiber diameter as s function of UV irradiation time

4.2.1.4. Effect of HEA grafting on the pore characteristics

The influence of HEA grafting upon the pore properties were studied by the estimation of percentage porosity and pore diameter. Grafting did not have any noticeable effect on the porosity (Table 10) and pore size (Figure 29) of the mat. The porosity was maintained within 52 – 53 % even after grafting.

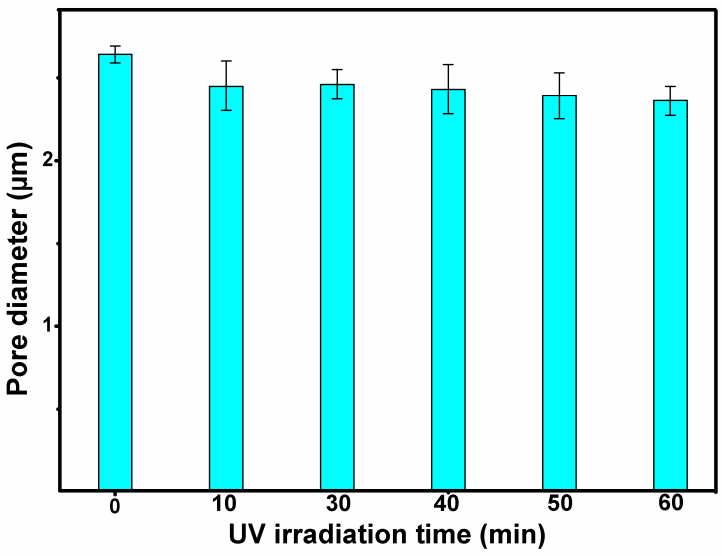

Figure 29. Effect of HEA grafting on the pore diameter

4.2.1.5. Effect of HEA grafting on the wetting characteristics of EVAL

Results of water contact angle and CWST measurements revealed that grafting led to reduction in the degree of hydrophobicity of electrospun EVAL. Neat EVAL mat had a contact angle of 126 ± 6 ° with water. A significant reduction in contact angles were observed as a result of UV treatment (Table 10). Within an exposure time of 10 minutes the contact angle decreased from 126 ° to 109 °. Upon 60 minutes of exposure, the contact angle decreased to 79 ° indicating substantial decrease in hydrophobicity. It may

also be noted that CWST of neat EVAL was 61.77 mN/m (Table 10) and could not get wet with water, but after grafting the value gradually increased with UV exposure time offering supporting evidence for improved wettability. The CWST for PHEA-g-EVAL, UV treated for 60 minutes, was beyond the limit of surface tension values of the selected solutions and it could not be measured (Table 10).

4.2.1.6. Effect of HEA grafting on the mechanical properties

Tensile stress-strain plots of the neat and PHEA-g-EVAL are shown in Figure 30 and the properties such as tensile strength, Young's modulus, elongation at break are summarized in Table 11. Grafting resulted in a significant decrease of tensile strength and Young's modulus whereas a substantial increase in the elongation at break was observed. This indicates that along with grafting UV exposure leads to certain extent of polymer chain scission as well. No clear trend of increase or decrease of glass transition temperature (T_g) or storage modulus was observed as a result of photografting (Table 11).

UV exposure time (min)	Properties (n=6)				
	Tensile strength (MPa)*	Elongation at break (%)*	Young's modulus (MPa)*	Tg (°C)	Storage modulus at 37 °C (MPa)
0	6.8 ± 0.5	42 ± 5	150 ± 14	82.6	56.2
10	5.9 ± 0.6	71 ± 9	136 ± 09	90.7	65.9
30	5.7 ± 0.5	85 ± 9	94 ± 09	66.2	107
40	5.7 ± 0.5	61 ± 11	111 ± 11	84.6	17.7
50	5.5 ± 0.8	48 ± 8	74 ± 08	80.7	49.3
60	4.8 ± 0.6	103 ± 4	100 ± 19	78.8	70.6

Table 11. Static and dynamic mechanical properties of electrospun mats as a function of UV exposure time

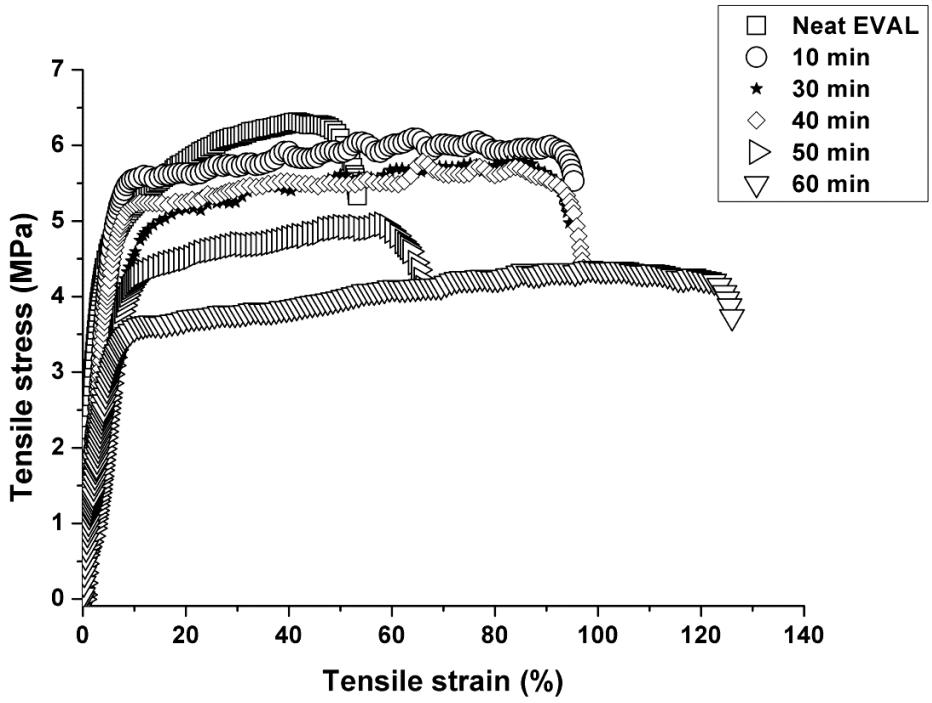

Figure 30. Stress-strain behavior of neat EVAL (indicated as '0') and PHEA-g-EVAL having different UV irradiation times

4.2.1.7. Effect of HEA grafting on hemocompatibility

Effect of HEA grafting on the hemocompatibility of EVAL was studied by analyzing the percentage hemolysis, RBC aggregation, plasma protein adsorption, platelet adhesion, coagulation assay,complement acivation, and blood cell consumption. A significant decrease in the percentage hemolysis (Table 12) was observed for all the grafted films as a function of UV treatment time. Hemolysis of neat EVAL was 2.3 ± 0.5 % whereas when it was grafted with HEA by exposing to UV for a period of 60 minutes the hemolysis decreased to less than 9 % of that observed for EVAL. The light

microscopy images of RBCs shown in Figure 31 revealed that RBC aggregation was more or less absent in the neat and HEA grafted EVAL compared to the positive contol.

UV exposure time (min)	Blood contacting properties (n=9)			
	Hemolysis (%)*	Plasma protein adsorption ($\mu g/mm^3$)*	Platelet consumption (%)*	
			PRP	WB
0	2.3 ± 0.5	7.2 ± 1.6	72 ± 15	96 ± 3
10	1.7 ± 0.5	4.6 ± 0.9	18 ± 6	61 ± 10
30	0.9 ± 0.2	4.3 ± 1.0	15 ± 10	61 ± 14
40	0.8 ± 0.3	3.7 ± 1.5	12 ± 3	71 ± 9
50	0.6 ± 0.2	3.4 ± 1.3	9 ± 7	71 ± 9
60	0.3 ± 0.1	0.2 ± 0.1	8 ± 5	70 ± 15

Table 12. *In vitro* hemocompatibility evaluation: Data of hemolytic evaluation, protein adsorption and platelet adhesion on electrospun mats as a function of UV exposure time

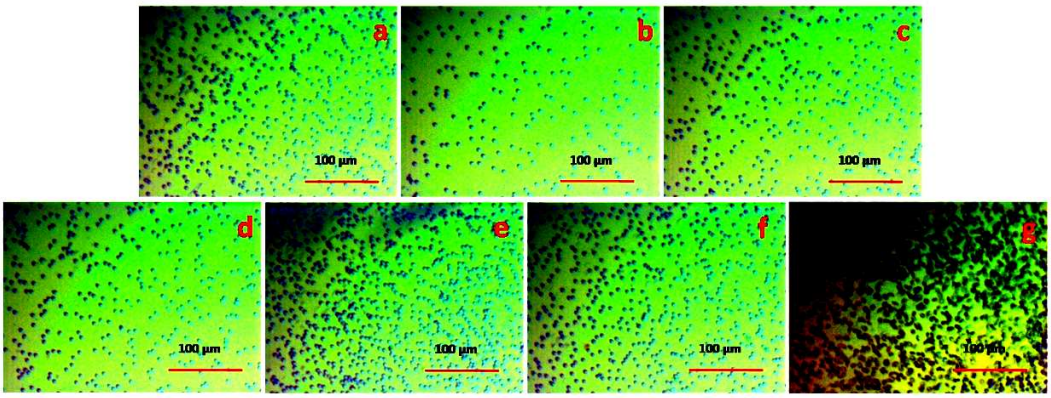

Figure 31. Light microscopy images of RBC aggregation studies conducted on electrospun mats: (a) Neat EVAL; (b-f) UV treated EVAL with treatment times 10, 30, 40, 50 & 60 minutes respectively; (g) Positive control

The plasma protein adsorption was also gradually decreasing with UV exposure time and the decrease was significant. When EVAL was exposed to UV for 60 minutes the observed reduction in plasma protein adsorption was about 97 % (Table 12). A quantitative estimation of adhered platelets from PRP as well as WB is also provided in Table 12. The results highlight that HEA grafting could result in a significant reduction in the platelet adhesion both from PRP and WB. The platelet adhesion was qualitatively studied by SEM analysis and the images are shown in Figure 32. Neat EVAL surface clearly showed a greater level of platelet adhesion. Aggregation of platelets were also observed in these pictures. However, it was interesting to note that all the HEA grafted EVAL mats showed very little platelet adhesion. Aggregates of platelets were also absent in these grafted EVAL.

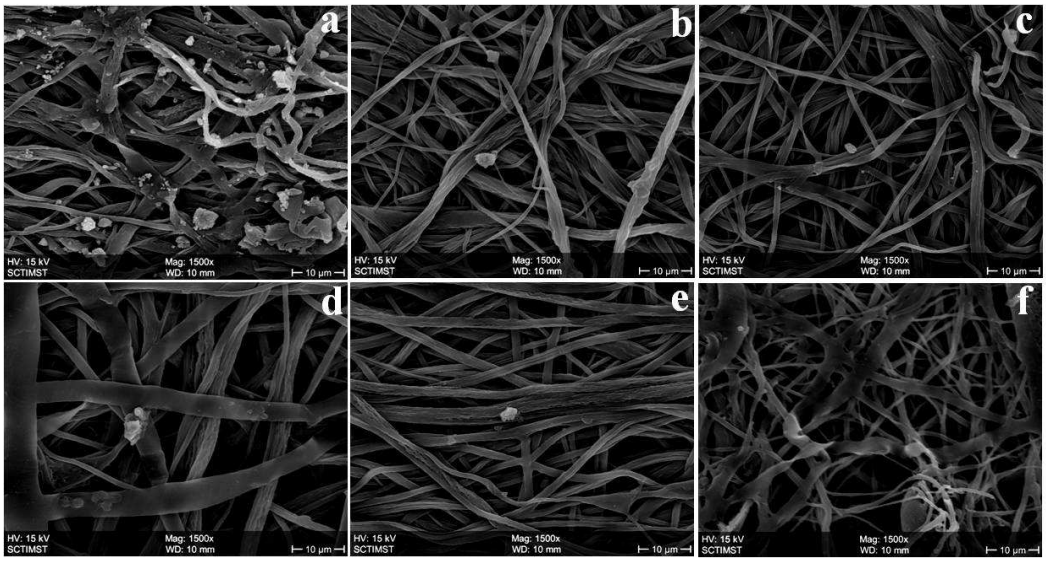

Figure 32. SEM images of electrospun mats after platelet adhesion studies: (a). Neat EVAL; (b-f). UV treated EVAL with treatment times 10, 30, 40, 50 & 60 min, respectively

The percentage change in the PTT and fibrinogen as a result of blood-material interactions is presented in Table 13. The change in PTT and fibrinogen levels were below 20 % for all the samples. The uncertainty level in these cases were 5 %. The presented data show that all the materials activated the coagulation cascade to a limited extent. However, the modification by HEA grafting did not seem to significantly influence the degree of activation. The results of complement activation test performed on HEA grafted EVAL is given in Table 13. There was a significant difference in the complement activation among the 3 sets of PHEA-g-EVAL (Table 13). In the case of EVAL, which was UV irradiated for 40 minutes, the level of C3a increased after PRP exposure. But when the UV irradiation times were 50 minutes and 60 minutes, the level of C3a decreased after PRP exposure. The effect of HEA grafting on the RBC and WBC consumption (Table 13) shows that electrospun EVAL has an inherent tendency for leukocyte adhesion. When the material was kept in contact with blood, the leukocyte adhesion of neat electrospun EVAL and PHEA-g-EVAL mat were close to each other. On the other hand, RBC adhesion was decreasing significantly with the increase in the degree of grafting/ UV exposure time (Table 13).

UV exposure time (min)	Blood contacting properties (n=6)				n=3
	PTT (%)	Fibrinogen (%)	WBC consumption (%)	RBC consumption (%)*	C3a (%)*
0	12.4 ± 3.5	6.9 ± 5.7	96 ± 2	68 ± 10	
10	14.1 ± 5.5	20.7 ± 11.8	99 ± 1	3.7 ± 1.8	
30	10.4 ± 4.7	21.1 ± 15.7	96 ± 3	5.1 ± 4.7	
40	15.6 ± 6.7	8.9 ± 3.4	97 ± 2	3.1 ± 2.9	7.4 ± 2.3
50	18.5 ± 5.9	11.4 ± 6.3	98 ± 2	4.5 ± 4.3	-17.9 ± 2
60	13.0 ± 5.0	10.2 ± 4.8	98 ± 1	3.9 ± 2.9	-9.9 ± 1.7

Table 13. *In vitro* hemocompatibility evaluation: Data of coagulation assay complement activation and interaction of blood cells on electrospun mats as a function of UV exposure time

4.2.1.8. Evaluation of leukodepletion efficiency of PHEA-g-EVAL membranes

From the data of *in vitro* hemocompatibility evaluation of all the HEA grafted EVAL membranes, comparing the degree of all the blood-material interactions, the grafted membranes obtained as a result of 60 minutes UV irradiation, PHEA-g-EVAL-60, was found to have desirable properties and this particular membrane system was fabricated to asymmetric filters. As mentioned earlier, the asymmetric filter was designed by placing the 4 layers of PHEA-g-EVAL-60 membranes obtained at a collection speed of 500 RPM as the top layers while a monolayer of PHEA-g-EVAL membrane collected at 1500 RPM served as the bottom layer. The SEM analyses of these membranes were performed and the images are provided in Figure 33. The fiber diameter and pore

properties were measured by image analysis and are provided in Table 14. The fiber diameter and porosity was not influenced by the collection speed, while the decrease in pore size confirms the asymmetry in the membrane assembly.

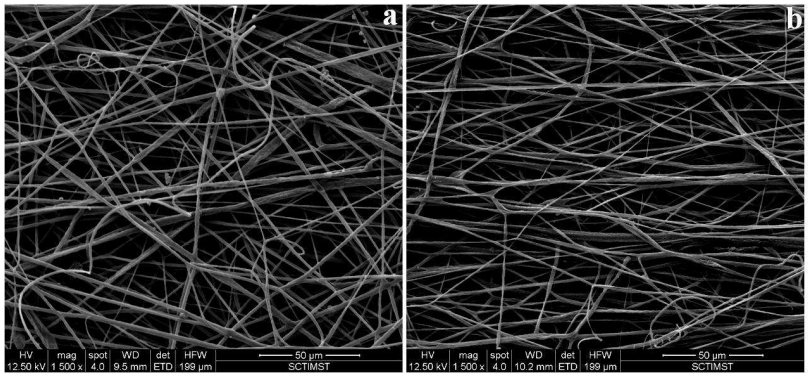

Figure 33. SEM images of PHEA-g-EVAL membranes in the asymmetric filter collected at different speeds; (a) 500 RPM and (b) 1500 RPM

Collection speed	Fiber diameter (µm)	Pore diameter (µm)	Porosity (%)
500 RPM	2.1 ± 0.2	18.3 ± 3.5	52 ± 0.3
1500 RPM	2.0 ± 0.4	12.0 ± 2.4	52 ± 0.6

Table 14. Membrane properties of PHEA-g-EVAL asymmetric filter

The whole blood filtration exepriments were performed according to the proceudre reported in section 3.5.3. The leukodepletion efficiency of the PHEA-g-EVAL-60 asymmetric filters were compared with that of the neat EVAL asymmetric filter in Figure 34. As expected, there was very significant reduction in the pletelet adhesion for the PHEA-g-EVAL-60 when compared to that of neat EVAL. However, it was also interesting that the WBC adhesion was noticeably reduced as a result of PHEA grafting[(Figure 34 (a)]. There was no change in the speed of filtration before and after

grafting [Figure 34 (c)], but the percentage hemolysis induced by the PHEA-g-EVAL-60 filter was approximately zero [Figure 34 (b)].

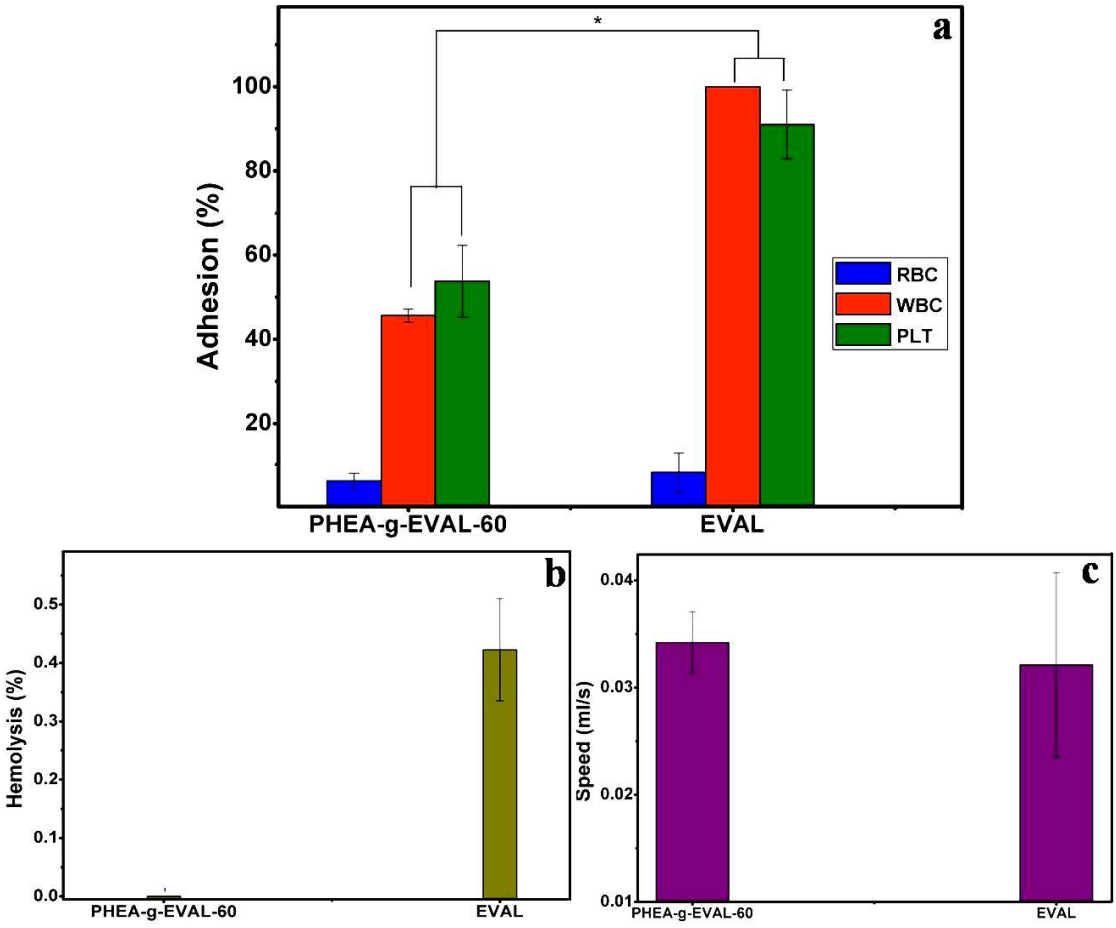

Figure 34. Comparison of leukodepletion efficiency of PHEA-g-EVAL-60 and neat EVAL asymmetric filter

The morphological and histological analysis of the filter membranes are provided in Figure 35 and Figure 36 respectively. The population of cells was comparatively poor on the various layers of the membranes in Figure 35. The microscopic images of the

stained cross-sections of the membrane assembly in Figure 36 also show a poor cell adhesion, which are in good agreement with the quantitative data and SEM images.

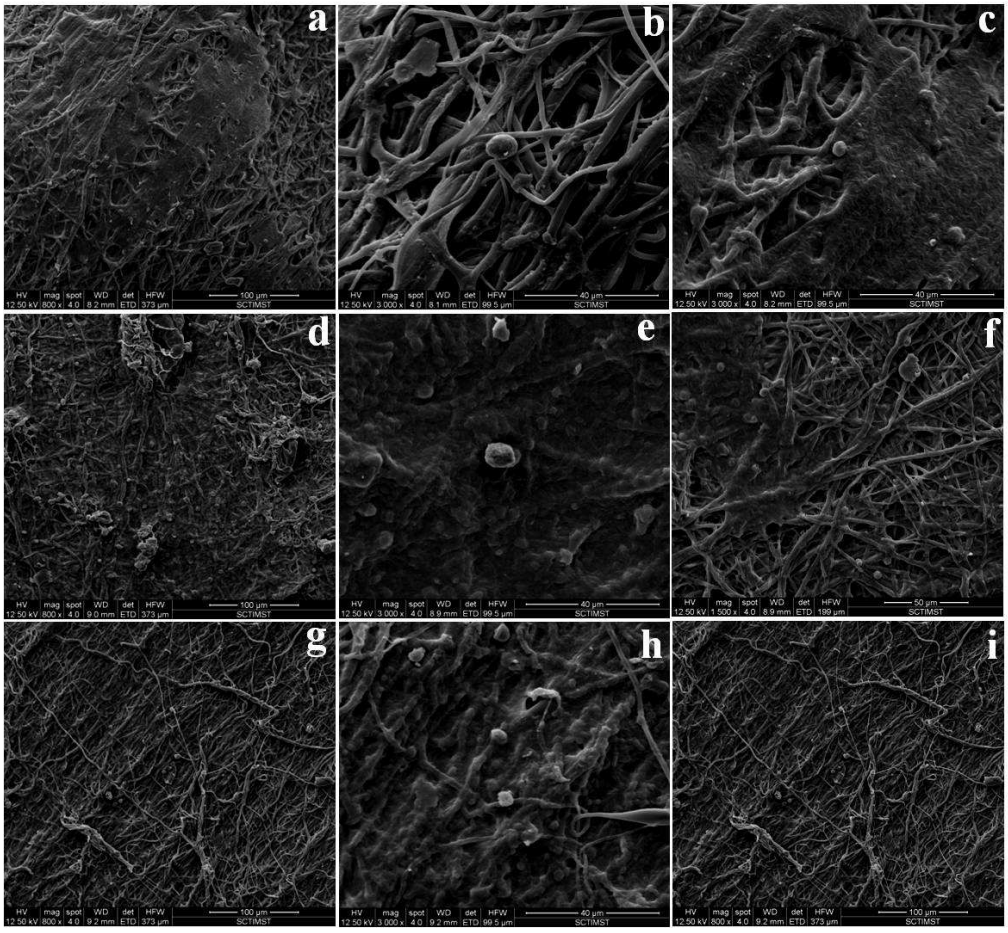

Figure 35. SEM analysis of adhered cells to the PHEA-g-EVAL-60 filter; (a-c) top layer, (d-f) middle layer and (g-i) bottom layer at different magnifications

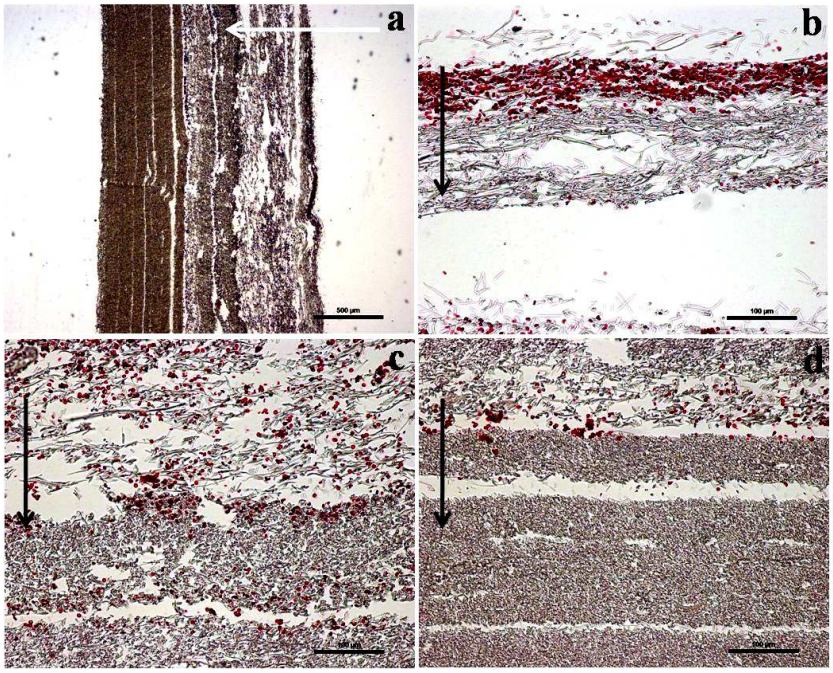

Figure 36. Histological examinations of stained cross sections of PHEA-g-EVAL-60 filter membrane assembly. The arrow indicates the direction of blood flow

4.2.2. Functionalization by incorporation of glycine

4.2.2.1. Surface characterization

The glycine incorporated EVAL membranes were characterized by the ATR-FTIR spectroscopy provided in Figure 37. The presence of glycine is confirmed by the appearance of a new peak at 1630 cm^{-1} corresponding to the COO stretch in the glycine. The smooth morphology of the fibers was maintained even after the incorporation of glycine, which is evident from the SEM photographs provided in Figure 38. The diameter of the fibers was measured from these images and is provided in Table 15. It was found that there was a decrease in the fiber diameter at higher glycine loading while the pore

size was gradually decreasing with increase in glycine loading. The percentage porosity was preserved even after the loading of glycine (Table 15).

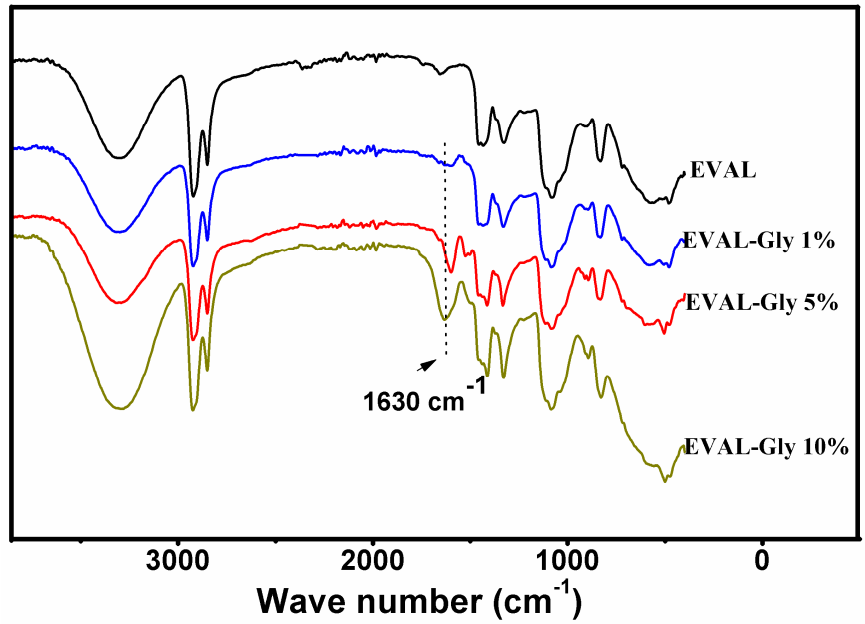

Figure 37. ATR-FTIR spectrum of EVAL-Gly membranes at various glycine loading

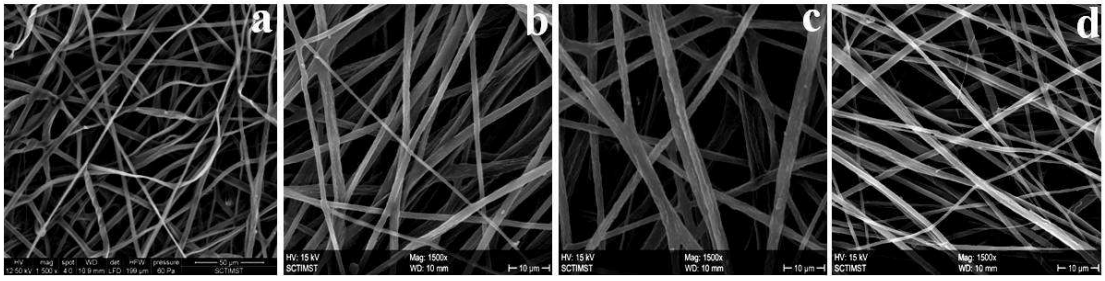

Figure 38. SEM pictures of EVAL-Gly membranes at various loadings; (a) neat EVAL, (b) EVAL-Gly-1%, (c) EVAL-Gly-5% and (d) EVAL-Gly-10%

Glycine Loading (%)	Fiber Diameter (µm)*	Pore Diameter (µm)*	Porosity (%)
0 (Neat EVAL)	1.8 ± 0.1	23.3 ± 5	53 ± 1.0
1	2.0 ± 0.2	13.0 ± 3	51 ± 0.2
5	2.1 ± 0.3	10.0 ± 2	52 ± 1.0
10	1.5 ± 0.3	6.0 ± 1	52 ± 0.2

Table 15. Fiber diameter and pore properties of EVAL-Gly membranes

The evaluation of wettability of the glycinated membranes were also carried out and the Figure 39 shows the effect of glycine loading on the WCA and CWST. It is interesting that the WCA was more or less uniform while the CWST values were enhanced as a result of glycine incorporation.

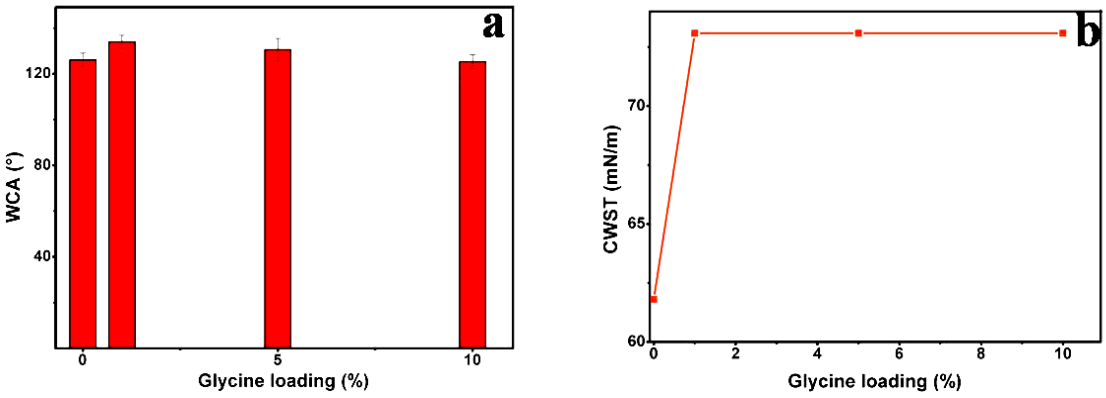

Figure 39. Wettability evaluation of EVAL-Gly membranes;
(a) WCA and (b) CWST

4.2.2.2. *In vitro* release study

The release study of glycine was also undertaken and the glycine released into the PBS at various time periods were quantitatively estimated by ninhydrin assay. From this, the cumulative release profile for various glycine loaded systems for a maximum period of 7 days was constructed and is given in Figure 40. It can be figured out that there was a burst release of glycine form all the glycine loaded membranes within 1 day and the release continued successively and was stabilized reaching 7 days. The quantity of glycine released at the end of 7 days were 4.0 ± 0.04 µg/mL, 6.1 ± 0.04 µg/mL and 6.2 ± 0.05 µg/mL for 1 %, 5 % and 10 % glycine loaded membranes respectively.

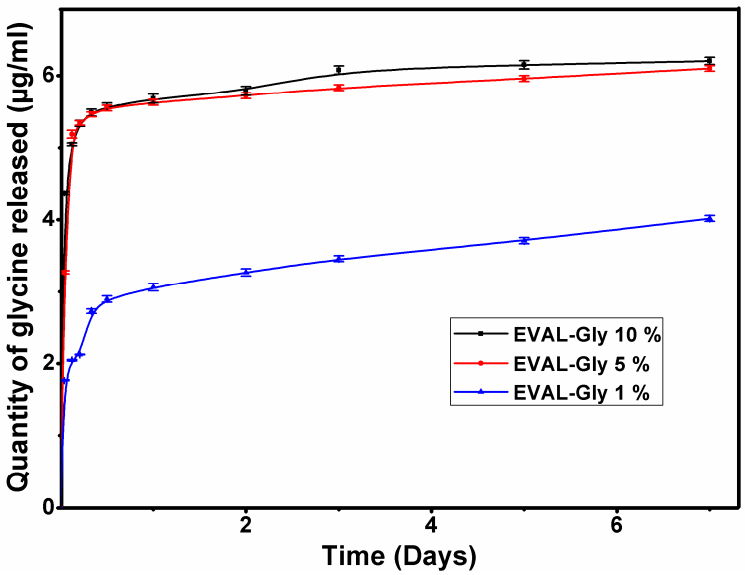

Figure 40. *In vitro* release profile of glycine from the various EVAL-Gly membranes

4.2.2.3. *In vitro* hemocompatibility evaluation

The effect of glycine incorporation on the blood-material interactions are provided in Table 16. There was no significant change in the plasma protein, WBC adhesion and platelet adhesion from whole blood. However the platelet adhesion was found to be gradually decreasing as a result of glycine incorporation. Noticeable decrease in the RBC adhesion and percentage hemolysis was also observed with glycine loading. The SEM images of the platelets adhered to the membranes after exposure to PRP (Figure 41) also support the quantitative data of platelet adhesion provided in Table 16.

Glycine loading (%)	Protein adsorption (%)	RBC adhesion (%) *	WBC adhesion (%)	Platelet adhesion (%)		Hemolysis (%) *
				WB	PRP *	
0	7.2 ± 1.6	68 ± 10	96 ± 2	96 ± 3	72 ± 15	2.3 ± 0.5
1	7.6 ± 2.5	13 ± 1	100 ± 0	99 ± 0	39 ± 6	0.4 ± 0.01
5	7.6 ± 2.0	60 ± 15	97 ± 2	94 ± 5	40 ± 3	0.3 ± 0.1
10	7.9 ± 1.7	25 ± 4	96 ± 5	96 ± 2	56 ± 8	0.3 ± 0.1

Table 16. *In vitro* hemocompatibility evaluation of EVAL-Gly membranes

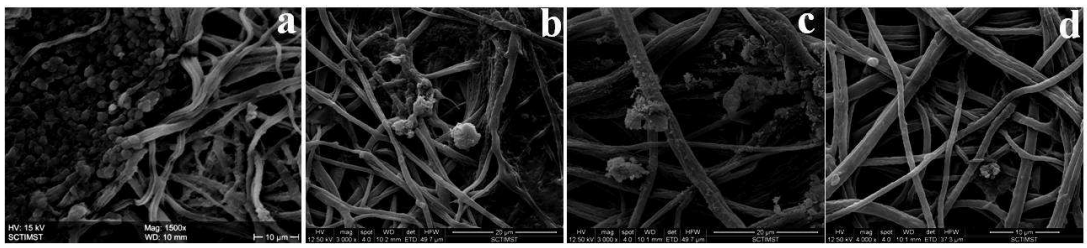

Figure 41. SEM images of EVAL-Gly membranes after exposure to PRP; (a) neat EVAL, (b) EVAL-Gly-1%, (c) EVAL-Gly-5% and (d) EVAL-Gly-10%

4.2.3. Functionalization of EVAL by SMDB

4.2.3.1. Surface characterizations

Figure 42 shows the ATR-FTIR spectra of neat and SMDB grafted EVAL. The peaks at 2923 cm^{-1} and 2850 cm^{-1} in the neat EVAL stand for the CH_2 asymmetric and symmetric stretches respectively. These peaks were still present in all the SMDB functionalized EVAL. Additionally, there was new peaks at 1740 cm^{-1} corresponding to the C=O stretch, 1540 cm^{-1} for the N-H stretch and at 1072 cm^{-1} corresponding to SO_3 stretch arising from the SMDB functionalization. The OH absorption peak in EVAL at 3303.5 cm^{-1} has been shifted to 3366 cm^{-1} for all the SMDB grafted films indicating successful functionalization. The morphological features before and after SMDB grafting of EVAL was studied by SEM and the images are provided in Figure 43. EVAL was electrospun to smooth, defect free cylindrical fibers and the no noticeable changes in the morphology of the fibers were observed after SMDB grafting. However, the average fiber diameter was found to be increasing significantly with increase in the UV irradiation period as a result of SMDB grafting (Figure 44). In Figure 45, the effect of SMDB functionalization on the WCA values of EVAL was studied. A significant decrease in the WCA of EVAL was observed as a function of UV irradiation time. The SMDB grafted EVAL became hydrophilic after 60 minutes of UV irradiation indicated by its WCA of 69 ± 11 °.

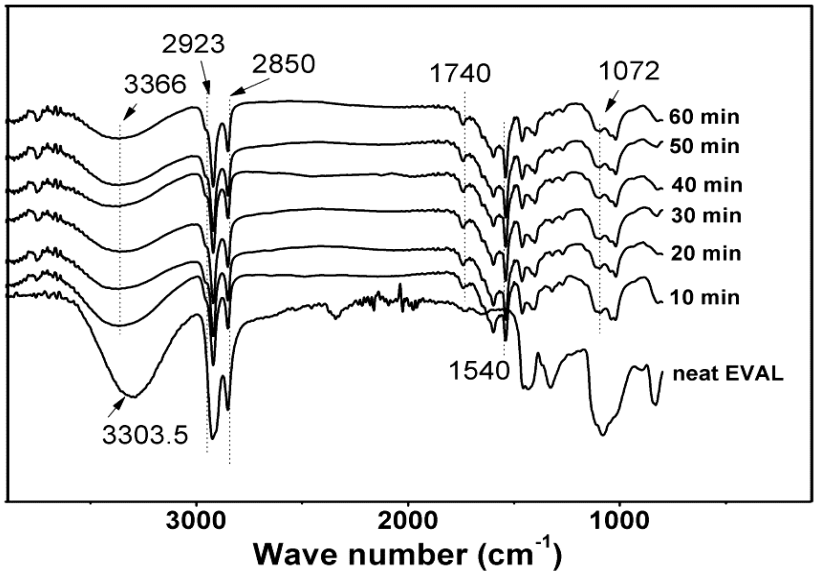

Figure 42. ATR-FTIR spectra of neat and PSMDB-g-EVAL obtained by various UV irradiation periods

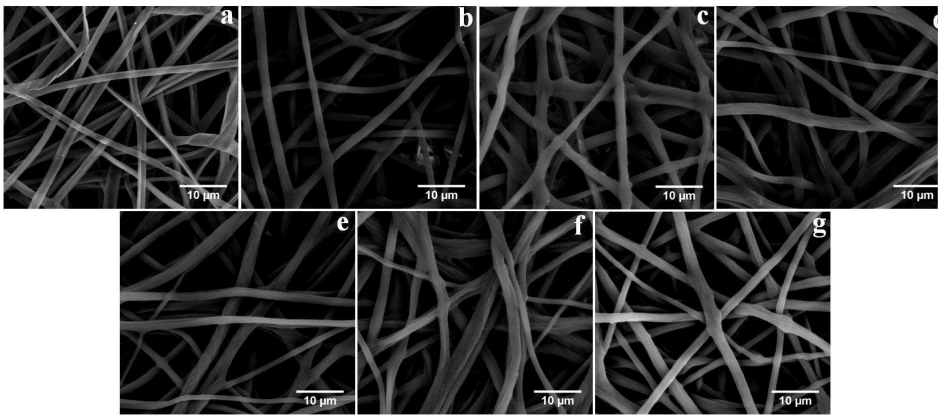

Figure 43. SEM pictures of (a) neat EVAL and (b-g) SMDB functionalized EVAL through UV irradiation periods 10, 20, 30, 40, 50 and 60 min, respectively

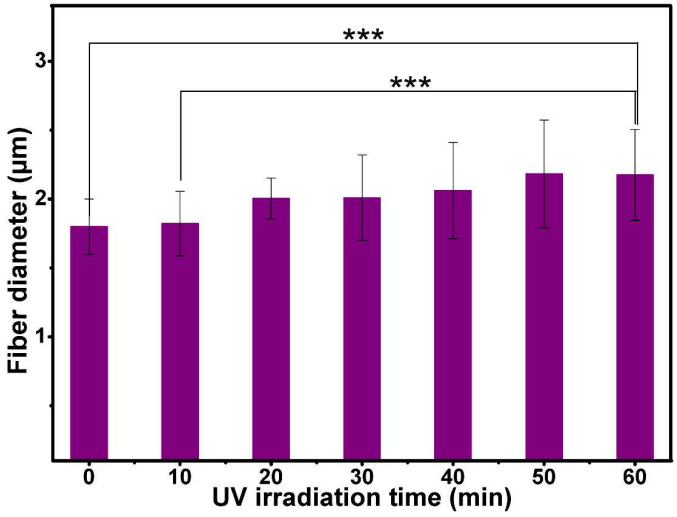

Figure 44. Effect of SMBD functionalization on the fiber diameter of EVAL as a function of UV irradiation periods. The '0' minutes stands for neat EVAL

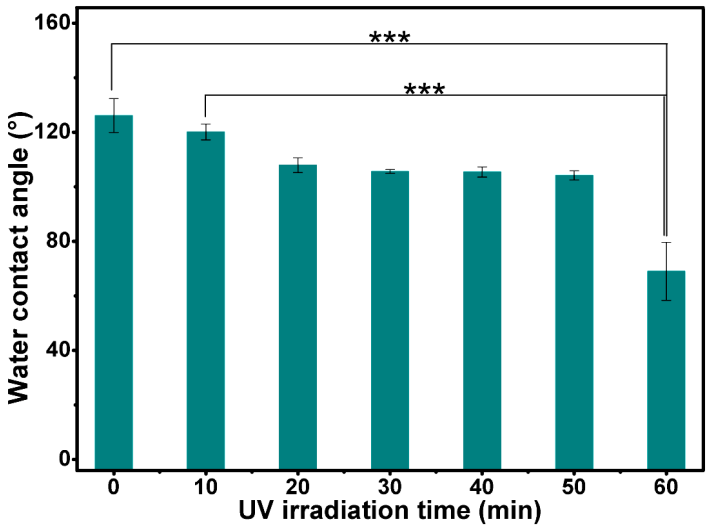

Figure 45. Effect of SMBD functionalization on water contact angle of EVAL as a function of UV irradiation periods. The '0' minutes stands for neat EVAL

4.2.3.2. Degree of Grafting

The estimated values of percentage degree of grafting are provided in Figure 46. A gradual increase in DG was observed as a function of UV irradiation period. The maximum DG obtained after 60 minutes UV irradiation was approximately 11 %.

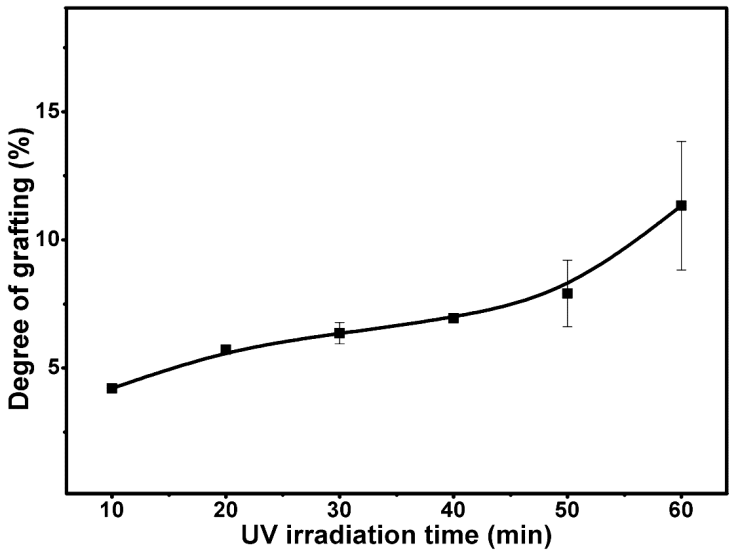

Figure 46. Degree of grafting of SMDB functionalized EVAL as a function of UV irradiation time

4.2.3.3. Pore size and porosity analysis

The pore characteristics of neat and SMDB grafted EVAL is provided in Table 17. The SMDB grafting had no considerable effect on the pore size of the membranes. The percentage porosity of neat and SMDB functionalized EVAL is expressed in Table 17. These porosities were neither altered by the functionalization.

UV irradiation time (min)	Pore size (μm), n=25	Porosity (%), n=3
Neat EVAL	23.3 ± 5	53 ± 1
10	21.5 ± 7	52 ± 0.5
20	20.3 ± 8	52 ± 0.7
30	18.7 ± 7	52 ± 0.7
40	19.6 ± 7	52 ± 0.4
50	18.9 ± 7	52 ± 0.4
60	22.2 ± 8	52 ± 1

Table 17. Effect of SMDB functionalization on the pore size and porosity of EVAL

4.2.3.4. *In vitro* hemocompatibility evaluation

The influence of SMDB grafting on the blood parameters was assessed by the *in vitro* hemocompatibility evaluation by means of plasma protein adsorption, platelet adhesion, blood cell consumption studies and hemolysis and the data are compared in Table 18. It can be seen that there was no significant change in the plasma protein adsorption as a result of SMBD grafting. The data on blood cell adhesion studies of neat and SMDB grafted EVAL are compared (Table 18). It can be inferred that the WBC consumption by neat EVAL was not significantly altered after grafting with SMDB, however, there was a dramatic decrease in the RBC consumption by neat EVAL after modification. The minimum modification time of 10 minutes could effectively reduce the RBC consumption of neat EVAL. However the SMDB functionalization did not particularly affect the adhesion of platelets from whole blood. As expected, the platelet

adhesion from PRP was remarkably reduced as result of SMDB grafting (Table 18 and Figure 47). It is obvious form these images that a higher amount of platelets were adhered on neat EVAL membrane while all the SMDB grafted EVAL membranes manifested an inhibition to platelets (Figure 47). The platelets were also compact on neat EVAL membrane. In addition, the adhered platelets on neat and SMDB grafted EVAL membranes demonstrated spherical morphology devoid of pseudopodium deformation (Figure 47). The haemolytic evaluation was also performed in order to understand the risks, if any, caused by the SMDB modification due to RBC damage. The results of which provided in Table 18, highlight that there was a highly significant and effective reduction in the percentage hemolysis as a result of SMDB grafting.

UV irradiation time (min)	Protein adsorption (µg/mm^3)	RBC adhesion (%) *	WBC adhesion (%)	Platelet adhesion (%)		Hemolysis (%) *
				PRP *	WB	
0	7.2 ± 1.6	68 ± 10.0	96 ± 2	72 ± 15	96 ± 3	2.3 ± 0.5
10	7.5 ± 0.8	3.4 ± 0.3	99 ± 1	52 ± 8	81 ± 9	0.18 ± 0.1
20	8.4 ± 0.5	3.2 ± 2.7	98.4 ± 0	41 ± 1	68 ± 26	0.18 ± 0.1
30	8.9 ± 1.7	7.9 ± 2.0	98.4 ± 0	52 ± 14	71 ± 7	0.20 ± 0.1
40	8.7 ± 0.7	8.6 ± 2.0	100 ± 0	44 ± 11	71 ± 9	0.1 ± 0.08
50	8.5 ± 0.5	3.2 ± 3.0	100 ± 0	43 ± 14	91 ± 3	0.08 ± 0.02
60	8.7 ± 0.3	9.5 ± 1.5	99 ± 1	40 ± 4	78 ± 17	0.08 ± 0.01

Table 18. *In vitro* hemocompatibility evaluation of PSMDB-g-EVAL obtained at various UV irradiation times

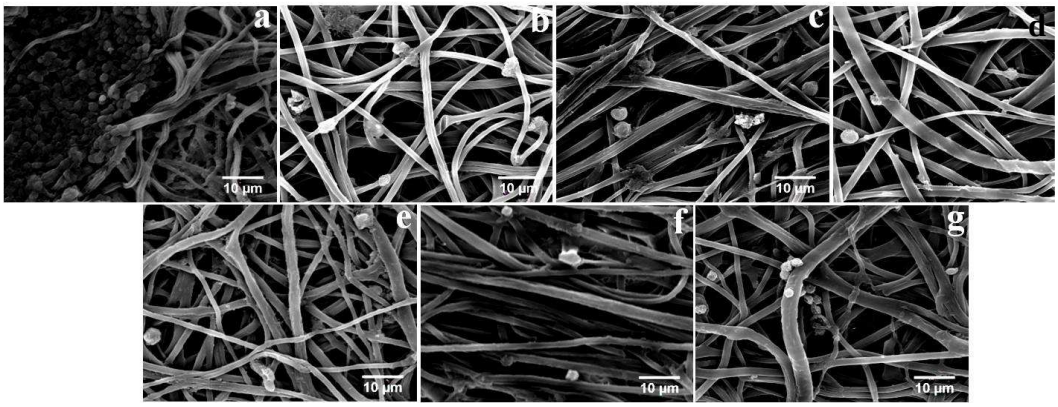

Figure 47. SEM images of membranes after exposure to platelets. (a) Neat EVAL and (b-g) SMDB functionalized EVAL with UV irradiation time 10, 20, 30, 40, 50 and 60 minutes respectively

4.2.3.5. Evaluation of leukodepletion efficiency of zwitterions bearing EVAL membranes: EVAL-Gly and PSMDB-g-EVAL membranes

The overall leukodepletion efficiency of the two zwitterionic EVAL membranes was compared. For this, from all the modified membranes, EVAL-Gly-1% and PSMDB-g-EVAL-60 were found to have ideal blood contacting and membrane properties. Hence these systems were fabricated into asymmetric filters for whole blood filtration. The SEM images of the top layer membranes (obtained at a speed of 500 RPM) is already given in Figure 38 and Figure 43, while image of the bottom layer placed in the filter, obtained at a collection rate of 1500 RPM, are provided in Figure 48 and the measured membrane parameters are provided in Table 19. It was observed that the fiber diameter and porosity for both the membrane systems remained unaltered with increase in the collection speed.

But the pore diameter was reduced with increase in the collection speed for both the zwitterions bearing membranes.

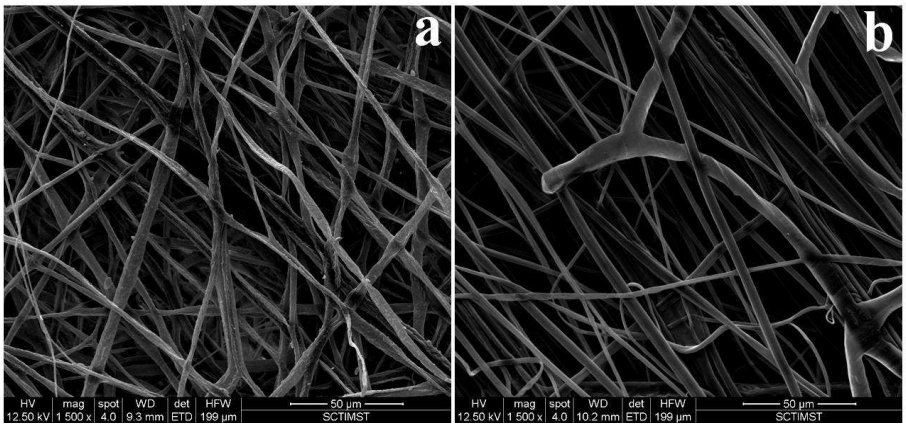

Figure 48.: SEM images of (a) EVAL-Gly-1% and (b) PSMDB-g-EVAL membranes obtained at a speed of 1500 RPM

Membrane	Collection speed (RPM)	Fiber diameter (µm)	Pore diameter (%)	Porosity (%)
EVAL-Gly-1%	500	2.0 ± 0.2[a]	13.0 ± 3[a]	51 ± 0.2[a]
EVAL-Gly-1%	1500	2.0 ± 0.4	7.8 ± 1.5	52 ± 0.2
PSMDB-g-EVAL-60	500	2.3 ± 0.3[b]	22.2 ± 8[c]	52 ± 1[c]
PSMDB-g-EVAL-60	1500	2.4 ± 0.2	10.9 ± 2.7	52 ± 0.4

[a] Values taken from Table 15; [b] Values taken from Figure 44; [c] Values taken from Table 17

Table 19. Membrane properties of EVAL-Gly and PSMDB-g-EVAL asymmetric filters

Figure 49 shows the leukodepletion efficiency of both the zwitterionic membrane systems. It is very clear that no significant difference in platelet adhesion was observed

among the three filters. The WBC depletion efficiency of PSMDB-g-EVAL-60 membranes was lower than that of the neat EVAL and EVAL-Gly-1% membranes. Both the zwitterionic systems did not induce any hemolysis. But the EVAL-Gly-1% membranes offered resistance to blood flow and hence decreased the speed of filtration.

The distribution of cells on the filter membranes were also compared in Figure 50 to Figure 53. WBCs were seen on all layers of filters of both the membranes as indicated by the SEM images in Figure 50 and Figure 52. The microscopic images revealed a comparatively higher population of WBC throughout the EVAL-Gly-1% (Figure 51) than that on the PSMDB-g-EVAL-60 filter (Figure 53). These images thus support the quantitative data of cell adhesion provided in Figure 49.

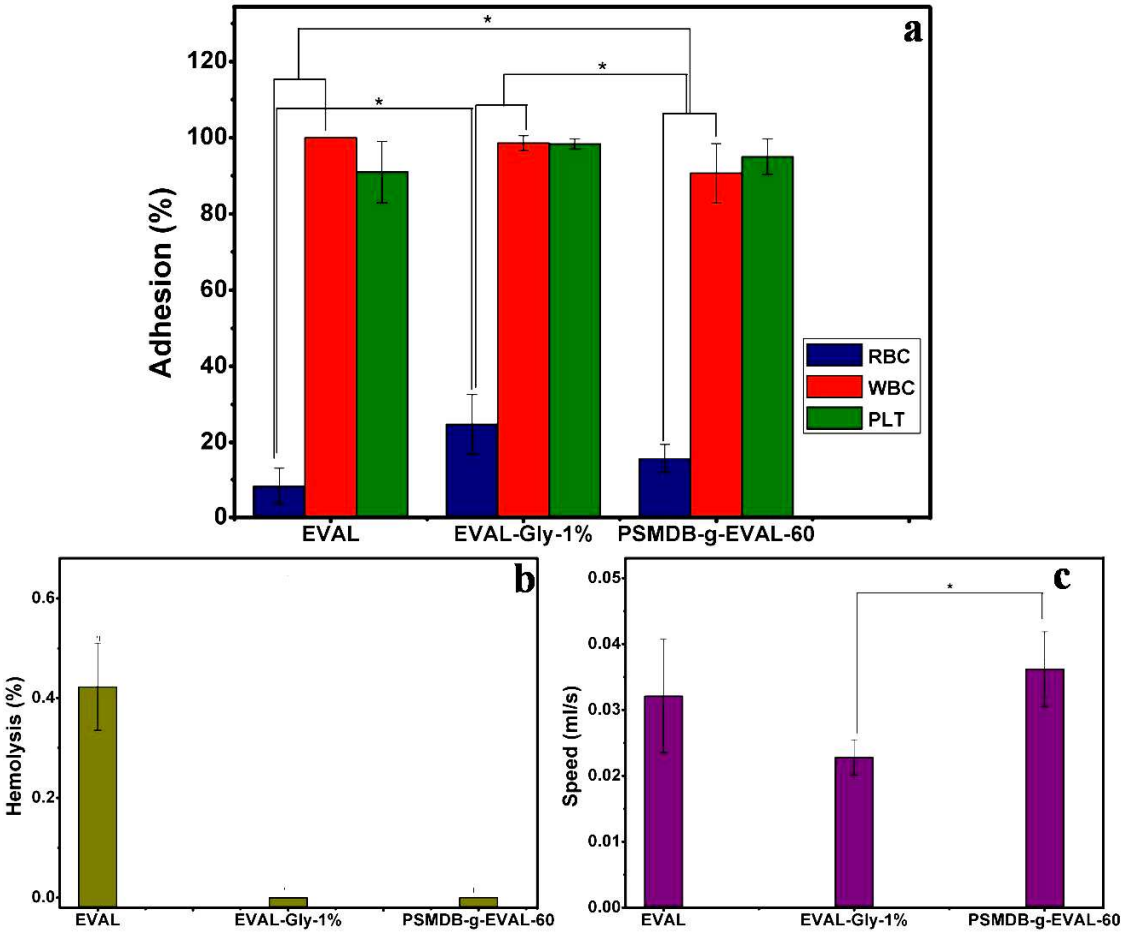

Figure 49. Comparison of leukodepletion efficiency of zwitterions bearing EVAL asymmetric filters- EVAL-Gly-1% and PSMDB-g-EVAL-60 with neat EVAL asymmetric filter

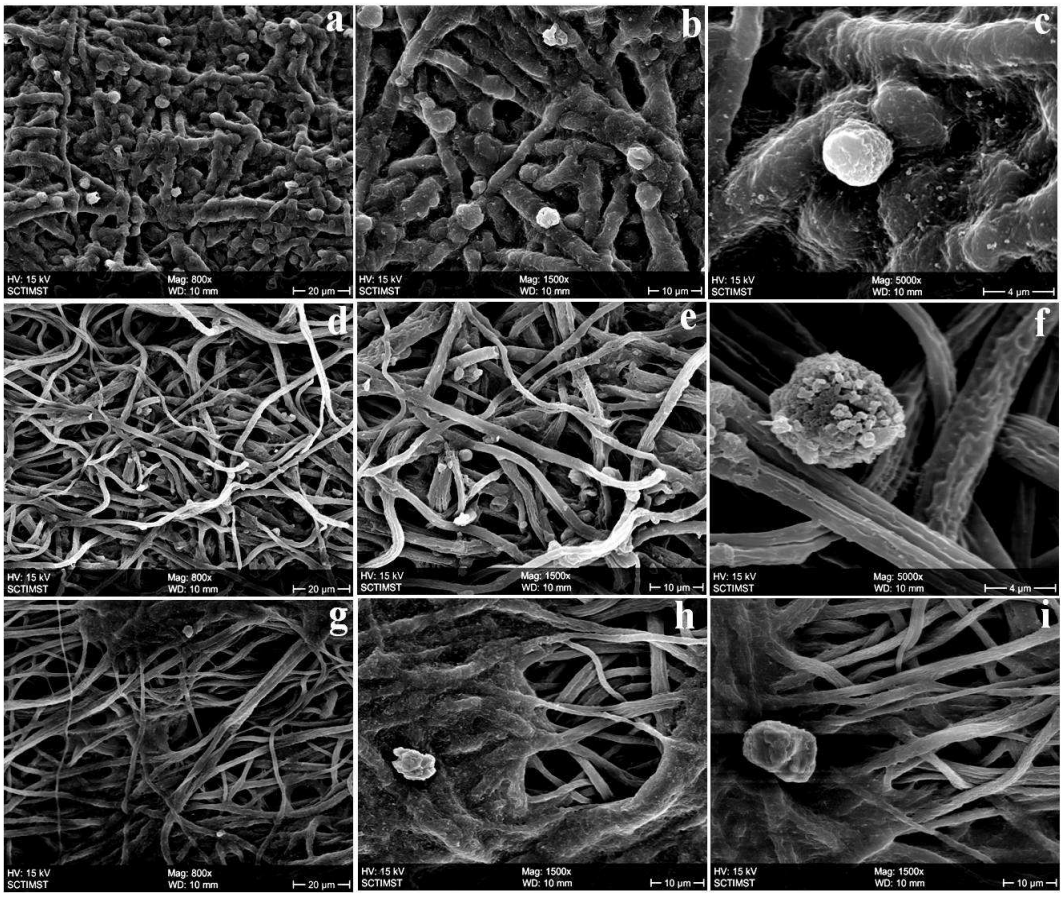

Figure 50. SEM analysis of adhered cells to the EVAL-Gly-1% filter; (a-c) top layer, (d-f) middle layer and (g-i) bottom layer at different magnifications

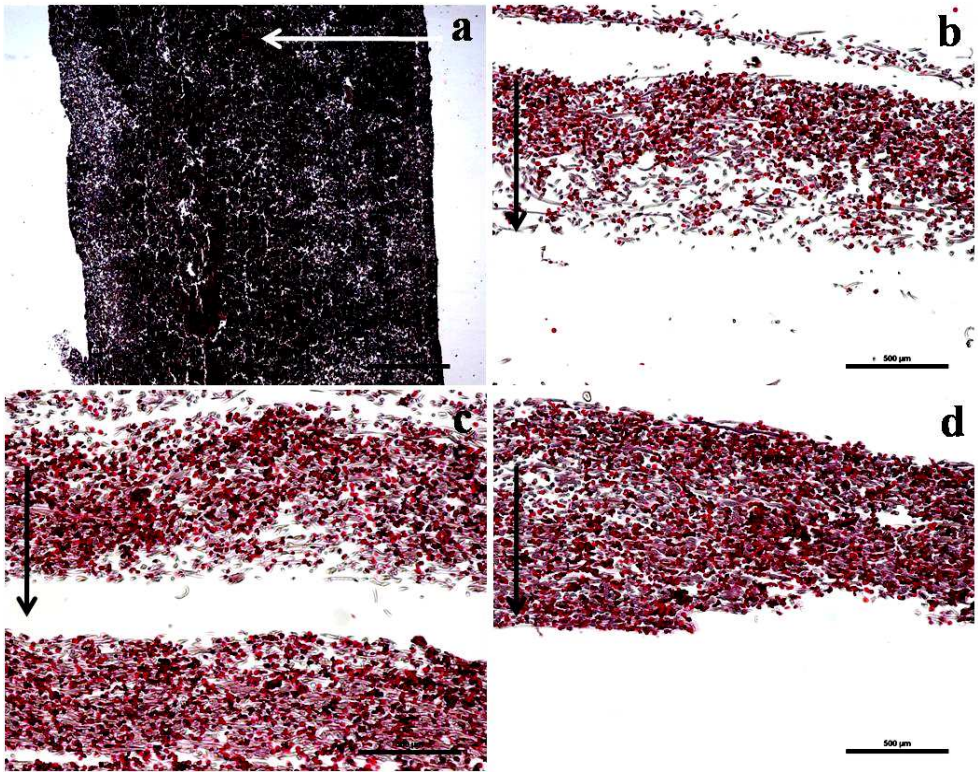

Figure 51. Histological examinations of stained cross sections of EVAL-Gly-1% filter membrane assembly. The arrow indicates the direction of blood flow

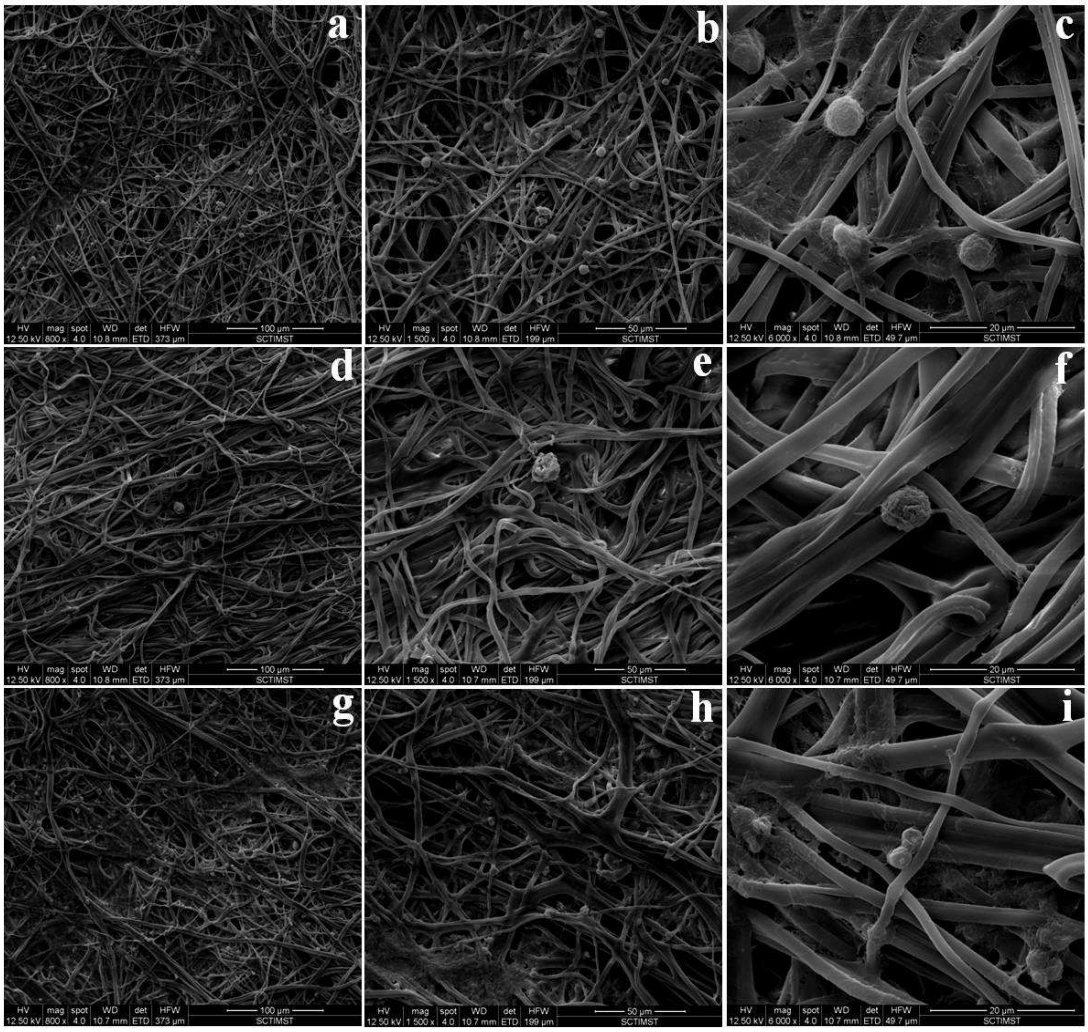

Figure 52. SEM analysis of adhered cells to the PSMDB-g-EVAL-60 filter; (a-c) top layer, (d-f) middle layer and (g-i) bottom layer at different magnifications

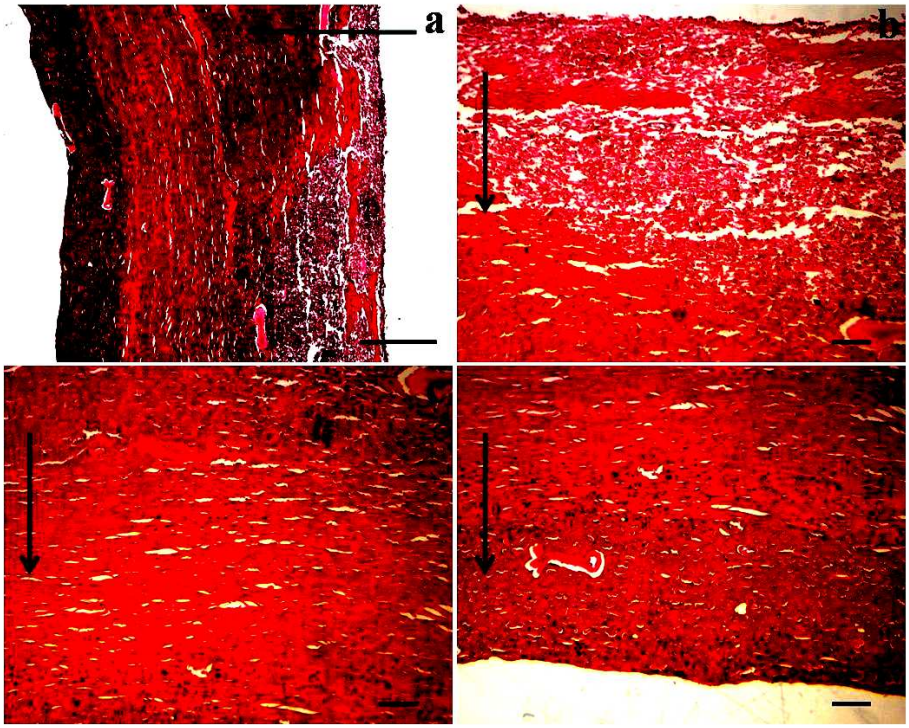

Figure 53. Histological examinations of stained cross sections of PSMDB-g-EVAL-60 filter membrane assembly. The arrow indicates the direction of blood flow

4.2.4. Fabrication and characterization of BSA immobilized EVAL membranes

4.2.4.1. Immobilization of BSA on EVAL membranes

BSA was immobilized on electrospun EVAL membranes via. self polymerizable dopamine spacer. The proposed mechanism for this reaction is provided in Figure 54. Dopamine readily polymerized to polydopamine (PD) attaches firmly to the EVAL membrane surface providing further functionalities for reacting with the BSA through its amino groups. The PD formation on EVAL membranes was visualized by the black

coloration to EVAL membranes in the Figure 8. The membranes were further characterized as described in the following sections

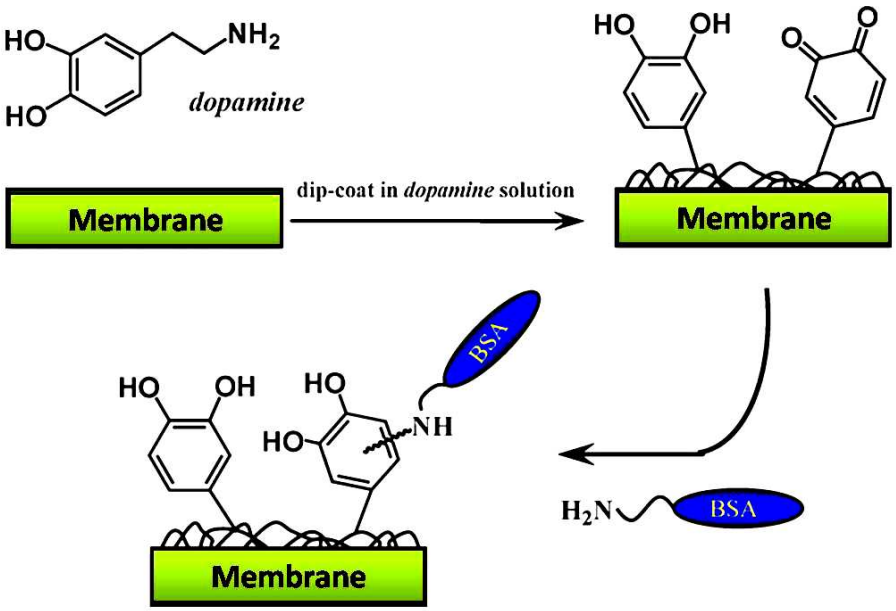

Figure 54. Mechanism of BSA immobilization on membrane via dopamine

4.2.4.2. Surface characterization

The ATR-FTIR spectra of neat EVAL, EVAL-polydopamine (EVAL-PD) and various BSA immobilized EVAL membranes (EVAL-BSA) are compared in Figure 55. It is clearly observed from the spectra that there was a new peak formation at 1604 cm^{-1} which indicates the presence of C=O groups derived from PD. After BSA immobilization, this peak was shifted to higher wave number, 1655 cm^{-1} which derives from the C=O moieties in BSA. The SEM pictures in Figure 56 show the formation of PD particles on the EVAL fiber surface. However, after the immobilization of BSA, the concentration of PD particles was reduced. The smooth morphology of the fibers was retained after BSA

immobilization, with a gradual increase in the fiber diameter with increase in the BSA concentration (Table 20). Interestingly, the pore sizes of the EVAL membranes were found to significantly reducing after the functionalization while the percentage porosity was decreased initially after the formation of PD particles and further increased after the BSA immobilization (Table 20). Hence the percentage porosity of the neat EVAL and EVAL-BSA membranes remained more or less uniform. Similarly, the WCA was found to reducing after the formation of PD layer, which indicates that the hydrophilicity of EVAL was slightly enhanced due to the incorporation of PD. However, the WCA was increased after the BSA immobilization (Table 20). So it has to be noted that the BSA chains offered hydrophobicity to the EVAL-PD membranes. The overall wettability of the EVAL-BSA membranes were similar to that of the neat EVAL.

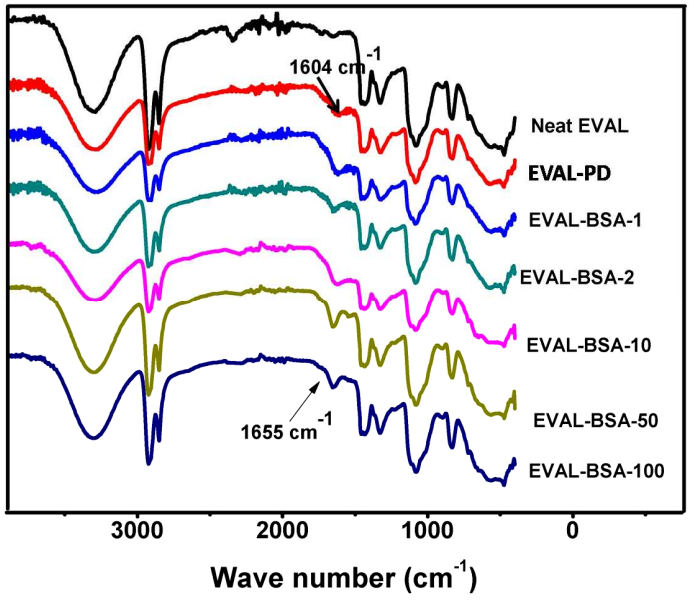

Figure 55. ATR-FTIR spectra of EVAL-BSA membranes

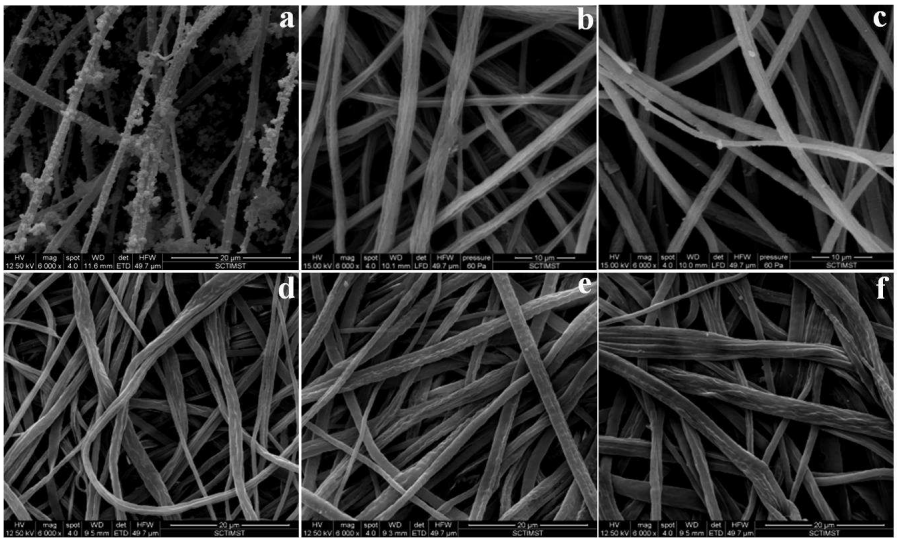

Figure 56. SEM images of (a) EVAL-PD, (b) EVAL-BSA-1, (c) EVAL-BSA-2, (d) EVAL-BSA-10, (e) EVAL-BSA-50 and (c) EVAL-BSA-100

Sample	WCA (°) *	Fiber diameter (µm) *	Pore diameter (µm)	Porosity (%)
Neat EVAL	126 ± 6	1.8 ± 0.1	23.3 ± 5	53 ± 1.0
EVAL-PD	115 ± 3	2.2 ± 0.3	-	49 ± 0.5
EVAL-BSA-1	129 ± 3	2.3 ± 0.3	17.9 ± 3.2	52 ± 0.3
EVAL-BSA-2	135 ± 7	2.5 ± 0.3	19.6 ± 3.4	53 ± 1.0
EVAL-BSA-10	125 ± 5	2.4 ± 0.2	16.2 ± 2.7	51 ± 0.2
EVAL-BSA-50	127 ± 1	2.7 ± 0.2	17.6 ± 3.2	52 ± 0.1
EVAL-BSA-100	118 ± 5	3.0 ± 0.1	13.9 ± 2.5	52 ± 0.4

Table 20. Properties of the EVAL-BSA membranes

4.2.4.3. *In vitro* hemocompatibility evaluation

Table 21 shows the effect of BSA immobilization on the various blood parameters. The plasma protein adsorption was found to be dramatically increasing with increase in the immobilized BSA concentration. The adhesion of RBCs was gradually reduced while no change in the WBC adhesion was recorded. The platelet adhesion showed different trends when the both the neat and BSA immobilized membranes were exposed to PRP and WB. No noticeable change in the platelet adhesion was observed when the samples were exposed to WB, while the platelets from PRP became repellant to the EVAL-BSA membranes. This is also evidenced from the SEM images of membrane exposed to PRP, provided in Figure 57. The percentage hemolysis was also initially decreasing at lower concentrations of BSA while the membranes, for which the BSA concentration was ≥ 50 g/L, induced very high hemolysis.

BSA concentration (g/L)	Protein adsorption (μg/mm^3)*	RBC adhesion (%)*	WBC adhesion (%)	Platelet adhesion (%)		Hemolysis (%)*
				PRP*	WB	
0 (neat EVAL)	7.2 ± 1.6	68 ± 10	96 ± 2.0	72 ± 15	96 ± 3	2.3 ± 0.5
1	19.0 ± 5.0	35 ± 5	99 ± 0.6	45 ± 3	98 ± 3	0.3 ± 0.04
2	19.0 ± 3.0	44 ± 5	98 ± 0.6	67 ± 12	94 ± 3	0.4 ± 0.1
10	18.0 ± 3.0	5 ± 2	97 ± 1.0	37 ± 8	84 ± 2	0.3 ± 0.05
50	23.0 ± 2.0	14 ± 5	96 ± 1.0	49 ± 8	95 ± 1	1.7 ± 0.1
100	20.0 ± 4.0	13 ± 4	96 ± 1.0	31 ± 3	99 ± 1	3.5 ± 1.0

Table 21. *In vitro* hemocompatibility evaluation of EVAL-BSA membranes

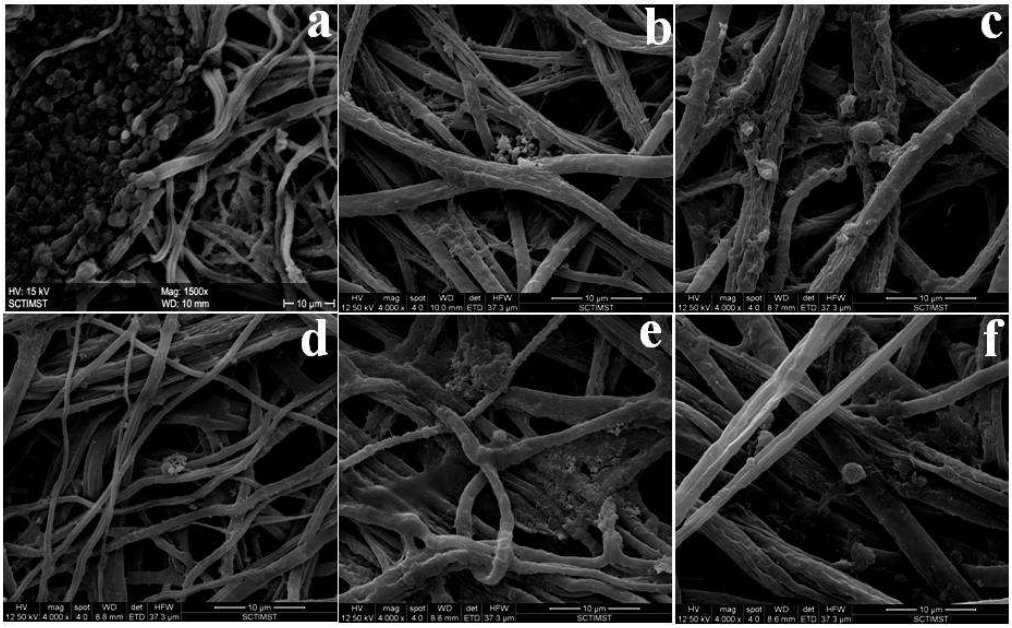

Figure 57. SEM images of EVAL-BSA membranes after exposure to PRP; (a) neat EVAL, (b) EVAL-BSA-1, (c) EVAL-BSA-2, (d) EVAL-BSA-10, (e) EVAL-BSA-50 and (f) EVAL-BSA-100

4.2.4.4. Evaluation of leukodepletion efficiency by EVAL-BSA membranes

From Table 21, it was understood that the EVAL-BSA-10 membranes possessed the ideal hemocompatibility desired for leukodepletion filter membranes. Hence these membranes were fabricated into asymmetric filters. The membrane properties of top and bottom layers in the asymmetric filter are recorded in Table 22. It can be seen that the pore size of the bottom layer, obtained at a collection speed of 1500 RPM was lower than that of the top layers whereas the percentage porosity and fiber diameter remained constant.

Collection speed	Fiber diameter (µm)	Pore diameter (µm)	Porosity (%)
500 RPM	2.4 ± 0.2[a]	16.2 ± 2.7[a]	51 ± 0.2[a]
1500 RPM	2.1 ± 0.5	10.7 ± 2.6	52 ± 0.3

[a] Values taken from Table 20

Table 22. Membrane properties of EVAL-BSA-10 asymmetric filter

Upon whole blood filtration, it was observed that the WBC adhesion on the EVAL-BSA-10 membranes was reduced significantly and the RBC adhesion was enhanced than those of neat EVAL [Figure 58 (a)]. No change in platelet adhesion was observed as a result of BSA immobilization. Interestingly, the speed of filtration was very much lower for the EVAL-BSA-10 filter than that of neat EVAL [Figure 58 (c)]. The percentage hemolysis induced by the EVAL-BSA-10 filter was found to be approximately zero [Figure 58 (b)].

Figure 59 and Figure 60 depicts the distribution of cells through the various layers of EVAL-BSA-10 asymmetric filter. From the microscopic images provided in Figure 60,

it can be visualized that all the layers were highly populated with cells. However, most of the WBCs were present in top and middle layers than bottom layer according to the SEM (Figure 59) and microscopic images (Figure 60). In addition, it can also be inferred that a higher amount of RBCs were present on EVAL-BSA-10 filter (Figure 60) than that of neat EVAL filter (Figure 16) which is in good agreement with the quantitative data given in Figure 58.

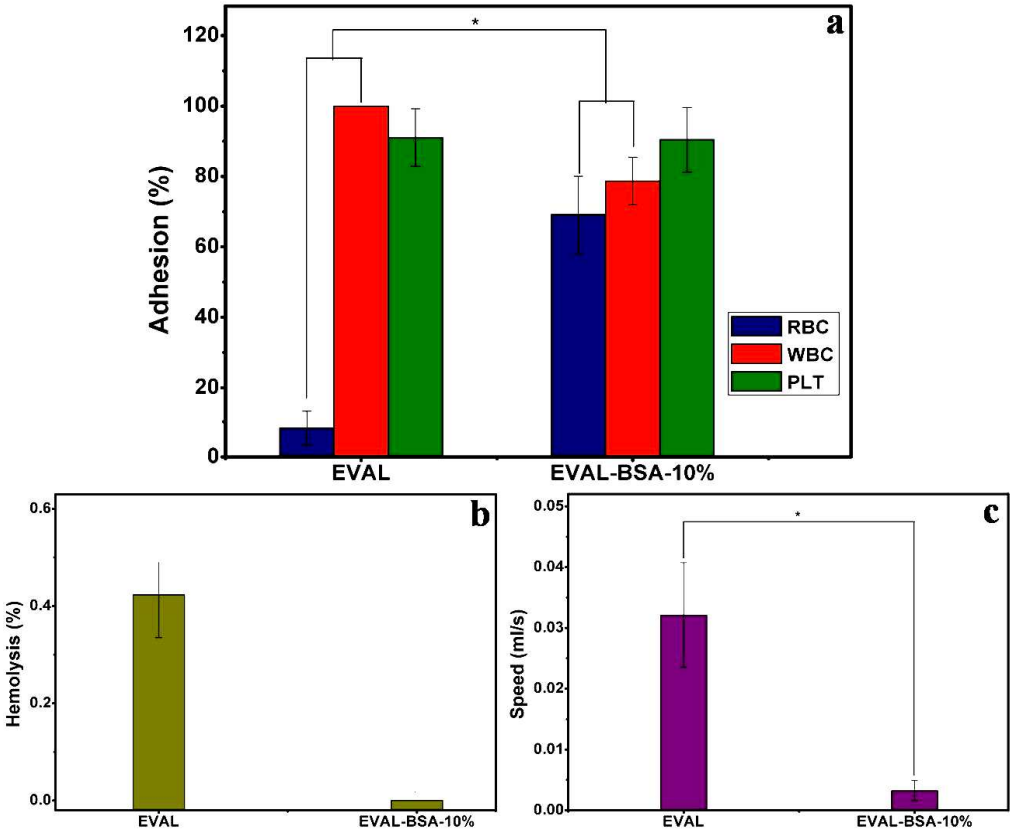

Figure 58. Comparison of leukodepletion efficiency of neat EVAL and EVAL-BSA-10 asymmetric filters

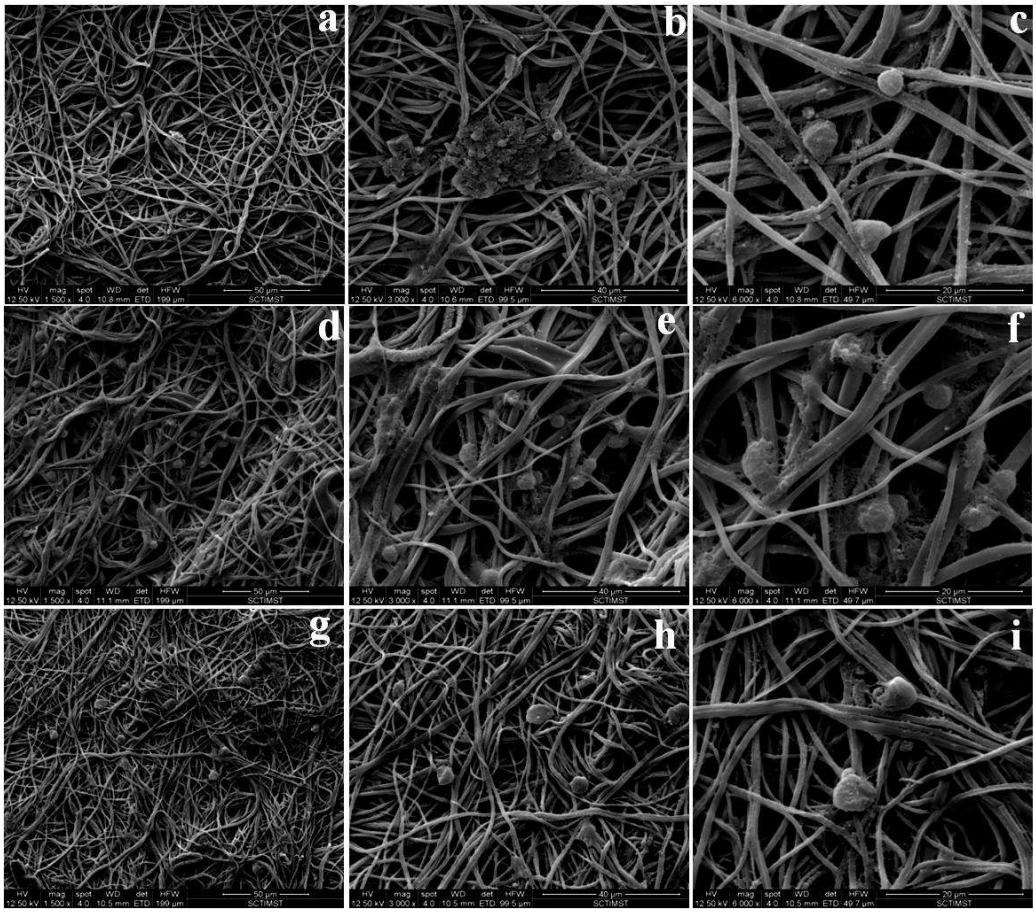

Figure 59. SEM analysis of adhered cells to the EVAL-BSA-10 filter; (a-c) top layer, (d-f) middle layer and (g-i) bottom layer at different magnifications

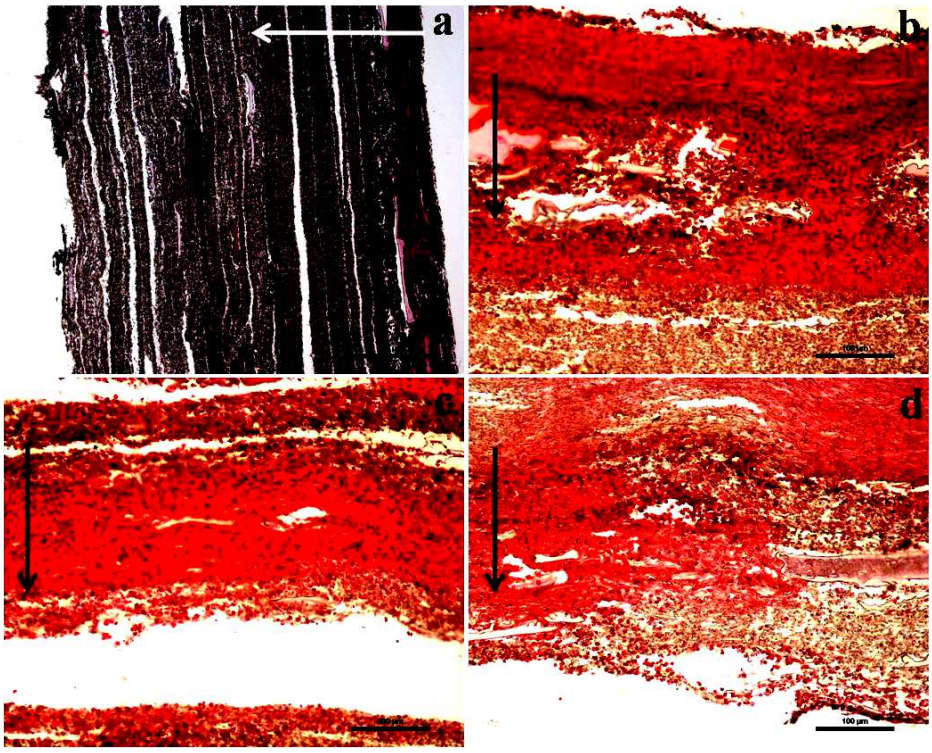

Figure 60. Histological examinations of stained cross sections of EVAL-BSA-10 filter membrane assembly. The arrow indicates the direction of blood flow

4.3. Comparison of leukodepletion efficiency of the various modified and unmodified filters

The leukodepletion efficiencies of various electrospun membrane based filters viz PAN, neat EVAL, PHEA-g-EVAL-60, EVAL-Gly-1%, PSMDB-g-EVAL-60 and EVAL-BSA-10 were compared with each other in Figure 61. The efficiencies were also correlated with their corresponding WCA. It can be seen that out of the 6 filters compared each have a different surface chemistry and wettability. The PAN, neat EVAL, EVAL-Gly-1% and EVAL-BSA-10 was found to hydrophobic while PHEA-g-EVAL-60 and

PSMDB-g-EVAL-60 were hydrophilic. The leukodepletion by hydrophobic PAN filter was much poor than the hydrophobic neat EVAL filter. The overall efficiency was decreased in the PHEA-g-EVAL-60 than that in neat EVAL. Among the two zwitterions bearing EVAL membranes, the PSMDB-g-EVAL-60 was highly hydrophilic while the other one, EVAL-Gly-1%, was highly hydrophobic. The PSMDB-g-EVAL, being the most hydrophilic system, gave sufficiently high leukodepletion efficiency. In case of EVAL-BSA-10 filter, the membranes were hydrophobic, but its leukodepletion efficiency was lower than that of neat EVAL and EVAL-Gly-1%.

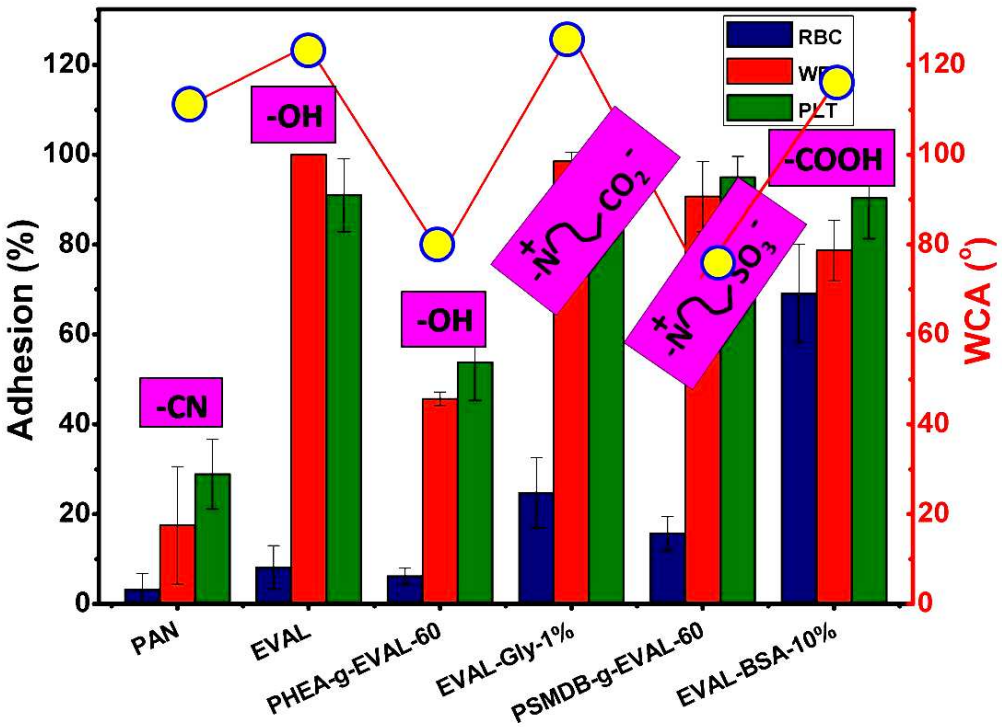

Figure 61. Comparison of wettability, surface chemistry and leukodepletion efficiency of the developed filters

CHAPTER 5

DISCUSSION

Chapter 5 contains the discussion and interpretation of the study results detailed in Chapter 4. The major findings of this study are correlated with published literature in the relevant field and interpretations made wherever possible.

5.1. Fabrication and characterization and evaluation of leukodepletion efficiency of electrospun membranes

The concept of fragmentation of whole blood into various blood components has brought great contributions to the transfusion based therapies. However, the risks associated with such component based therapies were later disclosed from clinical trials and practices. Thus it was identified that WBCs present in the donor blood cause several complications in the recipient (Högman, 1997; Kim *et al.*, 2009; Mijović *et al.*, 1983). These catastrophes strongly recommended the leukodepletion of blood and blood products. Membrane based filtration of blood has been proven as the most versatile method for leukocyte depletion. A numbers these kinds of filters are available in market and made the filtration process much easier.

The present study was aimed to fabricate a novel electrospun fiber based membrane filter out of suitable blood compatible polymers for effective removal of leukocytes from whole blood. Electrospinning has been proven successful for the

generation of fibroporous matrices for various applications including biomedical applications. Filter membranes are one among the noteworthy uses of electrospun membranes. A number of electrospun polymers have reported to be best membranes for the purification of air and water (Guibo *et al.*, 2013; Gule *et al.*, 2012; Zhang *et al.*, 2010). Yet it seems like electrospinning has been concealed by the various other conventional techniques when concerned with the fabrication of leukodepletion membranes.

The present study focused on fabrication of membrane materials by electrospinning of highly blood compatible EVAL and PAN. Electrospinning of EVAL has also been reported by previous researchers from its solution in various solvents like 2-propanol/water mixture 70/30 and 80/20 compositions, HFIP etc. (Kenawy *et al.*, 2003; Namekawa *et al*., 2014; Xu *et al.*, 2011). Some peculiarities like clogging during the electrospinning of EVAL at a rate of 10 mL/h were observed. Similar effects during the spinning of EVAL were also reported earlier (Kenawy *et al.*, 2003).

DMF was used for the electrospinning of PAN as reported by previous researchers due to its favorable boiling point and excellent conductivity (Jeun *et al.*, 2015). The PAN-DMF solution has a pale yellow color due to the conjugation of CN bonds and the resulting PAN fibers were highly delicate and fluffy to handle (Ji and Zhang, 2008). Due to variation in the collector speed, it was expected that the device is an asymmetric filter device consisting of upper layers of more porous membranes than the bottom layer.

It is appropriate to study the morphological features and pore properties of the electrospun membrane to assess their performance. Both the EVAL and PAN membrane fabricated by electrospinning was composed of fine, well packed, regular and smooth network of fibers (Figure 10). Varying the flow rate of EVAL significantly altered the fiber diameter. The maximum fiber diameter obtained was 3 μm at a flow rate of 1 mL/min (Table 7). Increasing the fiber diameter further beyond this limit resulted in loss of polymer solution through dripping. The fiber diameter was not much influenced by the rotating speed of the collector (Table 7).

The suitability of the electrospinning technique was disclosed from the tuned pore properties of the membranes. The pore properties of the electrospun membranes were investigated by means of ImageJ analysis. It was Ghasemi-Mobarakeh *et al* who introduced a novel method for porosity estimation by ImageJ analysis from the SEM images (Ghasemi-Mobarakeh *et al.,* 2007). The method is advantageous over to other methods of porosity estimation because it is very simple and measures the porosity of various surface layers of the electrospun membranes (Ghasemi-Mobarakeh *et al.,* 2007). The mean pores sizes of all the membranes were higher than the size of blood cells (Table 7). This ensures sufficient entrapment of leukocytes in the fibrous network while allowing the RBCs to deform and percolate through the pores. The higher porosity of the membranes generated by method of electrospinning is also expected to facilitate smooth flow of the blood.

The use of solvents in the process of electrospinning is sometimes disfavored when the resulting membrane are intended to be used for biomedical applications. Hence the evaluation of toxicity for the electrospun membranes is of great importance. The findings reveal that there was a good interaction of the L929 cells with both electrospun EVAL and PAN membranes (Figure 12). The morphology of the cells was preserved when grown on both (Figure 12). The hemolysis caused by electrospun EVAL and PAN was negligible and is less than 2 %, in the *in vitro* study, which is safe according to the reports of Dhandhayuthappani *et al* (Table 8) (Dhandayuthapani *et al.*, 2012).

The developed membranes out of electrospun EVAL and PAN have been evaluated experimentally by filtering whole blood. The results presented in Figure 14 emphasize that EVAL filter resulted in high leukocyte removal as compared to the commercially available filter while the PAN filter showed very poor WBC depletion efficiency. The retention of other components like RBCs and platelets was also established. The RBC adhesion to the EVAL filter membrane was comparable to the control while no significant change in platelet adhesion was observed. Interestingly, the RBC and platelet adhesion on the PAN filter was noticeably lower than those on the control. The performances of the filters towards leukodepletion are mediated by the physico-chemical and morphological properties of the membranes. The surface chemistry, surface roughness, wettability, pore size, porosity and fiber packing of the membranes are believed to play pivotal roles in determining its leukodepletion efficiency (Matheis *et al.*, 2002).

The chosen grade of EVAL and PAN is inherently hydrophobic as indicated by their water contact angle despite of the hydroxyl bearing vinyl alcohol segments in EVAL (Figure 11). Thus the membrane surfaces are supposed to invite the proteins in their environment and this pre-adsorbed protein may triggers further transport of leukocytes and platelets. There are no available reports on the interaction of CN groups on leukocytes. However, previous reports by Curtis *et al* strongly suggest that the hydroxyl functionalities in the material surface play a vital role in leukocyte adhesion (Curtis *et al*., 1983). But other relevant properties of the developed membranes also need to be studied well to interpret the efficiencies (Bruil *et al.,* 1994).

Several researchers have suggested the possible mechanisms of leukodepletion by membranes but the exact mechanism is not yet manifested (Bruil *et al.,* 1995, Natori *et al.,* 2006). Here the approach of designing the asymmetric membranes in the filter was intended for the sieving of leukocytes due to the varying pore sizes and facilitating RBCs and platelets to pass through. Interestingly, the SEM photographs for the membranes after filtration, highlights that the leukocytes were trapped by sticking to the fibers immediately when they came in contact with them (Figure 15 and Figure 17). However, the pore size and porosity, both in top layer and bottom layer, was helpful for the fine passage of RBCs and was the reason for the high RBC retention after filtration for both EVAL and PAN filter. The leukocytes were even widely spread throughout reflecting a good interaction with the electrospun EVAL membrane (Figure 15). Obviously, the vivid vision of leukocytes sticking to the fibers in the SEM images strongly support that leukodepletion mechanism was predominantly adhesion (Figure 15 and Figure 17). But

the PAN filter membranes had a very weak interaction with the WBCs as observed from the SEM images. At the same time, the microscopic images also reveal a comparatively lower population of WBCs than those on EVAL filter membranes (Figure 16 and Figure 18). These images also support the results of adhered cell counts after filtration. So from these observations, it may be concluded that the leukocytes are removed by the developed filer by means of adhesion mechanism rather than sieving.

The assessment of true efficiency of leukodepletion by filters is ascertained from the magnitude of the cell adhesion/retention. The filters are found to be reliable if the residual leukocyte count after filtration is below a threshold of 10^6 while the exact count varies according to different guidelines. However, all the guidelines strongly agree to the maximum retention of other functional and viable blood components. Here the residual leukocyte count after filtration through the EVAL electrospun membrane filter was zero or in other words, the filter could achieve 100 % leukodepletion while the results of PAN filter was not satisfactory (Figure 14). Apparently, the RBC retention was significantly comparable to the commercial filter while 5-10 % of RBC loss due to adhesion to filters is accepted (Sharma *et al.*, 2014). Unlikely, the retention of platelets was less pronounced. It is also noticeable that the commercial filter was poor in platelet retention and there was no significant change in platelet retention between the commercial filter and the EVAL filter. It may be noted that platelets have a tendency to adhere to material surfaces and this issue of platelet adhesion is always encountered wherever whole blood is filtered. As a consequence, the commercial leukodepletion filters are employed after the removal of platelets by centrifugation of blood (Natori *et al.*, 2006). It was shown by previous

researchers that the adhered platelets play a key role in promoting the subsequent leukocyte adhesion to the filter membranes (Kjeldsen-Kragh and Golebiowska, 2002). Hence the presented results are in good agreement with this fact.

The duration of filtration is also important in predicting the efficiency of filters. The method of leukodepletion by filtration is less time consuming when compared to other leukoreduction methods, but further optimization to reduce the filtration time would be desirable. The filtration time for developed EVAL and PAN electrospun membrane filters was observed to be comparable to that for the commercial one [Figure 14 (c)]. Contradictory results were previously observed by Guo *et al* when they placed an electrospun PBT layer at the exit of filter composed of meltblown PBT layers. The filtration time was dramatically increased from 2.5 minutes to 65 minutes due to the smaller pore size and poor wettability of the electrospun PBT layer (Guo *et al.*, 2013).

Thus, the results obtained for PAN filter suggested that electrospun PAN membranes were not suitable for fabrication of highly efficient leukodepletion filter. So it was excluded from the study. But the overall performance of the electrospun EVAL leukodepletion filter clearly indicates that it is comparable to the performance of commercial filter in complete removal of leukocytes and recovery of other functional components. Even though the significant adhesion of platelets is not acceptable, approach of any surface modification technique for improving the surface properties of the electrospun EVAL membrane is expected to generate a platelet retardant and more efficient leukodepletion filter. Hence the developed EVAL filter as such may be useful

for the removal of both leukocytes and platelets from whole blood and if modified properly it may be an excellent leukodepletion filter competitive to the marketed filter.

The study also investigated the effect of filter structure, fiber diameter, pore diameter and porosity upon the leukodepletion efficiency of EVAL filter. Previous study by Bruil *et al* also investigated the effect of filter structure on the leukocyte depletion efficiency of open cellular polyurethane membranes with pore sizes varying from 15 μm - 65 μm (Bruil *et al.*, 1991). They concluded that asymmetric filter was advantageous to the symmetric filter in all respects of leukodepletion including WBC adhesion, RBC retention and hemolysis (Bruil *et al.*, 1991). The present studies with electrospun non-woven EVAL membranes are also in well agreement with this (Figure 19). Notwithstanding the higher pore size of the EVAL-S filter than the bottom layer of EVAL-AS filter, there was a plugging of the cells as evidenced from the data of cell adhesion (Figure 19), SEM (Figure 20) and microscopic images (Figure 21) of various layers of EVAL-S filter. Obviously the RBC retention through the EVAL-S filter was also not satisfactory. So from the light of these data it has to be inferred that the leukodepletion by electrospun non-woven are not influenced by the membrane pore size however sufficient pore size may help in retention of other functional components.

It was also disclosed from Figure 22 and Figure 24 that non-woven membranes composed of electrospun nanofibers had a low capacity for leukocyte removal. Umegae *et al* and Shirokaze *et al* investigated on the effect of diameter of the fibers in the PET non-woven fabric on the leukocyte removal efficiency (Shirokaze, 2002; Umegae *et al.*, 1988). They found that very high leukocyte removal was obtained when the average fiber

diameter varied from 1.7 μm to 3 μm. The efficiency of leukocyte removal significantly reduced when the fiber diameter was increased beyond 3 μm (Shirokaze, 2002; Umegae *et al.,* 1988). However no data is available on how the leukocyte removal is affected when the fiber diameter is lower than 1.7 μm. In another study by Guo *et al,* the authors found that the use of a single layer of electrospun PBT membrane having an average fiber diameter of approximately 468 nm assembled with commercially available melt-blown PBT membranes with an average fiber diameter of approximately significantly enhance the leukodepletion efficiency of the filter (Guo *et al.*, 2013). Excluding these, there are no other reported studies on the effect of fiber diameter on leukodepletion efficiency. The obtained results seemed to favor the findings of Umegae *et al* and Shirokaze *et al* as a very good leukodepletion with electrospun EVAL filters with fiber diameters 1.8 μm and 3 μm was observed (Figure 22, Figure 15, Figure 16, Figure 25 and Figure 26) (Shirokaze, 2002; Umegae *et al.*, 1988). The enhanced filtration time when the fiber diameter was lowered to 0.7 μm is thus assigned to the high resistance offered by the blood due to the small pores size, also supported by the findings of Guo *et al* [Figure 22 (b)] (Guo *et al.,* 2013).

5.2. Preparation, characterization and biological evaluation PHEA-g-EVAL

Photografting is a versatile method for modifying the surface properties of membranes or thin films (Khulbe *et al.,* 2010). For the present studies, BP was used as the photoinitiator. BP mediated photoinitiation has been used by several authors for surface

grafting and also for post modification of various polymeric membranes (Nady *et al*., 2011; Ulbricht *et al.*, 1996; Wang *et al*., 2007; Ye *et al.*, 2015). UV mediated reaction is shown in Figure 62. In the presence of UV irradiation BP gets converted into a singlet species having a short-life time. This singlet species soon relaxes into a triplet state. At this point it can abstract hydrogen from the EVAL backbone by inelastic collision and creates an active site on the polymer surface. This can initiate the graft polymerization of HEA monomer onto EVAL surface.

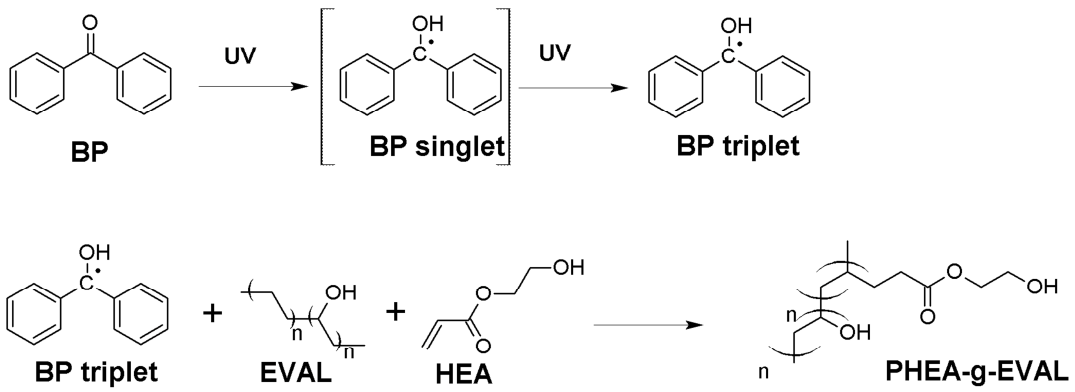

Figure 62. Mechanism of BP mediated photografting of HEA onto EVAL matrix

The method of photografting by the addition of monomer and initiator prior to irradiation is almost similar to the "pre-swelling grafting method" reported earlier (Jansen and Ellinghorst, 1985). It is a special grafting approach in which the trunk polymer is swollen in the monomer before irradiation. As a result, the monomer gets absorbed by the polymer matrix and the subsequent irradiation generates the graft copolymer and homopolymer. Such homopolymers get locked inside the trunk polymer which cannot be removed by any known methods. Hence it becomes difficult to distinguish between

homopolymerization and “true grafting”. The method followed in the current study was not very different from this, and the chances of forming the homopolymer, PHEA, along with graft polymer cannot be ruled out.

In the ATR-FTIR spectra (Figure 27), the appearance of a new peak at 1735.6 cm^{-1} indicates the formation of carbonyl group derived from grafted HEA. The peak corresponding to O-H stretch in EVAL shifted from 3288cm^{-1} to 3360 cm^{-1} for all the grafted films. The peak is found to be broadening with its intensities decreasing with increase in UV exposure time. This can be attributed to the increase in the intermolecular hydrogen bonding, the amount of which is proportional to the concentration of available hydroxyl groups. The observed increase in the DG also supports HEA grafting (Table 10). It may be noted that DG is a direct measure of the weight gained by the EVAL mat as a result of UV irradiation. Since an extensive extraction procedure have been carried out, it is likely that all the unreacted monomer and soluble homopolymer formed, if any, would have extracted out. So it can be inferred that increase in DG is an evidence for HEA grafting.

Changes in morphology of fibers as a result of HEA grafting are shown in Figure 28. These SEM images reveal that the electrospun EVAL mats consisted of smooth and continuous fibers. The fibre diameter was found to be increasing with increase in the exposure time in the beginning (up to 40 minutes) [Figure 28 (g)]. This is possibly because grafting might be the dominating reaction at these initial stages (Jansen and Ellinghorst, 1985). As the reaction progresses grafting sites might deplete and homopolymer formation might dominate. Little change in the fibre diameter occurred at

this stage. Similar observations have been reported elsewhere when glycidyl methacrylate was grafted onto linear poly(ethylenimine) (Xu *et al.*, 2010). The SEM images reveal that as a result of grafting fibers of different layers fuse together into a three dimensional network. Wrinkling of the fibers are also observed as a result of grafting. The wrinkle formation is possibly due to the collapse of the cylindrical fiber surface when the liquid HEA monomer present on the surface and core of the fibres get converted into solid polymer through grafting and homopolymerization. The EVAL fibers, which had in fact been "wet" with the HEA monomers, were converted to "dry" PHEA-g-EVAL fibers with fused and wrinkled morphological features. This process increased the diameters of PHEA-g-EVAL fibers greater than that of neat EVAL fibers. Both these observations are more and more predominant with increase in UV exposure time (Figure 28). These changes in the fiber morphology and fiber diameter after UV exposure further confirms grafting.

The pore characteristics of electrospun fibroporous mats play a crucial role in determining the physico-chemical properties, biological activity and biodegradability. The pore diameter and percentage porosity was calculated using image analysis technique and found that both of these parameters did not vary significantly even after HEA grafting (Table 10 and Figure 29). The porosity and pore size was dependant on the fiber diameter rather than DG. It was observed that there was only a slight increase in the fiber diameter after grafting. As a result the porosity and pore size did not change substantially. Despite the increase in the fiber diameter, pore diameter remained more or less constant even after

60 minutes of UV exposure. So it can be inferred that the photografting of HEA could preserve the pore characteristics of electrospun EVAL.

It is not uncommon to modify hydrophobic polymers with hydrophilic moieties so as to enhance its hydrophilicity. In the present study also grafting of HEA resulted in a significant reduction in the hydrophobicity of EVAL polymer (Table 10). The EVAL was in fact hydrophobic with a contact angle 126 ± 6 ° (Table 10) with water, in spite of the hydroxyl functionalities derived from the vinyl alcohol segment. All the grafted electrospun mats were not as hydrophobic as neat EVAL. This is clear from the data generated from contact angle measurements and CWST values. There was a non-linear variation in the WCA values with different UV irradiation periods. One possible reason is the formation of highly hydrophilic homopolymer, PHEA. Depending on the amount of PHEA formed, the values of WCA would vary. Another reason is the uneven surface of the mat formed due to grafting, homopolymerization, washing and drying. So while measuring the WCA, exact point of contact between the surface of the polymer and water droplet could not be detected with precision. With increase in DG, contact angle decreased and the CWST values increased (Table 10). The EVAL surface became very hydrophilic after 60 minutes of UV exposure as the water droplet placed on these mats got wet and spread during contact angle measurement itself. Zhou *et al* found that the water contact angle for EVAL with 44 mol % ethylene was 90 ° and decreased to 65 ° when modified with PC (Zhou *et al.,* 2007). The effect of grafting on the wettability of EVAL was also estimated by CWST. This method was previously studied by Lewis *et al*, where polyethylene terephthalate (PET) nonwoven fabric was coated with a copolymer of

MPC and lauryl mathacrylate (LMA), from alcohol-aqueous derived and alcohol only copolymer solutions (Lewis *et al.,* 2000). The copolymer coating enhanced the wettability of neat PET, indicated by the rise in CWST from 50 mN/m to 58 mN/m and 65 mN/m for alcohol only and aqueous-alcohol copolymer coating solutions, respectively (Lewis *et al.*, 2000). Yang *et al* presented similar reports of improved wettability after grafting various hydrophilic monomers to poly(butylene terephthalate) nonwoven fibrous matrices (PBTNFM) (Yang *et al.*, 2011). The CWST of unmodified PBTNFM increased after grafting and was influenced by the type of monomer and UV exposure time. HEA grafted PBTNF could achieve a CWST of 87 mN/m, (50 mN/m for the neat PBTNFM), after irradiating with UV for 49 minutes (Yang *et al.,* 2011). With electrospun EVAL, HEA grafting could increase the CWST to 81 mN/m when the UV exposure time was 50 minutes (Table 10).

The mechanical properties of the electrospun matrices also play a significant part in determining the end use of the material. Usually mechanical properties such as tensile strength, elongation at break, etc. for the electrospun fibroporous mats are a function of fiber properties like orientation, fiber size, fiber-fiber bonding, porosity, etc. (Wang *et al.,* 2004). The stress-strain properties of electrospun EVAL and HEA grafted EVAL follows that of a typical semi-crystalline polymer (Figure 30). The technique of electrospinning also allows control over the mechanical properties of biomaterials. For instance, hot pressed EVAL membranes had a tensile strength of 13.39 ± 0.45 MPa, Young's modulus of 326.78 ± 15.57 MPa and fracture strain of 39.59 ± 5 % (Zhou *et al.,* 2007). Ample differences in these properties were noticed in the studies as well.

Electrospun EVAL, before modification by HEA grafting, exhibited a tensile strength 6.8 ± 0.5 MPa, Young's modulus 150 ± 14 MPa and elongation at break 42 ± 5 % (Table 11). HEA grafting resulted in decreased tensile strength and Young's modulus and increased elongation at break which would possibly due to polymer degradation caused by UV radiation initiated reactions between BP triplet and EVAL chains. The grafted HEA chains would reduce the interaction between the EVAL chains and this could be another reason for the decreased tensile strength. Increased fracture strains and decreased Young's moduli of grafted EVAL mats could be attributed to the plasticization by the polymerized HEA chains within the EVAL matrix (Table 11). The T_g of neat electrospun EVAL was 82.6 °C (Table 4). Changes in T_g and the storage modulus were observed as a result of modification but a clear trend could not be deduced (Table 11). This is probably due to the variation in the degree of homopolymerization happening within the matrix.

Assessment of biocompatibility of polymeric materials is a vital part in developing new biomaterials, or when modifying any existing material. Hemocompatibility is an essential criterion while selecting any material for blood contacting applications. Here the influence of HEA grafting on the hemocompatibility of EVAL was studied quantitatively and qualitatively by monitoring the changes in blood composition and blood-material interactions when these fibers were kept in contact with blood *in vitro*. So properties such as hemolysis, plasma protein adsorption, RBC aggregation, platelet adhesion, coagulation, complement activation and blood cell consumption were studied. Hemolysis can happen at any circumstances where a material in contact with RBCs is in a highly stressed condition and can be altered by physical or

chemical modification. Electrospun EVAL showed a hemolysis of 2.3 ± 0.5 % before grafting (Table 12). With HEA grafting, the hemolysis decreased significantly. Hemolysis of all the HEA grafted EVAL mats fell within the acceptable level of 5 % (Table 12) (Dhandayuthapani *et al.*, 2012). HEA grafting also affected the protein adsorption, platelet adhesion and aggregation properties of EVAL. Reduced hydrophobicity of HEA grafted EVAL decreased the plasma protein adsorption onto EVAL (Table 12), which is the triggering factor for platelet adhesion. Thus the HEA grafted EVAL was found to be a platelet repellant material compared to neat EVAL. Similar observations were reported by Zhou *et al* when a melt molded micro-porous EVAL membrane with ethylene contents 27, 38 and 44 mol %, were modified with PC moieties (Zhou *et al.,* 2007). The grafted PC moieties could enhance the hydrophilicity of EVAL and further could suppress the BSA adsorption (Zhou *et al.,* 2007). Lin *et al* also highlighted the triggering action of protein adsorption to platelet adhesion. They concluded that heparin immobilization on polyacrylonitrile membrane, prepared by phase inversion method, could enhance the hydrophilicity and ultimately decreased the plasma protein adsorption and platelet adhesion from human PRP (Lin *et al.,* 2004). The absence of RBC aggregation before and after HEA grafting also contribute to the hemocompatibility of HEA grafted EVAL (Figure 31). Exposure of PRP onto neat and HEA grafted EVAL altered PTT and expression of fibrinogen (Table 13). The prolonged PTT obtained for the materials tested seemed to favor the proposed end use of the material. The change in clottable fibrinogen level may be ascribed to smaller degree of platelet activation. However, the effect of HEA grafting on the degree of fibrinogen adsorption by EVAL was negligible (Table 13).

Complement activation is another important factor determining the hemocompatibility of biomaterials or medical devices. Polymeric materials can initiate the complement activation via the alternative pathway. The phenomenon involves a series of sequential events resulting in the release of several anaphylotoxin peptide fragments of the complement proteins (Marconi *et al.,* 2000). C3a is one among several other peptides of such kind and the quantification of generated C3a is a general way of assessing the complement activation. Here the HEA grafted EVAL were screened and selected samples were evaluated for the complement activation. The HEA grafted EVAL obtained at higher UV irradiation periods were evaluated. The results highlight that there was a significant change in the percentage of generated C3a after exposure to plasma as a function of UV irradiation time (Table 13). It is also noteworthy that C3a generated after PRP exposure was lower in the case of EVAL mats UV irradiated for 50 and 60 minutes. The percentage of C3a generated for the 40 and 60 minutes of UV irradiated EVAL mats fall within the uncertainty level of 10 %. In the latter case, since the adsorption and desorption of C3 to the materials cannot be neglected, the lower concentration of the C3a after exposure may be due to the un-activated desorbed C3 (Hussain *et al*., 1998; Marconi *et al.,* 2000). Therefore, it can be inferred that the HEA grafted EVAL did not activate the complement system. The cell adhesion to the materials is also a significant issue in deciding the hemocompatibility. It was observed that electrospun neat EVAL had a tendency to attract the leukocytes and RBCs. The leukocyte consumption nature of EVAL was preserved even after HEA grafting (Table 13). This can be attributed to the fibrous texture due to electrospinning and presence of hydroxyl groups (Curtis *et al.,* 1986). The

concentration of hydroxyl groups was also increased after UV treatment as a consequence of HEA grafting. The studies of Curtis *et al* also support this observation. In addition, the increase in the fiber diameter after grafting provided more adhesion sites for leukocytes (Curtis *et al*., 1986; Curtis *et al.*, 1983; Lee *et al.*, 2001). At the same time the RBC adhesion was found to be decreasing with increase in the degree of grafting with HEA (Table 13). This phenomenon can be clarified on the basis of hydrophobic interaction of the presented polymers with the lipid bilayer of RBCs (Liu *et al*., 2012). The reduced hydrophobicity after HEA grafting and the introduction of hydroxyl groups onto the EVAL backbone were effective in reducing the RBC adhesion onto the electrospun EVAL fibers (Liu *et al.*, 2012). The present studies suggest that grafting of HEA would reduce RBC adhesion and this method is suitable for modification of any existing filter material. The leukodepletion efficiency of the PHEA-g-EVAL membranes was also studied. It is interesting to note that the WBC adhesion as well as the platelet adhesion was significantly reduced after the grafting. This is attributed to the enhanced hydrophilicity of the PHEA-g-EVAL membranes that there could be formation of a hydration layer around the membrane on their immediate contact with blood (Kitano *et al.*, 2005). This hydration layer is supposed to be strong due to the strong hydrogen bonding interactions between the OH groups from the membrane and the surrounding water molecule. In such a case the leukocyte pseudopodia were unable to reach the fibers for attachment (Lin and Chuang, 2000; West *et al.*, 2004). The present studies suggest that grafting of HEA would reduce platelet adhesion and this method is suitable for modification to enhance the overall hemocompatibility of any existing filter material.

5.3. Preparation, characterization and biological evaluation of EVAL membranes functionalized with zwitterionic systems

5.3.1. Preparation and characterization of EVAL-Gly

Glycine, the simplest amino acid, is a less considered system for modifying the properties of polymers. It has particularly accepted as a model system for studying the polymorphic crystallization behavior (Chew *et al.,* 2007; Poornachary *et al.,* 2007). Several researchers have carried out the modification of various polymers by incorporation of glycine containing peptides and other glycine derivatives, especially a glycine derived zwitterions, glycine betaine (GB) (Moideen K *et al.*, 2016; Pepinsky *et al.,* 1958). Notwithstanding its non toxicity and biofunctionality, the incorporation of pure crystalline glycine to polymer matrix by direct methods has not been executed much. In the present study, an effort was made to incorporate glycine to the EVAL fibers by electrospinning and to examine its effect on the various blood-material interactions.

Figure 37 confirms the presence of glycine in the EVAL matrix due to the appearance of a peak corresponding to the COO in the glycine. When compared with the previous studies by Isakov *et al* where glycine was present in free form and Yu *et al* where glycine was in the grafted form, the position of this peak was observed to be somewhere in between the corresponding wavelengths reported by them (Isakov *et al.*, 2011; Yu *et al.,* 2014). This hints that the incorporated glycine is bonded to the EVAL by hydrogen bonding interactions. Moreover the intensity of the peak at 3288 cm^{-1} in EVAL for the OH stretch has been increased predominantly in the EVAL-Gly-10 % which is

accounted for the OH stretch of EVAL associated with HN - - - O stretch as a result of the interactions between glycine and EVAL (Isakov *et al.,* 2011).

Little effect was observed on the morphological appearance of the EVAL fibers after addition of glycine (Figure 38). However, the noticed decrease in the fiber diameter and pore diameter at higher glycine loading is owing to the enhanced charge density of the polymer solution imparted by the polar glycine which in turn caused a greater stretching force experienced by each fiber while electrospinning (Table 15) (Hemmat *et al.*, 2015). The wettability of EVAL membranes was not affected by the glycine loading (Figure 39). This seems to contradict the preceding reports, however, it has to be assumed that the concentration of glycine specified in the current study was deficient to raise the hydrophilicity and wettability of EVAL (Moideen K *et al.*, 2016).

It is consequential to analyze the release characteristics of glycine since the released glycine is expected influence the various blood parameters when in contact with whole blood (Lyapina *et al*., 2003). It can be seen from Figure 40 that there was a burst release of glycine during the initial phase, and the release was sustained after 2 days. Minute concentrations of glycine were released to the PBS within the initial hours and it is necessary to understand the effect of these by the *in vitro* blood compatibility evaluation.

5.3.2. Preparation and characterization of PSMDB-g-EVAL

The sulfobetaine systems possessing zwitter ionic moieties are receiving a lot attention as highly blood compatible materials in recent years (Chen *et al*., 2005; Yuan *et*

al., 2003a). Thus several polymeric biomaterials including membrane materials have been easily modified so far either by coating or by covalently linking with various kinds of sulfobetaines in order to enhance their hemocompatibility. The present study focused on functionalizing EVAL leukodepletion filter membranes with SMDB by UV grafting method.

The effect of modification of membranes that dramatically altered the physico-chemical and blood contacting properties of EVAL were investigated. The EVAL membranes were successfully functionalized by irradiating the membranes as such electrospun from mixture of photoinitiator and SMDB monomer. This was evidenced by the appearance of new absorption peaks corresponding to the amide and sulfonate groups in the ATR-FTIR spectra provided in Figure 42. The shifting of OH peak in neat EVAL to higher wave numbers also hints the functionalization with SMDB (Figure 42). These observations also agree well with the literature (Zhao *et al*., 2011).

No detrimental effects on the fiber morphology were observed after SMDB functionalization as visualized in the SEM images (Figure 43). However, the fiber diameter was remarkably increased with increase in the UV irradiation time. Successively, fiber diameter of neat EVAL was increased from 1.8 ± 0.1 µm to 2.3 ± 0.3 µm after 60 minutes UV irradiation (Figure 44). The increased fiber diameter can be ascribable to the formation of SMDB graft EVAL copolymer, mediated by the photoinitiator, as a result of UV irradiation (Zhao *et al*., 2010).

It is also important to highlight that the wettability of electrospun EVAL membranes was drastically affected by SMDB functionalization. A significant decrease in the WCA

of EVAL was observed as a function of UV irradiation time (Figure 44). The SMDB grafted EVAL became hydrophilic after 60 minutes of UV irradiation indicated by its WCA of 69 ± 11 °. It is also noteworthy that the WCA values vary proportionally to DG. This decrement in WCA values further supports the functionalization and emphasize that the grafted SMDB chains are hydrophilic in agreement with Chang *et al* (Chang *et al.*, 2012).

Figure 46 shows an increment in the DG as a function of UV irradiation time while the photoinitiator concentration was 4 wt %. However, the maximum DG obtained as a result of 60 minutes of UV irradiation was much lower than that obtained by Yang *et al* (Yang *et al.*, 2011). This difference can be attributed to the poor availability of the monomer and initiator when these are locked in the fibers during electrospinning. Hence the approach adopted in the current study permits the modification of membranes to improve the desired properties, but to a limited extent.

The pore properties before and after functionalization were also investigated by means of ImageJ analysis. The results presented show significant variation neither in the pore size nor in the percentage porosity as a result of SMBD functionalization (Table 17). Thus it seems that the functionalization retained the membrane pore characteristics.

5.3.3. Biological evaluation of EVAL-Gly and PSMDB-g-EVAL

It was also necessary to understand the effect of zwitterion functionalization on the extent of various interactions with blood components. Interestingly, both the functionalizations – incorporation of glycine and photografting of SMDB - did not seem to particularly influence the protein adsorption and WBC adhesion, however, drastically

reduced the RBC adhesion and hemolysis (Table 16 and Table 18). In case of the adhesion of platelets, surprisingly, the results presented a substantial difference when the functionalized EVAL was exposed to PRP and whole blood (Table 16 and Table 18). In order to manifest the mechanism of these interactions, the role of material parameters like surface chemistry, wettability and membrane pore properties needs to unveiled. Previous studies have shown that zwitterionic systems show reluctance to protein adsorption because of the formation of a hydration layer around its own charged groups (Kitano *et al*., 2005; Lin and Chuang, 2000; West *et al.*, 2004). However, in the presented data, the degree of grafting as well as the wettability was only marginally enhanced after the functionalization with SMDB while EVAL-Gly membranes were still hydrophobic. Hence it may be assumed that the interaction of the functionalized membranes with water was poor and thus the strength of the hydration layer was not sufficient to prevent the protein adsorption. Moreover, the proteins are amphoteric, having both positive and negative regimes. Hence at the interface, it might happen that the quaternary ammonium acid groups present in both glycine and SMDB interacts well with the counter charges in the protein. Thus it has to be concluded that the balance between the ionic interaction and the weak hydration layer resulted in the stability of protein adsorption. The disparities in the adhesion of WBCs, RBCs and platelets after functionalization can also be interpreted based on the hydration layer. When whole blood was allowed to pass through the zwitterion functionalized membranes, although the membrane pore size was pretty much larger than the size of WBCS, the pseudopodia of WBCs could readily penetrate the weak hydration layer and reached the fiber surface to attach firmly (Kitano *et al*., 2005). But,

when it was RBCs, since the lipid hydrophobic lipid bi-layer repelled the hydration layer and caused their fast deformation allowing most of the RBCs to pass through the membrane (Liu *et al.,* 2012). Hence it can also be inferred that little pressure was exerted on the RBCs which is evident from the decreased percentage of hemolysis after both type of zwitterion functionalizations. Accompanying the WBC adhesion, the platelets from whole blood were not able to interfere with the hydration layer. Nevertheless, the platelets from PRP were directly exposed to the hydration layer of the glycine and SMDB functionalized EVAL. In the same way, the SEM images of the EVAL membranes exposed to PRP distinctly indicate that there was a substantial adhesion as well as spreading of platelets on bare EVAL and the platelets seemed to be detached from the membrane surface after the zwitterion functionalization (Figure 41 and Figure 47). This hints that the there was some sort of platelet activation caused by the bare EVAL which prompted the platelets to extent their pseudopodia to hold the fiber surface (Kitano *et al*., 2005). However, the zwitterion functionalization could explicitly reduce the activation of platelets and thus ensured a decreased platelet adhesion.

As a result of whole blood filtration, the WBC adhesion from whole blood on PSMDB-g-EVAL was lower than that of EVAL-Gly due to the higher hydrophobicity of EVAL-Gly (Figure 49). This in turn offered a resistance to blood flow and resulted in the increment in the duration of filtration. Additionally, there could be a high clogging by the adhered WBCs as evidenced from Figure 51 that the retention of RBCs was comparatively lower than that by the PSMDB-g-EVAL (Figure 53). However, the substantial platelet recovery from both the zwitterionic systems was not observed.

Therefore, on appraising the overall interactions by the various zwitterion functionalized EVAL membranes with the various blood components, the modifications imparting zwitterionic moities can be recommended for enhancing the hemocompatibility of various polymeric membranes and especially for blood filtration through non-woven membranes.

5.4. Preparation, characterization and biological evaluation of EVAL-BSA

Reducing the thrombogenecity associated with biomaterials by the proper surface modifications have been of keen interest for the researchers. Along with other successful methods, modification by coating or covalent attachment of albumin to the substrates have been proven versatile to reduce the protein adsorption, platelet adhesion and activation thereby enhancing the overall hemocompatibility for the blood contacting biomaterials (Liu *et al*., 2005; Maalej *et al.*, 1999). Various precursors have been used till date for the immobilization of BSA to the biomaterials. Among these, dopamine and polydopamine (PD) have acquired more attention (Jiang *et al*., 2011).

An attempted to covalently immobilize BSA onto electrospun EVAL membranes by means of pre-coating of polydopamine was executed. The mechanism for this reaction as proposed by Zhu *et al* is provided in Figure 54 (Zhu *et al*., 2011). Dopamine is neurotransmitter which readily undergoes oxidative polymerization to form PD particles/aggregates under alkaline conditions (Jiang *et al*., 2011). An import feature of this PD is that it makes a very strong attachment to the substrate by covalent and non-

covalent interactions like π- π interactions and electrostatic interactions (Lee *et al.,* 2006). Thus the newly generated PD layer remains stable and durable for a long time in all conditions excluding highly alkaline environment (Lee *et al.,* 2007). Thus the PD layer also furnishes its reactive functionalities for further attachment of desirable molecules and imparting the required properties to the substrate thereby. Consequently, lot many polymers have been functionalized by attachment of different molecules by means of adherent PD layer in order to enhance the wettability, cell adhesion and biocompatibility (Lee *et al*., 2009; Waite, 2008).

The formation of PD and its further reaction with BSA on EVAL surface have been evidenced by structural, morphological, and wettability analysis. A new peak corresponding for the C=O stretch in PD has been featured in the ATR-FTIR spectra (Figure 55). Many researchers have also noted this peak confirming the attachment of PD layer (Zhu *et al*., 2011). Further after the BSA immobilization, this peak was replaced by another peak which could be primarily due to the C=O stretch of Amide I band derived from BSA. Interestingly no other peaks of Amide I band were visible at lower wavelength (Figure 55). This leads to the point that the NH_2 groups of BSA were involved in the reaction with PD. Thus it is also concluded that BSA was not simply physically adsorbed to the PD coated EVAL membrane, but covalently attached. Interestingly, the SEM images reveal the formation of PD particle aggregates on EVAL surface [Figure 56 (a)]. Similar observation was also previously published by Jiang *et al* (Jiang *et al*., 2011). However, the concentration of PD particles disappeared after reacting with BSA retaining the smooth morphology of the EVAL fibers. The progressive increment in the fiber

diameter after the reaction with BSA also supports to their successful immobilization (Table 20). The effect of BSA immobilization on the wettability of EVAL membranes has also been studied. The results presented indicate that the EVAL membranes became slightly hydrophilic after the PD formation (Table 20). This is obviously due to the presence of hydrophilic catecholic groups derived from the PD (Ball *et al.,* 2012). However, the WCA values were raised after BSA immobilization. This stipulates that the BSA chains were hydrophobic in nature. Similar observation was previously noted by Weng *et al* when BSA was immobilized to anatase TiO_2 film by means of pre-treated phosphoric acid (Weng *et al.*, 2008).

The effects of BSA immobilization were clearly visible from the data of *in vitro* hemocompatibility evaluation. The *in vitro* platelet adhesion was effectively decreased when the EVAL-BSA membranes were exposed to PRP, which is in accordance with many other studies (Table 21 and Figure 57) (De Queiroz *et al*., 1997; Zhang *et al*., 2013). It was surprising to note that the plasma protein adsorption and percentage hemolysis was gradually increasing with increase in the BSA concentration (Table 21). This may be ascribed to the active –COOH groups of the BSA, as they bring about an effective bonding between the various proteins in plasma. Moreover the BSA chains will also invite other proteins in the environment ultimately resulting in a high protein adsorption. In resemblance to this, a study Fu *et al* also demonstrated that –COOH groups encourages the protein adsorption as they observed EVAL membranes in-situ functionalized with citric acid had significantly higher protein adsorption than the unmodified EVAL (Fu *et al.*, 2016). Thus when whole blood was kept in contact with

EVAL-BSA membranes, most of the proteins was adsorbed to its surface (Fu *et al.*, 2016). The effects due to this phenomenon is also reflected in other parameters also the WBC adhesion and platelet adhesion from whole blood was maintained while the RBC adhesion was reduced (Table 21). The formation of a protein layer on the EVAL-BSA membrane surface will facilitate the fine adhesion of WBC and this WBC layer will further enhance the subsequent protein adhesion. So as a result of these adhesions, it is expected that pores of the membranes might be clogged with cells and proteins. In such a case the RBC might find it difficult to pass through the membrane pores. This was also evidenced by the application of a high succession while performing the *in vitro* blood cell consumption studies. Obviously, the RBCs were squeezed through the pores resulting in a high degree of lysis (Table 21).

Notwithstanding the several published reports on the *in vitro* hemocompatibility of BSA functionalized biomaterials, there is no previous data on the leukodepletion efficiency by such membranes. Hence the whole blood filtration experiments through EVAL-BSA membranes were carried out because such a data will be beneficial for the forthcoming investigations. Asymmetric filter, with different pores sizes for top and bottom layers, were fabricated and blood was allowed to percolate through the filter immediately after priming with PBS. The obtained results of cell adhesion highlights that the WBC adhesion was decreased after the filtration which shows that –COOH had a moderate affinity towards the leukocytes (Figure 58) (Yang *et al.,* 2011). Also there was a high platelet adhesion, but the quantity of which was not different from that of neat EVAL, which is in accordance with the *in vitro* study results. The poor retention of RBCs

and the significantly lower filtration speed through the EVAL-BSA filter suggests the pore plugging effect imparted by the adhered cells and proteins, as supported by the microscopic images (Figure 59). Thus the obtained results demonstrate that the BSA functionalization could alter the hemocompatibility of the EVAL membranes *in vitro*, however could not significantly improve the leukodepletion efficiency.

5.5. Correlation between surface chemistry, wettability and leukodepletion efficiency

In the present study, the leukodepletion efficiencies of the various electrospun membrane systems having a range of surface functionalities and wettability were investigated. So it is now ideal to arrive at a correlation between the material chemistry, wettability and leukodepletion efficiency. Previously Yang *et al* established such a correlation exclusively between the surface chemical composition and cell adhesion, however the wettability was not associated with these (Yang *et al*. 2011). From the various systems those were experimented in the study a general conclusion can be drawn that hydrophobic substrates promote WBC and platelet adhesion, thus providing high leukodepletion efficiencies (Lim and Cooper, 1990). Various modifications altered the WBC adhesion as well as the platelet adhesion. It is clear from Figure 61 that wherever the membranes were hydrophilic, there was a poor leukodepletion, however some modified systems gave excellent leukodepletion even with the hydrophilicity associated with them. The following facts can also be deduced from this comparison chart. -CN present in PAN did not show an effective interaction with the WBCs while the OH groups

had a strong affinity towards the WBCs. The better efficiency by EVAL-Gly-1% was exclusively due to the high degree of hydrophobicity and the presence of zwitterions than the other zwitterinoic sulfobetaine system. Thus it can be identified that the most hydrophilic system, the PSMDB-g-EVAL-60 membranes gave a sufficiently high leukodepletion and leads to the conclusion that the surface chemistry was in such a way to promote the leukocyte adhesion despite of the enhanced hydrophilicity and wettability. Similarly the PAN filter, being highly hydrophobic, could not offer a satisfactory leukodepletion performance and this may be due to the weak affinity of -CN functionality towards the leukocytes. The leukodepletion by EVAL-BSA-10 filter was a little lower than the EVAL despite of its high degree of hydrophobicity. This is because of the poor interaction of WBCs with the -COOH groups derived from BSA chains, while its own NH_2 groups were bound to the PD spacer while immobilization. Based on these facts, the relative order of leukodepletion efficiency for the systems with various functionalities those were explored in the current study can be given as –CN << -COOH < OH = $N^+(COO^-)$ < $N^+(SO_3^-)$. It is now inferable that the membrane modification by sulfobetaine moieties can be well executed for the various leukodepletion filters, however the hydrophilicity of the resulting membranes has to be tuned properly in order to accomplish 100 % leukodepletion. Such a data is expected to be beneficial for the forthcoming investigations while developing and designing efficient electrospun leukodepletion filter membranes.

CHAPTER 6

SUMMARY AND CONCLUSION

6.1. Summary and Conclusions

It has been identified and clinically proven that excess number of leukocytes in the donor blood might cause some adverse reactions in the recipient during the process of blood transfusion. Thus a number of commercial leukodepletion filters serves to reduce the leukocyte count to the safe limit in order to prevent the occurrence of these reactions, however, their high cost and significant platelet removal has prompted the researchers to go in search of alternative membrane materials which can overcome these limitations.

Electrospun polymeric non-woven membranes have not much been taken into serious consideration for developing leukodepletion filters. Hence the primary objective of the present study is to address the above problem by exploring the feasibility of electrospun poly(ethylene-co-vinyl alcohol) (EVAL) and polyacrylonitrile (PAN) membranes for leukodepletion. The morphological features of the membranes were studied by SEM analysis. The membranes were hydrophobic, biocompatible and non-hemolytic. Leukodepletion filters were designed out of these membranes by stacking them in an acrylic case and their efficiency was assessed by whole blood filtration. The developed EVAL asymmetric filter showed a high leukodepletion efficiency while the PAN asymmetric filter gave a poor performance therefore eliminated from further studies. Effect of fiber diameter and filter structure on the leukodepletion efficiency of EVAL

filters were also successfully deduced. Thus it was inferred from this initial phase of study that asymmetric EVAL filters with fiber diameter 1.8 - 3 μm and appropriate pore diameter could offer very good leukodepletion performance which was comparable to the commercially available filter. The morphology and distribution of the WBCs adhered to the filter was also examined by SEM and histological analysis. Notwithstanding, significant platelet loss by adhesion to EVAL filter membranes was also noted which needs to be considered further.

Several reports suggested that the adhesion of blood cells onto membranes during leukodepletion is highly dependent on their surface chemistry and wettability. So by tuning the surface properties in the most desirable way, it is possible to enhance the WBC adhesion, and the RBC and platelet retention. Hence the various approaches for modifying the EVAL membranes thereby altering their surface properties so as to reduce the platelet adhesion were adopted. Selected functional moieties including acrylates, zwitterionic systems and proteins which can inhibit selective platelet adhesion was carefully chosen for the modification. Thus EVAL membranes were modified by photografting with 2-hydroxyethyl acrylate (PHEA-g-EVAL) and N-(3-sulfopropyl)-N-methacroyloxyethyl-N,N- dimethylammonium betaine (PSMDB-g-EVAL), functionalization by incorporation of glycine (EVAL-Gly) and, immobilization of bovine serum albumin (EVAL-BSA). The PHEA-g-EVAL and PSMDB-g-EVAL membranes were prepared by UV induced photografting of the monomers with the aid of benzophenone photoinitiator. The UV irradiation time was varied in order to obtain membranes with different degree of grafting. Glycine was directly incorporated to the

EVAL membranes during electrospinning while BSA was immobilized to EVAL membranes utilizing the reactive polydopamine coating. Chemical characterization of the various modified systems using ATR-FTIR confirmed the successful modifications and the wettability studies demonstrated the hydrophilicity of the modified EVAL membranes were enhanced after the modification except for glycine functionalized and BSA functionalized membranes. The DG of PHEA-g-EVAL and PSMDB-g-EVAL membranes were found to be increasing with increase in the UV irradiation time. The effects of these modifications on the morphological properties of the membranes including the fiber diameter, pore diameter and percentage porosity were also well established. The release of glycine from the EVAL-Gly membranes was also investigated.

Prior understanding about the degree of various interactions of the modified EVAL membranes with blood is necessary before assessing their leukodepletion efficiency. Hence an *in vitro* hemocompatibility evaluation was performed and the various blood parameters like *in vitro* hemolysis, plasma protein adsorption, *in vitro* RBC aggregation, platelet adhesion, coagulation assay, complement activation and blood cell consumption were analyzed. All the modifications enhanced the overall hemocompaiblity of EVAL membranes by reducing the hemolysis, protein adsorption, RBC adhesion and reduced the platelet adhesion *in vitro* when the modified membranes were exposed to PRP except for EVAL-Gly and EVAL-BSA systems. Interestingly the protein adsorption remained unchanged in EVAL-Gly while it increased in EVAL-BSA at the same time increasing the hemolysis. The PHEA-g-EVAL membranes did not affect the coagulation

cascade and activate the complement system. The adhesion of WBC, RBC and platelets from whole blood were also varied to different degrees as a result of modifications.

The evaluation of performance of the various modified membrane systems towards leukodepletion efficiency was also undertaken by filtration of whole blood through asymmetric filters composed out of selected membranes from each modified systems. Thus PHEA-g-EVAL-60, PSMDB-g-EVAL-60, EVAL-Gly-1 and EVAL-BSA-10 membranes were evaluated. The overall leukodepletion efficiency of PHEA-g-EVAL-60 filter was significantly lower than that of neat EVAL filter while for all other membranes systems, the leukodepletion efficieny was not much different from that of neat EVAL. The filter membranes were further evaluated by SEM and histological analysis in order to get an idea about the distribution of cell through various layers.

It was also found admissible to derive a correlation between the surface chemistry, wettability and leukodepletion efficiency of the various electrospun membranes by analyzing the data collected for all the modified and unmodified systems. The presented data insinuate that hydrophobic membranes are best suited for leukodepletion filter but may be associated with high platelet adhesion. However, in order to design an ideal leukodepletion filter with high retention of other functional and viable components, membranes with appropriate surface chemistry and wettability has to be identified. From the various surface functionalities that were experimented, the zwitterions bearing sulfobetaine systems has proven to have the high affinity for leukocytes and giving a substantially high leukodepletion efficiency despite of the hydrophilicity. Thus, along

with the other current techniques, the technique of electrospinning can be explored in future for the fabrication of membranes for leukodepletion filters.

To conclude the thesis presented was an extensive attempt to disclose the potential of electrospinning technology for developing excellent leukodepletion filters with idealized properties. By the selection of suitable blood compatible polymers cost effective and highly efficient leukodepletion filter membranes can be easily fabricated by electrospinning. It was also shown that there are various surface modification perspectives which are practicable for altering the physico-chemical properties of the electrospun leukodepletion filter membranes in order to resolve the limitations of the commercialized leukodepletion filter. Further efforts in search of novel electrospun filter membranes are expected to lead to the commercialization of productive and profitable electrospun polymeric membrane based leukodepletion filters.

6.2. Limitations of the Study

The present study explored the feasibility of electrospinning technique for the fabrication of leukodepletion filters. The study also undertook the various modification strategies to improve the leukodepletion filters in detail and all the reported experiments were performed with small volume of blood. Nevertheless, the relation between the filter depth and volume of the blood filtered or the design strategies of the filter in order to achieve effective filtration of one unit of blood could not be evaluated due to limitations.

6.3. Future perspectives

In future, the work can be extended by electrospinning of various other blood compatible polymers and to inspect their leukodepletion efficiency. Thus various other membranes can also be identified. A detailed evaluation of blood-material interactions by studying the platelet activation and complement activation due to the material, filtration process and filter design can also be undertaken.

BIBLIOGRAPHY

Acconci C, Legallais C, Vijayalakshmi M, Bueno SMA. (2000) Depyrogenation of snake antivenom serum solutions by hollow fiber-based pseudobioaffinity filtration. *J Membr Sci.* 173: 235-45.

Agarwal S, Wendorff JH, Greiner A (2008) Use of electrospinning technique for biomedical applications. *Polymer.* 49: 5603-21.

Andreu G, Dewailly J, Leberre C, Quarre M, Bidet M, Tardivel R, Devers L, Lam Y, Soreau E, Boccaccio C (1988) Prevention of HLA immunization with leukocyte-poor packed red cells and platelet concentrates obtained by filtration. *Blood.* 72: 964-9.

Ariga H, Lee TH, Laycock ME, Mohr BA, Kalish LA, Yomtovian R, Gernsheimer T, Busch MP (2003) Residual WBC subsets in filtered prestorage RBCs. *Transfusion.* 43: 98-106.

Avramescu M-E, Sager W, Borneman Z, Wessling, M (2004) Adsorptive membranes for bilirubin removal. *J Chromatogr B: Biomed Sci Appl.* 803: 215-23.

Avramescu M, Sager W, Mulder M, Wessling M (2002) Preparation of ethylene vinylalcohol copolymer membranes suitable for ligand coupling in affinity separation. *J Membr Sci.* 210: 155-73.

Ball V, Del Frari D, Michel M, Buehler MJ, Toniazzo V, Singh MK, Gracio J, Ruch D (2012) Deposition mechanism and properties of thin polydopamine films for high added value applications in surface science at the nanoscale. *BioNanoScience.* 2: 16-34.

Barber T, Lambrecht L, Mosher D, Cooper SL (1978) Influence of serum proteins on thrombosis and leukocyte adherence on polymer surfaces. *Scanning Electron Microsc*. 792: 881-90.

Barhate R, Loong CK, Ramakrishna S (2006) Preparation and characterization of nanofibrous filtering media. *J Membr Sci*. 283: 209-18.

Bian K, Cunningham MF (2005) Nitroxide-mediated living radical polymerization of 2-hydroxyethyl acrylate and the synthesis of amphiphilic block copolymers. *Macromolecules.* 38: 695-701.

Blackshear PL, Anderson RJ (1978) Hemolysis thresholds in microporous structures. In: Bessis M, Shohet SB, Mohandas M (eds) *Red Cell Rheology*, Springer, New York, pp. 373-91.

Bowden RA, Slichter SJ, Sayers M, Weisdorf D, Cays M, Schoch G, Banaji M, Haake R, Welk K, Fisher L (1995) A comparison of filtered leukocyte-reduced and cytomegalovirus (CMV) seronegative blood products for the prevention of transfusion-associated CMV infection after marrow transplant. *Blood.* 86: 3598-603.

Bruil A, Beugeling T, Feijen J, Aken WG. (1995) The mechanisms of leukocyte removal by filtration. *Transfus Med Rev*. 9: 145-66.

Bruil A, Brenneisen LM, Terlingen JG, Beugeling T, van Aken WG, Feijen J (1994) *In vitro* leukocyte adhesion to modified polyurethane surfaces: II. Effect of wettability. *J Colloid Interface Sci.* 165: 72-81.

Bruil A, Oosterom HA, Steneker I, Al BJ, Beugeling T, van Aken WG, Feijen J (1993) Poly (ethyleneimine) modified filters for the removal of leukocytes from blood. *J Biomed Mater Res.* 27: 1253-68.

Bruil A, Van Aken W, Beugeling T, Feijen J, Steneker I, Huisman J, Prins H (1991) Asymmetric membrane filters for the removal of leukocytes from blood. *J Biomed Mater Res.* 25: 1459-80.

Buchholz D, Aubuchon JP, Snyder E, Kandler R, Piscitelli V, Pickard C, Napychank P, Edberg S (1994) Effects of white cell reduction on the resistance of blood components to bacterial multiplication. *Transfusion.* 34: 852-7.

Bueno SM, Legallais C, Haupt K, Vijayalakshmi M (1996) Experimental kinetic aspects of hollow fiber membrane-based pseudobioaffinity filtration: process for IgG separation from human plasma. *J Membr Sci.* 117: 45-56.

Callaerts A, Gielis M, Sprengers E, Muylle L (1993) The mechanism of white cell reduction by synthetic fiber cell filters. *Transfusion.* 33: 134-8.

Campbell J, Mackenzie M, Yentis S, Sooranna S, Johnson M (2012) An evaluation of the ability of leucocyte depletion filters to remove components of amniotic fluid. *Anaesthesia* 67, 1152-7.

Cao Y, Wang H, Yang C, Zhong R, Lei Y, Sun K, Liu J (2011) *In vitro* studies of PBT nonwoven fabrics adsorbent for the removal of low density lipoprotein from hyperlipemia plasma. *Appl Surf Sci.* 257: 7521-8.

Capasso A, Pisano A (2014) Leukocyte depletion of transfused blood to reduce perioperative mortality. In: Landoni, Giovanni, Ruggeri, Laura, Zangrillo, Alberto (eds) *Reducing Mortality in the Perioperative Period*, Springer, New York, pp. 85-92.

Chang Y, Chang W-J, Shih Y-J, Wei T-C, Hsiue G-H (2011) Zwitterionic sulfobetaine-grafted poly (vinylidene fluoride) membrane with highly effective blood compatibility via atmospheric plasma-induced surface copolymerization. *ACS Appl Mater Interfaces.* 3: 1228-37.

Chang Y, Chang Y, Higuchi A, Shih, Y-J, Li P-T, Chen W-Y, Tsai E-M, Hsiue G-H (2012) Bioadhesive control of plasma proteins and blood cells from umbilical cord blood onto the interface grafted with zwitterionic polymer brushes. *Langmuir*. 28: 4309-17.

Chen S, Zheng J, Li L, Jiang S (2005) Strong resistance of phosphorylcholine self-assembled monolayers to protein adsorption: insights into nonfouling properties of zwitterionic materials. *J Am Chem Soc.* 127: 14473-8.

Chew JW, Black SN, Chow PS, Tan RB, Carpenter KJ (2007) Stable polymorphs: difficult to make and difficult to predict. *Cryst Eng Comm.* 9: 128-130.

Chiang WY, Hu CM (1990) Studies of reactions with polymers. VI. The modification of PAN with primary amines. *J PolymSci Part A: Polym Chem.* 28: 1623-36.

Chu R (1999) Leukocytes in blood transfusion: adverse effects and their prevention. *Hong Kong Med J. 5*, 280-284.

Coffinier Y, Vijayalakshmi MA (2004) Mercaptoheterocyclic ligands grafted on a poly (ethylene vinyl alcohol) membrane for the purification of immunoglobulin G in a salt independent thiophilic chromatography. *J Chromatogr B: Biomed Sci Appl*. 808: 51-6.

Collier AC, Kalish LA, Busch MP, Gernsheimer T, Assmann SF, Lane TA, Asmuth DM, Lederman MM, Murphy EL, Kumar P (2001) Leukocyte-reduced red blood cell transfusions in patients with anemia and human immunodeficiency virus infection: the viral activation transfusion study: a randomized controlled trial. *J Am Med Assoc.* 285: 1592-1601.

Colson K (2010) Preparation and characterization of hydroxyapatite-alendronate composites.

Curtis A (1973) “Cell adhesion”. *Progress in biophysics and molecular biology, 27,* pp. 315IN7371IN9373IN11375-11370IN18372IN10374IN12384.

Curtis A, Forrester J, Clark P (1986) Substrate hydroxylation and cell adhesion. *J Cell Sci.* 86: 9-24.

Curtis A, Forrester J, McInnes C, Lawrie F (1983) Adhesion of cells to polystyrene surfaces. *J Cell Biol.* 97: 1500-6.

De Queiroz AA, Barrak ÉR, Gil HA, and Higa, O. Z. (1997). Surface studies of albumin immobilized onto PE and PVC films. *J Biomater Sci, Polym Ed*. 8: 667-81.

de Vries, AJ, Gu Y, van Oeveren W (2005) The clinical effects and mechanisms of leukocyte depletion filters during cardiac surgery. *Ann Card Anaesth.* 8: 117.

DeWitt D, Finley M, Lawin L (2005) Blends comprising ethylene-vinyl acetate copolymer and poly (alkyl (meth) acrylates or poly (aromatic (meth) acrylates); implantable medical device; permit stents releasing the bioactive agent over time in vivo; provide clear coats, durability, biocompatibility, and release kinetics; drug delivery device. U.S. Patent Application No. 11/099,997.

Dhandayuthapani B, Varghese SH, Aswathy RG, Yoshida Y, Maekawa T, Sakthikumar D (2012) Evaluation of antithrombogenicity and hydrophilicity on Zein-SWCNT electrospun fibrous nanocomposite scaffolds. *Int J Biomater*. 2012: 1-11.

Dzik S (1993) Leukodepletion blood filters: filter design and mechanisms of leukocyte removal. *Transfus Med Rev.* 7: 65-77.

Ertel SI, Chilkoti A, Horbetti TA, Ratner BD (1992) Endothelial cell growth on oxygen-containing films deposited by radio-frequency plasmas: the role of surface carbonyl groups. *J Biomater Sci, Polym Ed*. 3: 163-83.

Fisher M, Chapman JR, Ting A, Morris PJ (1985) Alloimmunisation to HLA antigens following transfusion with leucocyte-poor and purified platelet suspensions. *Vox Sang.* 49: 331-5.

Fleming A (1926) A simple method of removing leucocytes from blood. *Br J Exp Pathol.* 7: 281-286.

Food and Drug Administration (FDA) (1996) Recommendations and licensure requirements for leukocyte-reduced blood products. FDA Memorandum, May 29.

Food and Drug Administration (FDA) (2012). Guidance for Industry: Pre-storage leukocyte reduction of whole blood and blood components intended for transfusion. US Department of Health and Human Services. Center for Biologics Evaluation and Research. September.

Forrester J, Lackie J (1984) Adhesion of neutrophil leucocytes under conditions of flow. *J Cell Sci.* 70: 93-110.

Frühauf N, Dumpich O, Kaudel C, Kasimir-Bauer S, Oldhafer K (2001) Filtration of malignant cells: tumour cell depletion in an ex vivo model using a leukocyte adhesion filter. *Perfusion.* 16: 51-5.

Fu Q, Wang X, Si Y, Liu L, Yu J, Ding B (2016) Scalable fabrication of electrospun nanofibrous membranes functionalized with citric acid for high-performance protein adsorption. *ACS Appl Mater Interfaces.* 8: 11819-29.

Garvin JE (1961) Factors affecting the adhesiveness of human leucocytes and platelets *in vitro*. *J Exp Med*. 114: 51-73.

Gérard E, Bessy E, Hénard G, Ducoroy L, Verpoort T, Marchand-Brynaert J (2011) Surface modification of poly (butylene terephthalate) nonwoven by photochemistry and biofunctionalization with peptides for blood filtration. Journal of Polymer Science Part A: Polymer Chemistry 49: 5087-99.

Ghasemi-Mobarakeh L, Semnani D, Morshed M (2007) A novel method for porosity measurement of various surface layers of nanofibers mat using image analysis for tissue engineering applications. *J Appl Poly Sci.* 106: 2536-42.

Greenwalt TJ, Gajewski M, McKenna JL (1962) A new method for preparing buffy coat-poor blood. Transfusion. 2: 221-9.

Greiner A, Wendorff JH (2007) Electrospinning: a fascinating method for the preparation of ultrathin fibers. *Angew Chem, Int Ed.* 46: 5670-3.

Grinnell F, Feld MK (1981) Adsorption characteristics of plasma fibronectin in relationship to biological activity. *J Biomed Mater Res.* 15: 363-81.

Guibo Y, Qing Z, Yahong Z, Yin Y, Yumin Y (2013) The electrospun polyamide 6 nanofiber membranes used as high efficiency filter materials: filtration potential, thermal treatment, and their continuous production. *J Appl Polym Sci.* 128: 1061-9.

Guidoin R, Taylor K, Bain W (1977) Blood filter evaluation. *Biomater, Med Devices, Artif Organs.* 5: 317-36.

Gule NP, de Kwaadsteniet M, Cloete TE, Klumperman B (2012) Electrospun poly (vinyl alcohol) nanofibres with biocidal additives for application in filter media, 1–properties affecting fibre morphology and characterisation. *Macromol Mater Eng.* 297: 609-17.

Guo S, Ke Q, Wang H, Jin X, Li Y (2013) Poly (butylene terephthalate) electrospun/melt-blown composite mats for white blood cell filtration. *J Appl Polym Sci.* 128: 3652-59.

Hassan MA, Yeom BY, Wilkie A, Pourdeyhimi B, Khan SA (2013) Fabrication of nanofiber meltblown membranes and their filtration properties. *J Membr Sci.* 427: 336-44.

He J-H, Liu Y, Mo L-F, Wan Y-Q, Xu L (2008) Electrospun nanofibres and their applications. iSmithers, United Kingdom.

Hemmat A, Ghoreishi S, Sabet JK (2015) Effect of salt additives on the fabrication of poly (vinylidene fluoride-co-hexafluropropylene)(PVDF-HFP) nanofiber membranes for air gap membrane distillation. *Procedia Mater Sci.* 11: 370-5.

Henschler R, Rüster B, Steimle A, Hansmann H, Walker W, Montag T, Seifried E (2005) Analysis of leukocyte binding to depletion filters: role of passive binding, interaction with platelets, and plasma components. *Ann Hematol.* 84: 538-44.

Hoffstein S, Weissmann G, Pearlstein E (1981) Fibonectin is a component of the surface coat of human neutrophils. *J Cell Sci.* 50: 315-27.

Högman CF (1997) Cellular blood components: preparation, preservation, leukodepletion and indication. *Baillière's Clin Anaesthesiol.* 11: 241-59.

Huang X-J, Huang X-D, Che A-F, Xu Z-K, Yao K (2006) Suppression of cell adhesion on polyacrylonitrile-based membranes by the anchoring of phospholipid moieties. *Chin J Polym Sci.* 24: 103-6.

Huang X-J, Xu Z-K, Wan L-S, Wang Z-G, Wang J-L (2005) Surface modification of polyacrylonitrile-based membranes by chemical reactions to generate phospholipid moieties. *Langmuir* 21: 2941-7.

Hussain M, Murali C, Willi P, Sharma C, Bhuvneshwar G, Sreekumar R (1998) Comparative complement activation study of polypropylene hollow fibres of two different makes in static condition. *J Biomater Appl.* 12: 300-20.

Isakov D, Gomes EDM, Bdikin I, Almeida B, Belsley M, Costa M, Rodrigues V, Heredia A (2011) Production of polar β-glycine nanofibers with enhanced nonlinear optical and piezoelectric properties. *Cryst Growth Des.* 11: 4288-91.

Ishihara K, Aragaki R, Ueda T, Watenabe A, Nakabayashi N (1990) Reduced thrombogenicity of polymers having phospholipid polar groups. *J Biomed Mater Res.* 24: 1069-77.

Iwasaki Y, Yamasaki A, Ishihara K (2003) Platelet compatible blood filtration fabrics using a phosphorylcholine polymer having high surface mobility. *Biomaterials* 24: 3599-604.

Jansen B, Ellinghorst G (1985) Modification of polyetherurethane for biomedical application by radiation-induced grafting. I. Grafting procedure, determination of mechanical properties, and chemical modification of grafted films. *J Biomed Mater Res.* 19: 1085-99.

Jeun J-P, Kim H-B, Oh S-H, Park J-K, Kang P-H (2015) Effects of electron beam irradiation on the electrospinning of polyacrylonitrile. *J Nanosci Nanotechnol.* 15: 5942-5.

Ji L, Zhang X (2008) Ultrafine polyacrylonitrile/silica composite fibers via electrospinning. *Mater Lett.* 62: 2161-4.

Jiang J, Zhu L, Zhu L, Zhu B, Xu Y (2011) Surface characteristics of a self-polymerized dopamine coating deposited on hydrophobic polymer films. *Langmuir*. 27: 14180-7.

Jin G, Yao Q, Zhang S, Zhang L (2008) Surface modifying of microporous PTFE capillary for bilirubin removing from human plasma and its blood compatibility. *Mater Sci Eng: C.* 28: 1480-8.

Jindal KK, McDougall J, Woods B, Nowakowski L, Goldstein MB (1989) A study of the basic principles determining the performance of several high-flux dialyzers. *Am J Kidney Dis.* 14: 507-11.

Johnson J, Mijović V, Brozović B (1983) Evaluation of a new filter for leucocyte depletion of blood. *J Clin Pathol.* 36: 1200-1.

Kataoka K, Okano T, Sakurai Y, Nishimura T, Inoue S, Watanabe T, Maruyama A, Tsuruta T (1983) Differential retention of lymphocyte subpopulations (B and T cells) on the microphase separated surface of polystyrene/polyamine graft copolymers. *Eur Polym J.* 19: 979-84.

Kenawy E-R, Layman JM, Watkins JR, Bowlin GL, Matthews JA, Simpson DG, Wnek GE (2003) Electrospinning of poly (ethylene-co-vinyl alcohol) fibers. *Biomaterials* 24: 907-13.

Khulbe K, Feng C, Matsuura T (2010) The art of surface modification of synthetic polymeric membranes. *J Appl Polym Sci.* 115: 855-95.

Kim EJ, Yeo GD, Pai CM, Kang IK (2009) Preparation of surface-modified poly (butylene terephthalate) nonwovens and their application as leukocyte removal filters. *J Biomed Mater Res Part B: Appl Biomater*. 90: 849-56.

Kitano H, Tada S, Mori T, Takaha K, Gemmei-Ide M, Tanaka M, Fukuda M, Yokoyama Y (2005. Correlation between the structure of water in the

vicinity of carboxybetaine polymers and their blood-compatibility. *Langmuir*. 21: 11932-40.

Kjeldsen-Kragh J, Golebiowska E (2002) Back-priming of the RCM1™ leucocyte-reduction filter: consequences for filtration efficacy. *Vox Sang.* 82: 127-30.

Klein E (1998) The modern history of haemodialysis membranes and controllers. *Nephrology*. 4: 255-65.

Kvarstein B (1969) Effects of proteins and inorganic ions on the adhesiveness of human leucocytes to glass beads. *Scand J Clin Lab Invest.* 24: 41-8.

Lane TA, Anderson KC, Goodnough LT, Kurtz S, Moroff G, Pisciotto PT, Sayers M, Silberstein LE (1992) Leukocyte reduction in blood component therapy. *Ann Intern Med.* 117: 151-62.

Lang EV, Lang JH, Lasser EC (1988) Adherence of granulocytes to nylon fibers. Evidence for a plasma granulocyte adherence factor. *Thromb Res.* 50: 243-8.

Ledent E, Berlin G (1996) Factors influencing white cell removal from red cell concentrates by filtration. *Transfusion.* 36: 714-8.

Lee E, Vernucci P, Williams S (2002) Leukocyte reduction filtration media. U.S. Patent No. 6,337,026.

Lee H, Dellatore SM, Miller WM, Messersmith PB (2007) Mussel-inspired surface chemistry for multifunctional coatings. *Science.* 318: 426-30.

Lee H, Rho J, Messersmith PB (2009) Facile conjugation of biomolecules onto surfaces via mussel adhesive protein inspired coatings. *Adv Mater.* 21: 431-4.

Lee H, Scherer NF, Messersmith PB (2006) Single-molecule mechanics of mussel adhesion. *Proc Natl Acad Sci.* 103: 12999-3003.

Lee JH, Park JW, Lee HB (1991) Cell adhesion and growth on polymer surfaces with hydroxyl groups prepared by water vapour plasma treatment. *Biomaterials* 12: 443-8.

Lee Y-S, Livingston Arinzeh T (2011) Electrospun nanofibrous materials for neural tissue engineering. *Polymers* 3: 413-26.

Lewis AL, Hughes PD, Kirkwood LC, Leppard SW, Redman RP, Tolhurst LA, Stratford PW (2000) Synthesis and characterisation of phosphorylcholine-based polymers useful for coating blood filtration devices. *Biomaterials* 21: 1847-59.

Li S-F, Chen J-P, Wu W-T (2007) Electrospun polyacrylonitrile nanofibrous membranes for lipase immobilization. *J Mol Catal B: Enzym.* 47: 117-24.

Lim F, Cooper SL (1990) The effect of surface hydrophilicity on biomaterial-leukocyte interactions. *ASAIO Trans/Am Soc Artif Intern Organs.* 37: 146-7.

Lin JC, Chuang WH (2000) Synthesis, surface characterization, and platelet reactivity evaluation for the self-assembled monolayer of alkanethiol with sulfonic acid functionality. *J Biomed Mater Res.* 51: 413-23.

Lin W-C, Liu T-Y, Yang M-C (2004) Hemocompatibility of polyacrylonitrile dialysis membrane immobilized with chitosan and heparin conjugate. *Biomaterials* 25: 1947-57.

Liu T-Y, Lin W-C, Huang L-Y, Chen S-Y, Yang M-C (2005) Hemocompatibility and anaphylatoxin formation of protein-immobilizing polyacrylonitrile hemodialysis membrane. *Biomaterials.* 26: 1437-44.

Liu Z, Jiao Y, Wang T, Zhang Y, Xue W (2012) Interactions between solubilized polymer molecules and blood components. *J Controlled Release.* 160: 14-24.

Lyapina L, Pastorova V, Golubeva M, Grigorieva M (2003) Role of Glycine in Blood Coagulation Processes. *Biol Bull Russ Acad Sci.* 30: 492-5.

Maalej N, Albrecht R, Loscalzo J, Folts JD (1999) The potent platelet inhibitory effects of S-nitrosated albumin coating of artificial surfaces. *J Am Coll Cardiol.* 33: 1408-1414.

MacGregor RR, Spagnuolo PJ, Lentnek AL (1974) Inhibition of granulocyte adherence by ethanol, prednisone, and aspirin, measured with an assay system. *N Engl J Med.* 291: 642-6.

Marconi W, Cordelli S, Napoli A, Piozzi A (2000) Polymeric systems based on derivatives of ethylene-vinyl alcohol copolymers. *J Bioact Compat Polym.* 15: 257-71.

Maruyama A, Tsuruta T, Kataoka K, Sakurai Y (1987) Polyamine graft copolymer for separation of rat B and T lymphocytes. Role of ionic interaction between polymer matrix and lymphocytes. *Makromol Chem, Rapid Commun.* 8: 27-30.

Matheis G, Moritz A, Scholz M (2002) Leukocyte depletion in cardiac surgery and cardiology: Karger Medical and Scientific Publishers.

Matsumura K, Hyon S-H, Nakajima N, Iwata H, Watazu A, Tsutsumi S (2004) Surface modification of poly (ethylene-co-vinyl alcohol): hydroxyapatite immobilization and control of periodontal ligament cells differentiation. *Biomaterials.* 25: 4817-24.

McAllister K, Sazani P, Adam M, Cho MJ, Rubinstein M, Samulski RJ, DeSimone J M. (2002) Polymeric nanogels produced via inverse microemulsion polymerization as potential gene and antisense delivery agents. *J Am Chem Soc.* 124: 15198-207.

Meer PF, Pietersz RN, Nelis JT, Hinloopen B, Dekker WJ, Reesink HW (1999) Six filters for the removal of white cells from red cell concentrates, evaluated at 4 C and/or at room temperature. *Transfusion.* 39: 265-70.

Meryman H, Hornblower M (1986) The preparation of red cells depleted of leukocytes. *Transfusion.* 26: 101-6.

Mijović V, Brozovic B, Hughes A, Davies T (1983) Leukocyte-depleted blood A comparison of filtration techniques. *Transfusion.* 23: 30-2.

Moideen KI, Isloor AM, Garudachari B, Ismail A (2016) The effect of glycine betaine additive on the PPSU/PSF ultrafiltration membrane performance. *Desalin Water Treat.* 1-11.

Morley D, Feuerstein I (1989) Adhesion of polymorphonuclear leukocytes to protein-coated and platelet adherent surfaces. *Thromb Haemostasis.* 62: 1023-8.

Morudu LJ (2011) The indications of leukodepleting blood or blood products, and the importance of using bedside blood-product filters during neonatal transfusion. *Professional Nursing Today.* 16: 22-5.

Nady N, Franssen MC, Zuilhof H, Eldin MSM, Boom R, Schroën K (2011) Modification methods for poly (arylsulfone) membranes: a mini-review focusing on surface modification. *Desalination.* 275: 1-9.

Namboodiri AG, Parameswaran R (2013) Fibro-porous polycaprolactone membrane containing extracts of Biophytum sensitivum: A prospective antibacterial wound dressing. *J Appl Polym Sci.* 129: 2280-6.

Namekawa K, Schreiber MT, Aoyagi T, Ebara M (2014) Fabrication of zeolite–polymer composite nanofibers for removal of uremic toxins from kidney failure patients. *Biomater Sci.* 2: 674-9.

Nandakumar A, Fernandes H, de Boer J, Moroni L, Habibovic P, van Blitterswijk CA (2010) Fabrication of bioactive composite scaffolds by electrospinning for bone regeneration. *Macromol Biosci.* 10: 1365-73.

Narick C, Triulzi DJ, Yazer MH (2012) Transfusion-associated circulatory overload after plasma transfusion. *Transfusion.* 52: 160-5.

Nataraj S, Yang K, Aminabhavi T (2012) Polyacrylonitrile-based nanofibers—a state-of-the-art review. *Prog Polym Sci.* 37: 487-513.

Natori SH, Gomei Y, Higuchi A (2006) Synthesis and performance of amphiphilic copolymers for blood cell separation. *J Biomed Mater Res Part B: Appl Biomater*. 78: 318-26.

Natori SH, Kurita K (2007a) Blood cell separation using amphiphilic copolymers containing N, N-dimethylacrylamide. *J Biomed Mater Res Part B: Appl Biomater*. 81: 419-26.

Natori SH, Kurita K (2007b) Blood cell separation using crosslinkable copolymers containing N, N-dimethylacrylamide. *Polym Adv Technol.* 18: 263-7.

Nie C, Ma L, Xia Y, He C, Deng J, Wang L, Cheng C, Sun S, Zhao C (2015) Novel heparin-mimicking polymer brush grafted carbon nanotube/PES composite membranes for safe and efficient blood purification. *J Membr Sci.* 475: 455-68.

Novotny V, van Doorn R, Witvliet MD, Claas F, Brand A (1995) Occurrence of allogeneic HLA and non-HLA antibodies after transfusion of prestorage

filtered platelets and red blood cells: a prospective study. *Blood.* 85: 1736-41.

Nusbacher J (1992) Yersinia enterocolitica and white cell filtration. *Transfusion.* 32: 597-600.

Oh NW, Jegal J, Lee KH (2001) Preparation and characterization of nanofiltration composite membranes using polyacrylonitrile (PAN). I. Preparation and modification of PAN supports. *J Appl Polym Sci.* 80: 1854-62.

Okano T, Nishiyama S, Shinohara I, Akaike T, Sakurai Y, Kataoka K, Tsuruta T (1981) Effect of hydrophilic and hydrophobic microdomains on mode of interaction between block polymer and blood platelets. *J Biomed Mater Res.* 15: 393-402.

Oldhafer KJ, Stavrou GA, Donati M, Kaudel P, Frühauf NR (2013) Extracorporeal tumor cell filtration during extended liver surgery: first clinical use of leukocyte depletion filters-a case series. *World J Surg Oncol.* 11: 1-7.

Olson BJ, Markwell J (2007) Assays for determination of protein concentration. *Curr Protoc Protein Sci.*, 3.4. 1-3.4. 29.

Owens N, Gingell D, Trommler A (1988) Cell adhesion to hydroxyl groups of a monolayer film. *J Cell Sci.* 91: 269-79.

Pandey S, Vyas GN (2012) Adverse effects of plasma transfusion. *Transfusion.* 52: 65S-79S.

Pepinsky R, Vedam K, Hoshino S, Okaya Y (1958) Ferroelectricity in Di-Glycine Nitrate $(NH_2CH_2COOH)_2 \cdot HNO_3$. *Phys Rev.* 111: 430-2.

Petsch D, Deckwer W-D, Anspach FB, Legallais C, Vijayalakshmi M (1998) Endotoxin removal with poly (ethyleneimine)-immobilized adsorbers: Sepharose 4B

versus flat sheet and hollow fibre membranes. *J Chromatogr B: Biomed Sci Appl.* 707: 121-30.

Polliack A, Lampen N, Clarkson B, De Harven E, Bentwich Z, Siegal F, Kunkel H (1973) Identification of human B and T lymphocytes by scanning electron microscopy. *J Exp Med.* 138: 607-24.

Poornachary SK, Chow PS, Tan RB (2007) Influence of solution speciation of impurities on polymorphic nucleation in glycine. *Cryst Growth Des.* 8: 179-85.

Ramakrishna S, Fujihara K, Teo W-E, Lim T-C, Ma Z (2005) An introduction to electrospinning and nanofibers Vol 90: World Scientific, Singapore.

Rasp FL, Clawson C, Repine JE (1981) Platelets increase neutrophil adherence *in vitro* to nylon fiber. *J Lab Clin Med.* 97: 812-9.

Remya K, Joseph J, Mani S, John A, Varma H, Ramesh P. (2013) Nanohydroxyapatite incorporated electrospun polycaprolactone/polycaprolactone–polyethyleneglycol–polycaprolactone blend scaffold for bone tissue engineering applications. *J Biomed Nanotechnol.* 9: 1483-94.

Rich A, Harris AK (1981) Anomalous preferences of cultured macrophages for hydrophobic and roughened substrata. *J Cell Sci*. 50: 1-7.

Rider J, Want E, Winter M, Turton J, Pamphilon D, Nobes P (2000) Differential leucocyte subpopulation analysis of leucodepleted red cell products. *Transfusion Med.* 10: 49-58.

Sahu S, Verma A (2014) Adverse events related to blood transfusion. *Ind J Anaesth.* 58: 543-51.

Sakurada Y, Sueoka A, Kawahashi M (1987) Blood purification device using membranes derived from poly (vinyl alcohol), and copolymer of ethylene and vinyl alcohol. *Polym J.* 19: 501-13.

Saufi SM, Ismail AF (2002) Development and characterization of polyacrylonitrile (PAN) based carbon hollow fiber membrane. *Songklanakarin J Sci Technol.* 24: 843-54.

Serious Hazards of Transfusion Steering Group (2002) Serious hazards of transfusion annual report 2001-2002. Manchester, UK: SHOT office, pp. 94-101.

Sharma DC, Rai S, Gupta S, Jain B (2014) Universal leukoreduction decreases the incidence of febrile nonhemolytic transfusion reactions to cellular blood components: A 5 year study. *International Blood Research and Reviews*. 2: 279-288.

Sharma R, Marwaha N (2010) Leukoreduced blood components: Advantages and strategies for its implementation in developing countries. *Asian J Transfus Sci.* 4: 3-8.

Shirokaze J (2002) Leukocytapheresis using a leukocyte removal filter. *Ther Apheresis.* 6: 261-6.

Sill TJ, von Recum HA (2008) Electrospinning: applications in drug delivery and tissue engineering. *Biomaterials.* 29: 1989-2006.

Sirchia G, Wenz B, Rebulla P, Parravicini A, Carnelli V, Bertolini F (1990) Removal of white cells from red cells by transfusion through a new filter. *Transfusion.* 30: 30-3.

Skalak R, Impelluso T, Schmalzer E, Chien S (1982) Theoretical modeling of filtration of blood cell suspensions. *Biorheology.* 20: 41-56.

Sniecinski I, O'donnell M, Nowicki B, Hill L (1988) Prevention of refractoriness and HLA-alloimmunization using filtered blood products. *Blood.* 71: 1402-7.

Steneker I, Biewenga J (1990) Histological and immunohistochemical studies on the preparation of leukocyte-poor red cell concentrates by filtration: The filtration process on cellulose acetate fibers. *Vox Sang.* 58: 192-8.

Steneker I, Luyn M, Wachem P, Biewenga J (1992) Electronmicroscopic examination of white cell reduction by four white cell-reduction filters. *Transfusion.* 32: 450-7.

Sueoka A (1997) Present status of apheresis technologies: Part 1. Membrane plasma separator. *Ther Apheresis.* 1: 42-8.

Thankam FG, Muthu J (2014) Influence of physical and mechanical properties of amphiphilic biosynthetic hydrogels on long-term cell viability. *J Mech Behav Biomed Mater.* 35: 111-22.

Ulbricht M, Matuschewski H, Oechel A, Hicke H-G (1996) Photo-induced graft polymerization surface modifications for the preparation of hydrophilic and low-proten-adsorbing ultrafiltration membranes. *J Membr Sci*. 115: 31-47.

Umegae M, Nishimura T, Kuroda T, Kato H (1988) Development of filtration lymphocytapheresis and its clinical application. *Jpn J Artif Organs.* 17: 413-6.

Van Oss CJ (1975) Phagocytic engulfment and cell adhesiveness as cellular surface phenomena. Dekker, pp. 143-152

Vaughan JM (1939) Blood Tranfusion Outfit. *Br Med J.* 2: 1084-5.

von Ahsen N, Müller C, Serke S, Frei U, Eckardt K-U (2001) Important role of nondiagnostic blood loss and blunted erythropoietic response in the anemia of medical intensive care patients. *Crit Care Med.* 29: S141-S150.

Waite JH (2008) Surface chemistry: mussel power. *Nat Mater.* 7: 8-9.

Wan Kim S, Jacobs H (1996) Design of nonthrombogenic polymer surfaces for blood-contacting medical devices. *Blood Purif.* 14: 357-72.

Wang M, Jin H-J, Kaplan DL, Rutledge GC (2004) Mechanical properties of electrospun silk fibers. *Macromolecules.* 37: 6856-64.

Wang M, Yuan J, Huang X, Cai X, Li L, Shen J (2013) Grafting of carboxybetaine brush onto cellulose membranes via surface-initiated ARGET-ATRP for improving blood compatibility. *Colloids Surf B: Biointerfaces.* 103: 52-8.

Wang Z-G, Wan L-S, Xu Z-K (2007) Surface engineerings of polyacrylonitrile-based asymmetric membranes towards biomedical applications: An overview. *J Membr Sci*. 304: 8-23.

Ward G (2005) Nanofibres: media at the nanoscale. *Filtr Separat.* 42: 22-4.

Waters JH, Tuohy MJ, Hobson DF, Procop G (2003) Bacterial reduction by cell salvage washing and leukocyte depletion filtration. *Anesthesiology.* 99: 652-5.

Weng Y, Hou R, Li G, Wang J, Huang N, Liu H (2008). Immobilization of bovine serum albumin on TiO_2 film via chemisorption of H_3PO_4 interface and effects on platelets adhesion. *Appl Surf Sci.* 254: 2712-9.

Wenz B (1986) Leukocyte-poor blood. *Crit Rev Clin Lab Sci.* 24: 1-20.

West SL, Salvage JP, Lobb EJ, Armes SP, Billingham NC, Lewis AL, Hanlon GW, Lloyd AW (2004) The biocompatibility of crosslinkable copolymer

coatings containing sulfobetaines and phosphobetaines. *Biomaterials.* 25: 1195-204.

Wosek J (2015) Fabrication of composite polyurethane/hydroxyapatite scaffolds using solvent-casting salt leaching technique. *Adv Mater Sci.* 15: 14-20.

Xu C, Xu F, Wang B, Lu T (2011) Electrospinning of poly (ethylene-co-vinyl alcohol) nanofibres encapsulated with Ag nanoparticles for skin wound healing. *J Nanomater.* 2011: 1-7.

Xu X, Zhang J-F, Fan Y (2010) Fabrication of cross-linked polyethyleneimine microfibers by reactive electrospinning with in situ photo-cross-linking by UV radiation. *Biomacromolecules.* 11: 2283-9.

Xu Z-K, Nie F-Q, Qu C, Wan L-S, Wu J, Yao K (2005) Tethering poly (ethylene glycol) s to improve the surface biocompatibility of poly (acrylonitrile-co-maleic acid) asymmetric membranes. *Biomaterials.* 26: 589-98.

Yang C, Cao Y, Sun K, Liu J, Wang H (2011) Functional groups grafted nonwoven fabrics for blood filtration—The effects of functional groups and wettability on the adhesion of leukocyte and platelet. *Appl Surf Sci.* 257: 2978-83.

Ye H, Chen L, Li A, Huang L, Zhang Y, Li Y, Li H (2015) Alkali-responsive membrane prepared by grafting dimethylaminoethyl methacrylate onto ethylene vinyl alcohol copolymer membrane. *J Appld Polym Sci*. 132: 41775-

Yomtovian R, Gernsheimer T, Assmann SF, Mohandas K, Lee TH, Kalish LA, Busch MP (2001) WBC reduction in RBC concentrates by prestorage filtration: multicenter experience. *Transfusion.* 41: 1030-6.

You I, Kang SM, Byun Y, Lee H (2011) Enhancement of blood compatibility of poly (urethane) substrates by mussel-inspired adhesive heparin coating. *Bioconjugate Chem.* 22: 1264-9.

Young T-H, Lin C-W, Cheng L-P, Hsieh C-C (2001) Preparation of EVAL membranes with smooth and particulate morphologies for neuronal culture. *Biomaterials.* 22: 1771-7.

Yu Y-H, Chan C-C, Lai Y-C, Lin Y-Y, Huang Y-C, Chi W-F, Kuo C-W, Lin H-M, Chen P-C (2014) Biocompatible electrospinning poly (vinyl alcohol) nanofibres embedded with graphene-based derivatives with enhanced conductivity, mechanical strength and thermal stability. *RSC Adv.* 4: 56373-84.

Yuan J, Lin S, Shen J (2008) Enhanced blood compatibility of polyurethane functionalized with sulfobetaine. *Colloids Surf B: Biointerfaces.* 66: 90-5.

Yuan J, Zhang J, Zang X, Shen J, Lin S (2003a). Improvement of blood compatibility on cellulose membrane surface by grafting betaines. *Colloids Surf B: Biointerfaces.* 30: 147-55.

Yuan J, Zhang J, Zhu J, Shen J, Lin S, Zhu W, Fang J (2003b). Reduced platelet adhesion on the surface of polyurethane bearing structure of sulfobetaine. *J Biomater Appl.* 18: 123-35.

Yui N, Sanui K, Ogata N, Kataoka K, Okano T, Sakurai Y (1983) Effect of crystallinity of polyamides on adhesion-separation behavior of granulocytes. *J Biomed Mater Res.* 17: 383-8.

Zhang C, Jin J, Zhao J, Jiang W, Yin J (2013) Functionalized polypropylene non-woven fabric membrane with bovine serum albumin and its hemocompatibility enhancement. *Colloids Surf B: Biointerfaces.* 102: 45-52.

Zhang H, Nie H, Yu D, Wu C, Zhang Y, White CJB, Zhu L (2010) Surface modification of electrospun polyacrylonitrile nanofiber towards developing an affinity membrane for bromelain adsorption. *Desalination.* 256: 141-7.

Zhang J, Yuan J, Yuan Y, Zang X, Shen J, Lin S (2003) Platelet adhesive resistance of segmented polyurethane film surface-grafted with vinyl benzyl sulfo monomer of ammonium zwitterions. *Biomaterials.* 24: 4223-31.

Zhao J, Shi Q, Luan S, Song L, Yang H, Shi H, Jin J, Li X, Yin J, Stagnaro P (2011) Improved biocompatibility and antifouling property of polypropylene non-woven fabric membrane by surface grafting zwitterionic polymer. *J Membr Sci*. 369: 5-12.

Zhao Y-H, Wee K-H, Bai R (2010) Highly hydrophilic and low-protein-fouling polypropylene membrane prepared by surface modification with sulfobetaine-based zwitterionic polymer through a combined surface polymerization method. *J Membr Sci.* 362: 326-33.

Zhou J, Meng S, Guo Z, Du Q, Zhong W (2007) Phosphorylcholine-modified poly (ethylene-co-vinyl alcohol) microporous membranes with improved protein-adsorption-resistance property. *J Membr Sci*. 305: 279-86.

Zhu L-P, Jiang J-H, Zhu B-K, Xu Y-Y (2011) Immobilization of bovine serum albumin onto porous polyethylene membranes using strongly attached polydopamine as a spacer. *Colloids Surf B: Biointerfaces.* 86: 111-8.

Zingg W, Neumann A, Strong A, Hum O, Absolom D (1981) Platelet adhesion to smooth and rough hydrophobia and hydrophilic surfaces under conditions of static exposure and laminar flow. *Biomaterials.* 2: 156-8.

Zwarts F, de Vries AJ (2002) Aspects of leucocyte and fat filtration during cardiac surgery. *Perfusion.* 17.

LIST OF PUBLICATIONS

Publications from thesis

1. **P.V. Mayuri,** Anugya Bhatt, A. Sabareeswaran and P. Ramesh. 'A novel leukodepletion filter from electrospun poly(ethylene-vinyl alcohol) membranes and evaluation of its efficiency'. International Journal of Polymeric Materials and Polymeric Biomaterials 2016, 65 (4); 183-190.

2. **P.V. Mayuri,** Anugya Bhatt, Roy Joseph and P. Ramesh. 'Effect of photografting 2-hydroxyethylacrylate on the hemocompatibility of electrospunpoly(ethylene-co-vinyl alcohol) fibroporous mats'. Materials Science and Engineering Part C 2016, 60; 19–29.

3. **P.V. Mayuri,** Anugya Bhatt and P. Ramesh. 'Sulfobetaine functionalized electrospun poly(ethylene-co-vinyl alcohol) membranes for blood filtration'. (Under communication).

4. **P.V. Mayuri,** Anugya Bhatt and P.Ramesh. 'Effect of fiber diameter on filtration efficiency of electrospun poly(ethylene-co-vinyl alcohol) leukodepletion membranes'. (Under communication).

5. **P.V. Mayuri,** Anugya Bhatt and P. Ramesh. 'Bovine serum albumin immobilized electrospun poly(ethylene-co-vinyl alcohol) membranes as effective leukodepletion filters'. (Under communication).

Other publications

1. **P.V. Mayuri** and P. Ramesh. 'Fabrication and characterization of silver nanoparticle impregnated uniaxially aligned fibre yarns by one-step electrospinning process'. Journal of Material Science 2016, 51 (5); 2739-2746.

Conference presentations

1. **P. V. Mayuri**, Anugya Bhatt, Sabareeswaran A and P. Ramesh. "A novel leukodepletion filter from electrospun poly(ethylene-co-vinyl alcohol) membranes" (Oral presentation). National conference on biopolymers and green composites, October 9-10, 2015 (BPGC-2015) organized by Centre for Biopolymer Polymer Science and Technology, Kochi.

2. **P. V. Mayuri,** Anugya Bhatt and P. Ramesh. "Sulfobetaine functionalized electrospun poly(ethylene-co-vinyl alcohol) membranes with enhanced hemocompatibility" (Poster presentation). National conference on material science and technology (NCMST), July 6-8, 2015 organized by Indian Institute of Space Science and technology, Thiruvananthapuram.

3. **P. V. Mayuri** and P. Ramesh. "Hemocompatible 2-hydroxyethyl acrylate grafted electrospun poly(ethylene-co-vinyl alcohol) fibers with improved hydrophilicity" (Poster presentation). International conference FAPS – MACRO, May 15-18, 2013 organized by Indian Institute of Science, Bangalore.

CURRICULUM VITAE

Personal

Name	:	Mayuri P. V.
Date of birth	:	18th May 1988
Marital status	:	Married
Phone number	:	9496759774
Address	:	Parappully House
		Lilly Nivas
		Elamkunnappuzha P. O.
		Ernakulam-682503
		Kerala, India
E-mail	:	pv.mayuri@gmail.com

Education

PhD Scholar (January 2011- present) at Sree Chitra Tirunal Institute for Medical Sciences and Technology, BioMedical Technology Wing, Thiruvananthapuram, Kerala, India. Supervisor : Dr. P. Ramesh

Master of Science in Chemistry (Polymer science) (2008-2010), School of Chemical Sciences, Mahatma Gandhi University, Kottayam, Kerala, India (Passed with First rank)

Bachelor of Science in Chemistry (Polymer science) (2005-2008), Cochin College, (Mahatma Gandhi University), Kochi, Kerala, India (Passed with First class and Distinction)

Professional Experience

October 2010 – December 2010: Project fellow at Sree Chitra Tirunal Institute for Medical Sciences and Technology, Trivandrum, Kerala, India. Project Supervisor: Dr. P. Ramesh.

January 2010 – June 2010: MSc. Project at IIT Chennai. Project Supervisor: Dr. Susy Varughese

Achievements

KSCSTE Research Fellowship -2010 was awarded

INSPIRE Fellowship 2011 (DST, India) was awarded

First prize in Quiz competition during National Conference on Biopolymers and Green composites 2015, organized by Centre for Biopolymer Science & Technology, Kochi

APPENDIX

Preparation of phosphate buffered saline (PBS) pH 7.4 (1000 ml)

The following salts were taken for 1000 ml of PBS

Sodium Chloride (NaCl)	- 8.00 g
Potassium Chloride (KCl)	- 0.20 g
Disodium hydrogen phosphate (Na_2HPO_4)	- 1.44 g
Potassium dihydrogen phosphate ($KH_2PO_{4)}$	- 0.24 g

These salts were completely dissolved in 1000 ml of distilled water. The pH of the resulting solution was checked. If the pH is higher than 7.4, drops of 0.1 N HCl is added until it becomes 7.4. If the pH is less than 7.4, required amount of 0.1 N NaOH is added to adjust the final pH to 7.4.